ver

# STUDIES ON GAMMA TRANSITIONS AND THEIR DIRECTIONAL CORRELATIONS IN GERMANIUM-74 AND PROMETHIUM-147

Zin Aung

M.S.,Missouri; M.Sc.Lond.

A Thesis submitted

for the degree of

DOCTOR OF PHILOSOPHY

in the University of London

Bedford College

London

1973

CONTENTS

## Abstract

A 40 cc Ge(Li) detector has been used to study the gamma rays emitted in the decay of Cobalt-60, Arsenic-74 and Neodymium-147. A system for measuring directional correlations has been constructed with a fast-slow electronics arrangement utilising the Ge(Li) detector and a NaI(Tl) scintillation counter, and the directional correlations of gamma-gamma cascades in Germanium-74 and Promethium-147 have been studied.

# CHAPTER 1 INTRODUCTION

## 1.1 Gamma-Ray Spectroscopy

Nuclear spectroscopy can be roughly classified as the study of nuclear structure and the quantum mechanical properties of the ground state and excited levels of nuclei. In the early days the experimenter measured the energies and intensities of the alpha-,beta-,and gamma-radiations emitted in the decay of radioactive nuclei which gave information about the energy levels of excited nuclei. With the advances in experimental techniques, instrumentation and theoretical methods, the main aim of nuclear spectroscopy now is to determine not only the relative energy levels but also to determine the state characteristics (spins and parities), transition probabilities etc. For this reason in addition to measuring the energy and intensities of gamma rays and alpha-,and beta-groups, it is necessary to determine internal conversion coefficients, K/L ratios, and to do experiments on the spatial and temporal relationships of the radiations (i.e. angular correlations, studies of lifetimes of states etc.).

In the work reported in this thesis we are concerned only with gamma-ray spectroscopy; specifically, the measurement of the energies, the intensities, and the directional correlations of gamma rays.

## 1.2 Ge(Li) Detectors in Gamma-Ray Spectroscopy

The importance of semi-conductor detectors in gamma-ray spectroscopy is related to their excellent energy resolution (Typically about 3 keV compared to about 100 keV for NaI (Tl) at about 1 MeV coupled with detection efficiency orders of magnitude larger than that of other high resolution instruments (diffraction and external conversion magnetic spectrometers). Moreover, Ge(Li) and Si(Li) detectors, like scintillators and gaseous counters, work as multichannel devices permitting simultaneous measurement of the entire gamma ray spectrum.

The first successful attempts to utilize semiconductor detectors for gamma-ray spectroscopy were made using Si(Li) detectors; however, their practical use was limited to energies below 100 keV, because of the low atomic number of silicon. Freck and Wakefield (1962) succeeded in constructing the first germanium gamma ray spectrometer. Since then there has been rapid progress in the development of construction techniques which led to sensitive detector volumes of up to 100 $cm^3$ for the coaxial types. In addition the use of field effect transistor preamplifiers in the electronic chain and refinements in detector construction improved the energy resolution from 21 keV (Freck and Wakefield, 1962) to 1.4 keV (Heath et-al, 1966) for the 662 keV $^{137}Cs$ line.

The good energy resolution of the semi-conductor detector permits the relative determination of the energy of a gamma ray with very high precision. The absolute energy assigned to a gamma ray transition is then determined by comparison with reference gamma ray lines. Since only a few gamma ray lines are known with high precision, the energy intervals between the unknown peak and the reference peaks can be large. It is then desirable for the spectrometer system (detector plus associated electronics) to have a good linearity. According to theory which predicts a value of w (energy required to create an ion pair) which is independent of energy, the linearity of the Ge(Li) system must be excellent. Several measurements have been undertaken to check this and Berg and Kashy (1966) have reported a linearity value better than $\pm$ 0.03% in the range 662 to 2614 keV.

If all of the gamma ray energy is deposited in the detector by the photoelectric effect, Compton scattering and/or pair production the resulting pulse is deposited in the full energy peak. In the energy region 100 keV to 8 MeV most of the gamma rays are absorbed in the germanium detector by the Compton scattering process. If the detector is large enough a significant proportion of scattered gamma rays will be totally absorbed after undergoing a number of collisions. Others will be scattered out of the detector and will then produce an output pulse less than the full energy pulse. This generates a

Compton continuum below the full energy peak. The ratio of the peak height to the level of the plateau is called the peak-to-Compton ratio and is a useful measure of how easily low intensity gamma rays can be seen against a high background.

The efficiency of the germanium detector is usually defined as the percentage of $^{60}Co$ 1.33 MeV gamma rays that lose all of their energy in the detector compared with the percentage that lose all their energy in a 3 inch by 3 inch NaI(Tl) crystal with the measurement being made at 25 cm from the same source in both cases. The relative photopeak efficiency is therefore a function of the sensitive volume of the detector. There are now available detectors of about 100 $cm^3$ sensitive volume with efficiencies of 10 - 12%.

Since the development of the first Ge(Li) detectors these devices have been used extensively for nuclear decay scheme studies. Measurements with Ge(Li) detectors have given evidence of the existence of many new transitions, even in nuclei carefully investigated previously. The construction of large volume ($>$10 $cm^3$) coaxial detectors has also permitted improved coincidence measurements, at first in conjunction with scintillation counters but later with other Ge(Li) detectors. True coincidence pulses, because of the reduced line width, are accumulated in a small energy interval and therefore have a high probability of being separated from random peaks.

Before the widespread use of Ge(Li) detectors, gamma-gamma directional correlation measurements were made with NaI(Tl) detectors. The poor resolution of these detectors makes the determination of multipole mixtures of gamma rays difficult because of interference from gamma rays which are not resolved from the gamma ray in question. However, the development of large volume Ge(Li) detectors combined with the use of pulse height analysers capable of dividing spectra into thousands of channels have allowed a dramatic advance in the angular correlation technique. By recording a whole spectrum of gamma rays in coincidence with a selected gamma at different angles it is possible to study the directional correlation of a number ofcascades simultaneously.

## CHAPTER 2 THEORETICAL CONSIDERATIONS

### 2.1 Emission of Electromagnetic Radiation

Excited states of nuclei generally decay to lower states with the emission of electromagnetic radiation, i.e. gamma rays. Other modes of decay, e.g. internal conversion, $\beta$-decay, may also occur, depending on the particular state.

Classically a source of electromagnetic radiation is represented in terms of an oscillating distribution of electric or magnetic charges which constitutes a multipole. This representation has been carried over into quantum mechanical formalism to describe nuclear moments and to classify radiative transitions in nuclei. The radiation modes are quantised and are represented in terms of spherical harmonics $Y_{LM}(\theta, \phi)$ of rank L. That is, radiation represented by the rank L has multipolarity $2^L$, e.g. if L=1 the radiation is of dipole character. As shown by Heitler (1936) L represents the total angular momentum, of absolute magnitude $\hbar\,[L(L+1)]^{\frac{1}{2}}$, carried by $2^L$ - pole gamma radiation with respect to the source of the radiation field. Each multipole order can have two classes of radiation: electric $2^L$ pole (EL) and magnetic $2^L$ pole (ML) depending upon the parity associated with the radiation.

Consider a gamma transition between two states of specified angular momenta $(I_i, I_f)$ and parities $(\pi_i, \pi_f)$. The conservation of angular momentum and parity for the system of nucleus plus gamma rays imposes the following selection rules on the possible multipolarities of the gamma transition.

$$|I_i - I_f| \leq L \leq I_i + I_f$$

$$\Delta\pi \equiv \pi_i / \pi_f = (-1)^L \text{ for EL radiation}$$

$$= (-1)^{L-1} \text{ for ML radiation}$$

where $\Delta\pi = +1$ denotes no parity change

$\Delta\pi = -1$ denotes parity change

The multipole emission probabilities, which contain a term $(R/\ \ )^{2L}$, decline rapidly with increasing L and there is a sharp cut-off to even those higher order multipoles allowed by the momentum selection rule. Thus in practice one encounters only the lowest multipolarities. Another feature of electromagnetic radiation is that the probability of electric multipole emission is somewhat higher than that of the corresponding magnetic multipole emission. A consequence of this is that one frequently encounters multipole mixtures of the type ML with E(L+1), e.g. M1 and E2.

## 2.2 Multipole Transition Probabilities.

Quantum mechanically, the transition probability per second $T_{i \to f}$ for any process is given by the equation

$$T_{i \to f} = \frac{2\pi}{\hbar} \left| \langle f | H' | i \rangle \right|^2 \frac{dN}{dE}$$

where $H'$ is the Hamiltonian representing the perturbing interaction, $\langle f | H' | i \rangle$ is the matrix element of the interaction taken between the wave functions of the initial and final states and dN/dE is the number of final states per unit energy interval.

Because of this dependency on the wave functions of the states involved, theoretical gamma transition probabilities are calculated on the basis of a specific model of the nucleus. Generally they are calculated for the single particle shell model which is a very oversimplified picture of the nucleus. However, transition probabilities for other more realistic nuclear models as well as those measured experimentally can be conveniently expressed in terms of the results obtained for the single particle model.

When the basic quantum theory of multipole radiation is applied to this single particle model (Moszkowski , 1965) we obtain the following expression for the transition probability for emission of a photon of energy $E_\gamma$, angular momentum L,M and of electric or magnetic type with the nucleus going from a state i to a state f :-

$$T_{i\to f}(\sigma LM) = \frac{8\pi(L+1)}{L[(2L+1)!!]^2} \frac{1}{\hbar} \left(\frac{E_\gamma}{\hbar c}\right)^{2L+1} \left| \langle f | \mathcal{M}^{\sigma}_{LM} | i \rangle \right|^2$$

where $\mathcal{M}^{E}_{LM}$ and $\mathcal{M}^{M}_{LM}$ are the electric and magnetic multipole operators. The transition probability depends on the detailed nuclear structure only through the matrix element in the expression above. Therefore it is convenient to express the transition probability in terms of the reduced transition probability B(EL), or B(ML), which is essentially the square of the matrix element above summed over m-substates of the final state f and averaged over m-substates of the initial state i. That is,

$$T(\sigma L) = \frac{8\pi(L+1)}{L\left[(2L+1)!!\right]^2} \quad \frac{1}{\hbar}\left(\frac{E_\gamma}{\hbar c}\right)^{2L+1} \quad B(\sigma L)$$

The reduced transition probabilities are defined generally by

$$B(\sigma L) = \sum_{m_f(M)} \left|\langle f \,|\mathcal{M}_{LM}|\, i\rangle\right|^2$$

$$= (2I_i+1)^{-1} \left|\langle I_f \| \mathcal{M}_L \| I_i\rangle\right|^2$$

where $\langle I_f \| \mathcal{M}_L \| I_i\rangle$ is a reduced matrix element defined by the Wigner - Eckart theorem.

The $B(\sigma L)$ values on the Weisskopf single particle estimates are given by

$$B(EL) = \frac{e^2}{4\pi}\left(\frac{3}{L+3}\right)^2 \quad R^{2L}$$

and $B(ML) \approx 10\,(h/M_p cR)^2 \;\; B(EL)$

## 2.3 Decay Schemes and Nuclear Models

### 2.3.1 General

Our knowledge concerning nuclear structure is derived mainly from studies of the decay of radioactive nuclei; nuclear reactions also of course contribute to this knowledge especially at higher excitation energies. The information gained from these studies is presented as decay schemes and energy level diagrams. Nuclear models have been proposed to describe and predict nuclear properties associated with nuclear structure. Such properties are the angular momentum (spin), parity and moments of the ground state, as well as those of the excited states, their lifetimes, transition probabilities, etc..

The development of nuclear models has proceeded along two principal lines, namely, the strong interaction models in which the nucleons are strongly coupled to each other because of their strong and short range interactions and the independent particle models in which the nucleons are assumed to move independently in a common nuclear potential. The nuclear shell model and its developments into the single-particle shell model, the individual particle (many particle) shell model, and the j-j coupling model are examples of the independent particle model. The liquid drop model is an example of the strong interaction model. These two different approaches are combined to produce the unified model in which nucleons move **nearly** independently in a common, slowly changing, non-spherical potential. Both excitations of individual nucleons and collective motions involving the nucleus as a whole are considered.

When only the collective motions involving the nucleus as a whole are considered we arrive at the collective model. When the number of nucleons in a nucleus differs appreciably from the closed-shell magic numbers of the nuclear shell model, the extra nucleons outside the closed shells are thought to produce deformation of the nucleus. This explains the very large quadrupole moments and other shape dependent effects observed in these nuclei. The nucleus, when it is deformed into an ellipsoidal shape, is assumed to undergo rotational or vibrational collective motions. Even-even nuclei nearer the closed shells exhibit characteristic vibrational spectra which can be explained by the quadrupole vibrations of the nucleus about a spherical equilibrium shape.

### 2.3.2 Excited levels of Even-Even Nuclei

In all known even-even nuclei the ground state has zero spin and even parity. The first excited states are with a few exceptions $2^+$. The exceptions are almost always closed shell nuclei. The excitation energies of the first excited states are found to show a smooth variation with nucleon number reaching maxima at closed shells and minima in between (Scharff-Goldhaber, 1953). Especially small values of the $2^+$ excitation energy occur at the rare earths and the actinides (Perlman and Asaro, 1954). The higher excited states of the even-even nuclei also show some systematic behavior.

The low-energy excitation spectra of even-even nuclei can be roughly divided into three classes (i) intrinsic (closed-shell region), (ii) vibrational, and (iii) rotational. The position of the energy levels of nuclei in the closed-shell class(i) region can accounted for by the direct coupling of the nucleons in the unfilled shells. For example, the excited levels of $^{60}Ni$ are thought to consist of closed shells of neutrons and protons (N=Z=28) plus four neutrons in the ($2p_{3/2}$, $1f_{5/2}$, $2p_{1/2}$) states (Auerbach, 1967; Cohen et.al, 1967; Plastino et.al, 1966). The observed enchancement of the E2 transitions evidently results from the polarisation of the core by the outer particles. This polarisation does not alter the level schemes significantly but it effectively increases the charge of each outer nucleon.

As we move further away from the magic numbers, the shell model approach becomes too complicated from a computational point of view. However, the excitation spectra acquire a simple form. For nuclei moderately far removed from closed shell configurations, the spectra are most simply described as collective vibrations about a spherical equilibrium shape (Scharff-Goldhaber and Weneser, 1955). The second excited states are predominantly $2^+$, occasionally $4^+$, $0^+$ and sometimes an odd spin with odd parity ($3^-$). The ratio of the energies of the second and first excited states is usually around 2.2. The basic vibrational model considers the collective features of nuclei in terms of harmonic surface vibrations. It predicts a one-phonon (quantum of vibrational energy) first excited state of $2^+$, a two phonon quadrupole vibrational triplet of $0^+$, $2^+$, $4^+$, at twice the energy of the first excited state, a one-phonon octupole vibrational state of character $3^-$ at about the same energy as the $0^+$, $2^+$, $4^+$ triplet, etc. (See Meyer, 1970, for a review of this simple vibrational model). However, to remove the degeneracy of the two-phonon triplet of levels and other discrepancies with experimentally observed properties (i.e. concerning transition probabilities, static quadrupole moments etc.) it is necessary to introduce anharmonic terms and interparticle coupling effects (Scharff - Goldhaber and Weneser, 1955; Wilets and Jean, 1956; Raz, 1959; Davydov and Fillipov, 1958).

For even-even nuclei very far from closed shells ($155 < A < 185$, $A > 225$) the low energy spectra show very striking regularities with respect to energy spacing which are close to being proportional to $I(I+1)$, (the spins $I$ follow a unique sequence $0^+$, $2^+$, $4^+$, ...) which suggests an analogy with the energy levels of a symmetric top

$$E_I = \frac{\hbar^2}{2\mathcal{J}} I(I+1)$$ where $\mathcal{J}$ is the moment of

inertia of the top. Most of these spectra can be very accurately described in terms of the rotational model. In this model the nuclear shape is considered to be fixed and non-spherical but axially symmetric, i.e. essentially spheroidal (Bohr, 1952). Many bands of rotational levels have been observed. Sometimes several bands are seen in the same nucleus; they are considered to arise from different intrinsic states of motion, rotation of each configuration giving rise to levels with the I(I+1) spacing.

### 2.3.3 Excited Levels of Odd-mass Nuclei

The single-particle shell model offers a reasonable description of many general nuclear properties for nuclei in which either one proton or one neutron is present outside otherwise closed proton and neutron shells, or in which just one nucleon is missing from a closed shells configuration. This is true also for nuclei with one extra or missing nucleon outside closed subshells. However this model is not sophisticated enough to yield a detailed quantitative account of more model-sensitive properties like electric quadrupole and magnetic dipole moments, transition matrix elements etc., for the majority of nuclei which have several nucleons outside closed shells or closed subshells. Some improvement can however be achieved with the introduction of additional coupling rules and other refinements.

For odd-mass nuclei with an appreciable number of extra or missing nucleons outside closed shells or subshells the unified model which combines features of the collective and independent particle aspects of nuclei is found to be quite successful. The idea of this unified model is to extend the independent particle model and consider a collective vibration in terms of independent particles in a vibrating field. An odd-mass nucleus can be considered to consist of a single nucleon in a spin state $j$ coupled to an even-even core which can undergo collective vibrational motion. If the coupling is weak, i.e. there is little or no interaction between the particle and the core, the vibrational spectrum of the core persists and the electromagnetic transitions in the odd-mass nucleus are related to the corresponding transitions in the core purely by geometric factors. These results are independent of whether the core is vibrational or not. This weak coupling scheme is known as the core excitation model (Lawson and Uretsky, 1957; De-Shalit, 1961).

When the nucleus acquires a large permanent deformation (i.e. in the rotational region) the strong coupling limit of the unified model is employed in which one considers the relatively fast motion of the odd particle in a deformed field and subsequently the slower rotations of the entire system. The intrinsic structure of a deformed nucleus is considered to arise from the coupling of the extra-core particle to the core derived from the aligned wave functions of a nearby even-even nucleus. Use is made of the Nilsson model (1955) which calculates the single particle orbitals in a deformed shell-model potential.

In the transitional region between the spherical and deformed nuclei a similar approach in the unified model with intermediate coupling is employed (Bohr, 1952; Bohr and Mottleson, 1953). All but one of the nucleons are lumped together to form a core that is described in terms of collective coordinates. A coupling is introduced between the quadrupole vibrations of the core and the shell model states of the extra nucleon (Choudhury, 1954). In such calculations the phonon energy of the core vibrations, the strength of coupling between single particle motion and core vibrations, and the energy spacing between the single particle states are varied to reproduce the experimentally measured energy levels and spins.

The total Hamiltonian for the system of doubly even core plus an extra nucleon (proton in this case) is taken to be of the following form

$$H = H_{coll} + H_{s.p.} + H_{int} ,$$

where $H_{coll}$, $H_{s.p.}$ and $H_{int}$, are the Hamiltonian associated respectively with the harmonic quadrupole vibrations of the core, the motion of the odd nucleon in an effective average potential and the surface - particle interaction.

$H_{int}$ is given by

$$H_{int} = -(\pi/5)^{\frac{1}{2}} \xi \hbar\omega \sum_{\mu} (b_{\mu} + (-1)^{\mu} b^{+}_{-\mu}) Y_{2\mu}(\theta,\phi)$$

where $\hbar\omega$ is the phonon excitation energy of the doubly even core, $b_{\mu}$ and $b^{+}_{\mu}$ the annihilation and creation operators for phonons of spin 2 with z-component $\mu$ and $Y_{2\mu}$ a normalised spherical harmonic of the angular momentum coordinates of the particle. The dimensionless coupling parameter is defined by

$$\xi = k(5/2\pi\hbar\omega C)^{\frac{1}{2}}$$

where C is the nuclear surface deformation parameter and the coupling constant $k = \langle k(r) \rangle$ is a radial average.

The wave functions for the coupled system are expanded in the basis

$|j,NR;IM\rangle \equiv \sum_{m_j,M_R} \langle jm_j RM_R | IM\rangle |jm_j\rangle |NRM_R\rangle$ where the N-phonon state of the core with total angular momentum R and projection $M_R$ along the z-axis is coupled with the single particle state $|jm_j\rangle$ to give a total angular momentum I and projection M along the z-axis.

The eigenfunctions for the odd-proton nuclei at an energy $E^{(\alpha)}$ are constructed from the basis eigen vectors. The Schroedinger equation will then contain matrix elements which are functions of the parameters $\hbar\omega$, $\xi$ and $\Delta$. The solution is sought with the requirement that the eigenvalues $E^{(\alpha)}$ be a best fit to the experimental spectra and this is done by an iterative least squares procedure.

The energy levels of $^{147}$Pm have been calculated with this method by Choudhury and O'Dwyer (1967) and also by Heyde and Brussaard (1967). Their results are shown in Fig. 7.9 (See Chapter 7 section 6 ) together with the decay scheme resulting from the measurements of this work.

## 2.4 Directional Correlations of Gamma-gamma Cascades

The observation of the directional correlation of two successively emitted gamma radiations gives direct information of the angular momenta (spins) of the states involved and of the multipole character of the emitted radiation.

Take the case of a gamma-gamma cascade in which a nucleus decays from an initial level with spin $I_1$ through an intermediate level with spin $I_2$ to a final level with spin $I_3$ (See Fig. 2.1a). We assume that the intermediate state $I_2$ is sufficiently short lived so that it is not influenced by extra-nuclear fields. The directional correlation function $W(\underline{k}_1, \underline{k}_2)$ is defined as the probability that a nucleus decaying through the cascade $I_1 \rightarrow I_2 \rightarrow I_3$ emits the two radiations $\gamma_1$ and $\gamma_2$ in the directions $\underline{k}_1$ and $\underline{k}_2$ into the solid angles $d\Omega_1$ and $d\Omega_2$. The theoretical expression for

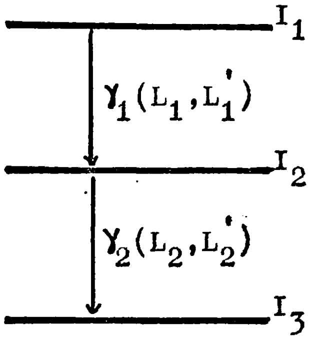


(a)

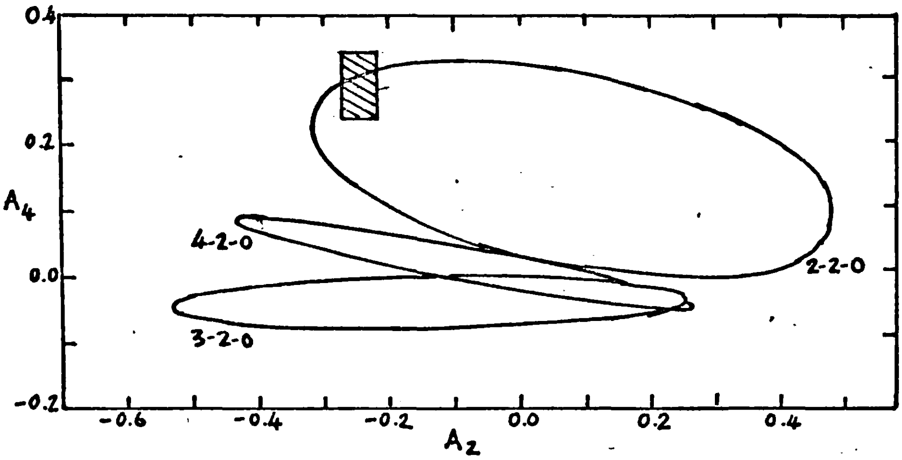


(b) Parametric plot of $A_2(\delta)$ vs $A_4(\delta)$

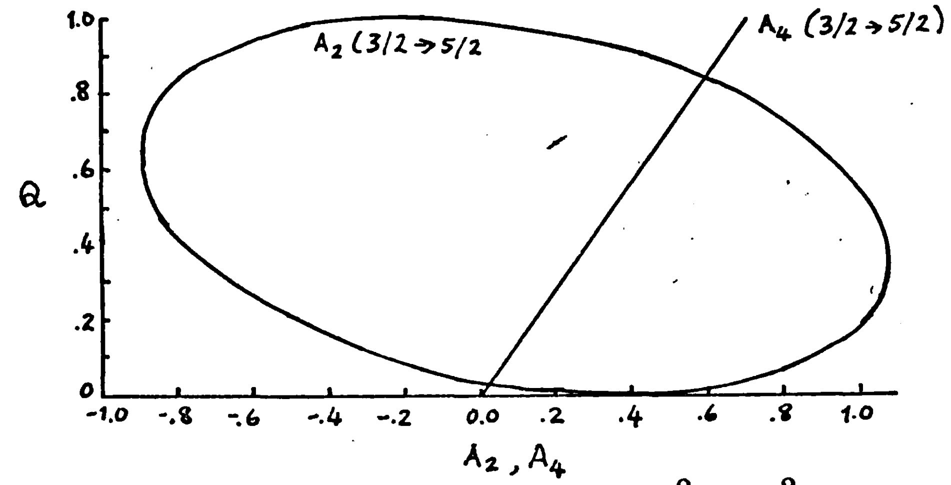


(c) Plots of $A_2$, $A_4$ vs $Q = \delta^2/(1+\delta^2)$

Fig.2.1 (a) a gamma-gamma cascade, (b) and (c) graphical methods of analysis of directional correlation data the correlation $W(\underline{k}_1, \underline{k}_2)$, or $W(\theta)$ where $\theta$ is the angle between the two directions $\underline{k}_1$ and $\underline{k}_2$, has been worked out for most cases of interest.

Generally, this is done by using first order perturbation theory and Fano's concept of the statistical or density matrix and then using Racah algebra to simplify and obtain the final result. Excellent reviews of the theory of gamma-gamma directional correlations have been given by Devons and Goldfarb (1957), Biedenharn (1960), Frauenfelder and Steffen (1965), and Steffen (1970). The last named review (Steffen, 1970) stresses symmetry considerations in the general theory of angular correlation phenomena.

For a two component cascade, the directional correlation function $W(\theta)$ can be shown to have the form

$$W(\theta) = \sum_{k\text{-even}} A_k(\gamma_1)\, A_k(\gamma_2)\, P_k(\cos\theta),$$

where $k = 0,2,4,\ldots$, $\theta$ is the angle between the propagation vectors of the two gamma-rays, and the $P_k\,(\cos\theta)$ are the normalised Legendre polynomials.

If each transition is a mixture of not more than two multipoles, the maximum value of k is the smallest of $2L_1'$, $2L_2'$ and $2I_2$. The constant $A_k(\gamma_1)$ is determined only by the parameters of the first transition, i.e., by $I_1$, $I_2$ and $L_1$, $L_1'$. Similarly $A_k\,(\gamma_2)$ depends on the parameters of the second transition only. Usually the normalisation

$A_0(\gamma_1) = A_0(\gamma_2) = 1$ is employed, and the highest value of k is usually 4 so that

$$W(\theta) = 1 + \sum_{k=2,4} A_k(\gamma_1) A_k(\gamma_2)\, P_k(\cos\theta)$$

The coefficients $A_k(\theta)$ are related to the spins and multipole mixing ratios as follows

$$A_k(\gamma_1) = \frac{1}{1+\delta_1^2}\Big[ F_k(L_1L_1I_1I_2) + (-1)^{L_1-L_1'}\, 2\delta_1 F_k(L_1L_1'I_1I_2) + \delta_1^2\, F_k(L_1'\, L_1'\, I_1\, I_2)\Big]$$

and

$$A_k(\gamma_2) = \frac{1}{1+\delta_2^2}\Big[ F_k(L_2L_2I_3I_2 + 2\delta_2 F_k(L_2L_2'\, I_3I_2) + \delta_2{}^2\, F_k(L_2'L_2'I_3I_2)\Big]$$

where $L_1' = L_1 + 1$ and $L_2' = L_2 + 1$

The F - coefficients can be calculated explicitly from theory and have been tabulated (Ferentz and Rosenzweig, 1955). The mixing ratio $\delta_1$ of the first transition is defined by

$$\delta_1 = \frac{\langle I_2 \| L_1'\pi_1' \| I_1\rangle}{\langle I_2 \| L_1\pi_1 \| I_1\rangle} = \frac{\langle I_2 \| L_1+1, \pi_1' \| I_1\rangle}{\langle I_2 \| L_1\, \pi_1 \| I_1\rangle}$$

That is, $\delta$ is the ratio of the reduced emission matrix elements (Becker and Steffen, 1969) for the particular multipole transitions concerned. The ratio of the intensities of the

$L_1 + 1$ and $L_1$ components is given by $\delta_1^{\,2}$.

The mixing ratio $\delta_2$ for the second transition may be defined in a similar way.

## 2.5. Analysis of Gamma-Gamma Directional Correlation Data

### 2.5.1 Least Squares Method

The directional correlation function is represented by

$$W(\theta) = A_0 + A_{22} P_2(\cos\theta) + A_{44} P_4 (\cos\theta)$$

Experimentally, the directional correlation of the gamma-gamma cascade is measured at a number of angles $\theta_i$. If the measured value of the correlation at angle $\theta_i$ is represented by $V(\theta_i)$, then a least squares procedure is used to obtain the best values of $A_0$, $A_{22}$, and $A_{44}$ by requiring that

$$\Delta = \sum_i (W(\theta_i) - V(\theta_i))^2 \text{ is a minimum.}$$

This leads to the equation

$$\partial\Delta/\partial A_k = 0 \qquad \text{where } A_k \text{ represents } A_0,\ A_{22} \text{ and } A_{44}$$

These are the normal equations of the least squares method and are linear in the unknowns. The least squares method is very conveniently expressed in terms of matrix notation. The directional correlation function may be represented very concisely by

$$W = PA$$

where $W$ is a column matrix having elements $W(\theta_i)$, $P$ is a rectangular matrix with elements $P_k\,(\cos\theta_i)$, $i$ labelling the rows and $k$ the columns. Finally $A$ is a column matrix with elements $A_0$, $A_{22}$, and $A_{44}$.

It may be shown that (See Ferguson, 1965) in matrix notation the normal equations are given by

$$\tilde{P}\,P\,A = \tilde{P}\,V$$

where the sign $\sim$ signifies transposition. All the parameters of these equations are known excepting the elements of $A$. Their solution gives the least squares fitted $A_k$'s which correspond to the minimum of $\Delta$.

The solution can be written formally

$$A = (\tilde{P}\,P)^{-1}\,\tilde{P}\,V = N^{-1}\,\tilde{P}\,V$$

where $N = \tilde{P}\,P$ is the normal matrix.

The above consideration assumes that all measurements at the different angles $\theta_i$ are equally accurate. Instead, if each measurement is given a weight $w_i$, the solution can be written

$$A = (\tilde{P}wP)^{-1}\,\tilde{P}wV$$

with $N = \tilde{P}wP$ where $w$ is a diagonal matrix whose diagonal elements are the weights, $w_i$.

The theoretical fitted values to the measured points are given by $W = PA$ with $A$ determined as outlined above.

The actual directional correlation coefficients are given by $A_2 = A_{22}/A_0$ and $A_4 = A_{44}/A_0$. They have to be corrected for finite solid angle effects later discussed in Chapter 4.

### 2.5.2 Errors of the Directional Correlation Coefficients

The standard deviation $\sigma_k$ of the fitted parameter $A_k$ is given by (Ferguson, 1965)

$\sigma_k^2 = \sigma_m^2 N_{kk}^{-1}$ where $N_{kk}^{-1}$ represent the diagonal elements of the inverse normal matrix $N^{-1}$, and $\sigma_m$ is the error of the measurements. $\sigma_m$ is obtained after the least squares fitting of the data, from the relation

$$\sigma_m^2 = \left[\sum_i (W(\theta_i) - V(\theta_i))^2\right]/(n-m)$$ where $m$ is the number of parameters calculated and $n$ the number of measured points.

Because the directional correlation coefficients are obtained as ratios of two parameters resulting from the fitting procedure, it is necessary to consider the correlation of the fitted parameters. A coefficient of correlation between two parameters is given by

$\rho_{kk'} = N_{kk'}^{-1} / \sigma_k \sigma_k'$ where $N_{kk'}$ are the off-diagonal elements of the inverse normal matrix.

If $S_2$ and $S_4$ are the standard deviations of the directional correlation coefficients $A_2$ and $A_4$

$$(S_2/A_2)^2 = (\sigma_2/A_{22})^2+(\sigma_0/A_0)^2 - 2\rho_{02}\ \sigma_0\sigma_2/A_0A_{22}$$

$$(S_4/A_4)^2 = (\sigma_4/A_{44})^2 + (\sigma_0/A_0)^2 - 2\rho_{04}\sigma_0\sigma_4 / A_0A_{44}$$

Measurements of the directional correlations reported in this work have been done at seven angles and the corresponding inverse normal matrix has been calculated and is shown in Table 2.1.

TABLE 2.1

Elements of the inverse normal matrix for measurements of unit weight at 7 angles

| k' | k=0 | 2 | 4 |
|---|---|---|---|
| 0 | 0.1820 | -0.0697 | -0.0993 |
| 2 | -0.0697 | 0.5949 | -0.3612 |
| 4 | -0.0993 | -0.3612 | 0.8669 |

Coefficients of correlation between the parameters $A_0$, $A_{22}$, and $A_{44}$ as obtained from the off-diagonal elements of the inverse normal matrix are

$$\rho_{02} = -0.2113;\ \rho_{04} = -.2499, \text{ and } \rho_{24} = -0.5032$$

## 2.5.3 Graphical Methods of Analysis

The values of $A_2$ and $A_4$ evaluated from the least squares fit to experimental data then can be compared to the theoretical values of $A_2$ and $A_4$ calculated for various spin sequences. The actual spin sequence can in many cases be identified uniquely and thereby a definitive or probable spin assignment to particular nuclear levels can be made. In most cases the comparison of the measured and theoretical values of the correlation coefficients can establish the multipole mixing ratios of the gamma transitions involved in the measured cascades.

Two of the most successful techniques for graphically accomplishing the comparisons discussed above are those of Coleman (1958) and Arns and Weidenbeck (1958). In the former method theoretically calculated values of $A_4$ are plotted against corresponding values of $A_2$ using $\delta_i$ (i =1 or 2) as a parameter. When this is done for different spin sequences, a family of ellipses results. The experimental values of $A_2$ and $A_4$ with their respective errors define a rectangular area in the $A_2$-$A_4$ plane. The proximity of this rectangle to a particular ellipse indicates the correct of most probable spin sequence and also a value of $\delta$. (See Fig. 2.1b). This method is particularly useful when only one transition of the cascade is of mixed multipolarity. In such cases theoretical values of $A_2$ and $A_4$ tabulated by Taylor et.al (1971) may be used.

In the method devised by Arns and Weidenbeck (1958) $A_2$ and $A_4$ are plotted against $\delta^2/1+\delta^2$ for various spin sequences and the experimental points compared to the theoretical values. The $A_2(\delta)$ curve is an ellipse whereas the $A_4(\delta)$ curve is a straight line, (See Fig 2.c). This method is very useful for analysing cascades in which both transitions are of mixed multipolarity. It is used in the analysis of the directional correlation of the gamma transitions in $^{147}$Pm and is presented in greater detail in Chapter 7.

## CHAPTER 3 INSTRUMENTATION

### 3.1 The Ge(Li) Detector

The detector used in measuring the gamma ray spectra reported in this thesis was an end drifted coaxial Ge(Li) crystal (Fig. 3.1). The sensitive volume of the detector is 40 $cm^3$ with a resolution of 3.5 keV for the 1332 keV gamma ray of $^{60}Co$. It has a photopeak efficiency of about 4% that of a 3" x 3" NaI(Tl) crystal at this energy; and the peak-to-Compton ratio is 16:1.

The detector is coupled to a charge-sensitive preamplifier NE 5287 A with a cooled FET stage. The preamplifier output is shaped and amplified by an ORTEC 485 amplifier with pole zero cancellation. The pulses are then fed into a multichannel analyser, Northern Scientific NS-606, which has a conversion gain of up to 2048 channels and a 512 channel memory. The analyser output is recorded by pen and on paper tape. The data on paper tape is later transferred onto punched cards at the University of London Computer Centre.

### 3.2 Computer Analysis of the Ge(Li) Spectra

The computer program called SAMPO divised by Routti and Prussin (1969) is used to analyse the gamma ray spectra. In this program a mathematical representation of the photopeak shapes and of the continuum under the photopeaks are determined directly from

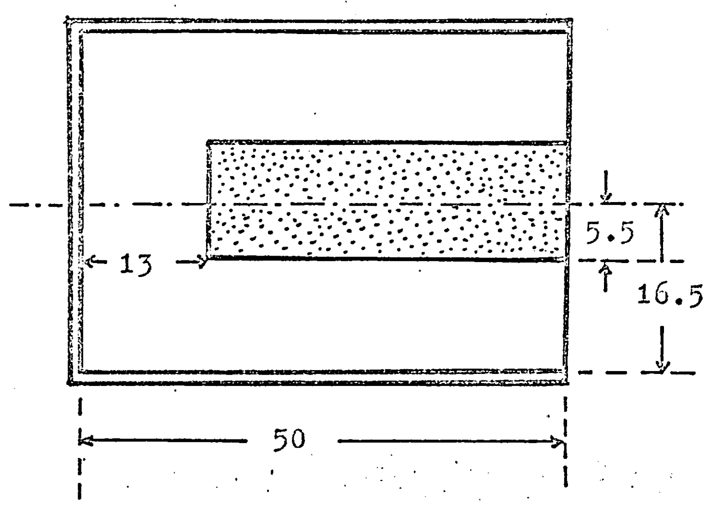


Fig. 3.1 End-drifted coaxial Ge(Li) detector of 40 cc sensitive volume. All dimensions are shown in mm.

well defined peaks in the measured spectrum. Data in the region of single peaks or multiple peaks are then fitted with the mathematical functions using the parameters obtained. The line shape (Gaussian with exponential tailings) calculations and fittings are performed using least squares procedures. An algorithm is also developed which enables an automatic search to be made for statistically significant peaks in the raw data. In addition to line shape calibrations the computer code also performs energy and efficiency calibrations, calculates relative intensities of the gamma peaks obtained, and provides complete statistical and calibration-error estimates. For establishing the goodness of fit for each peak the output also includes numerical and graphical representations of the fit.

## 3.3 Energy calibration of the Ge(Li) detector

Energy calibrations were done using standard sources of $^{60}Co$, $^{137}Cs$, $^{22}Na$, $^{152}Eu$ etc. In a preliminary search for peaks a linear interpolation between the calibration points was used. For a final accurate determination of the energies a polynomial least squares fit was made to the calibration points by minimising the expression

$$\chi^2 = \sum_{i=1}^{n} \frac{1}{D_i} \left[ E_i - \sum_{j=1}^{m} P_j C_i^{j-1} \right]^2$$

with respect to $p_j$, where

$P_j$ are the constants defining the calibration curve,

$C_i$ are the channel numbers,

$E_i$ are corresponding energies, and

$D_i$ the calibration uncertainties.

A calibration curve is shown in Fig 3.2

## 3.4 Relative Efficiency Calibration

To determine the relative intensities of the gamma rays it is necessary to know the relative efficiency of the detector at different energies. This was done by taking spectra of $^{226}Ra$ and $^{152}Eu$ sources which have lines with well known intensities. These nuclides provide the calibration points which are then fitted to the relative efficiency curve which is represented by

$$F = p_1 \left[ E^{p2} + p_3 \exp(p_4 E) \right]$$

where F is the efficiency

$p_1$, $p_2$, $p_3$, $p_4$ are constants determined in the fitting, and

E is the gamma energy in keV.

The relative efficiency curves for the 40 $cm^3$ Ge(Li) detector are shown in Fig. 3.3.

## 3.5 The Scintillation Counter

For the directional correlation studies a scintillation detector was used in conjunction with the Ge(Li) detector in a fast-slow coincidence arrangement.

The scintillation detector consisted of a cylindrical NaI(Tl) crystal, 1.5 inches diameter, 1 inch length, optically

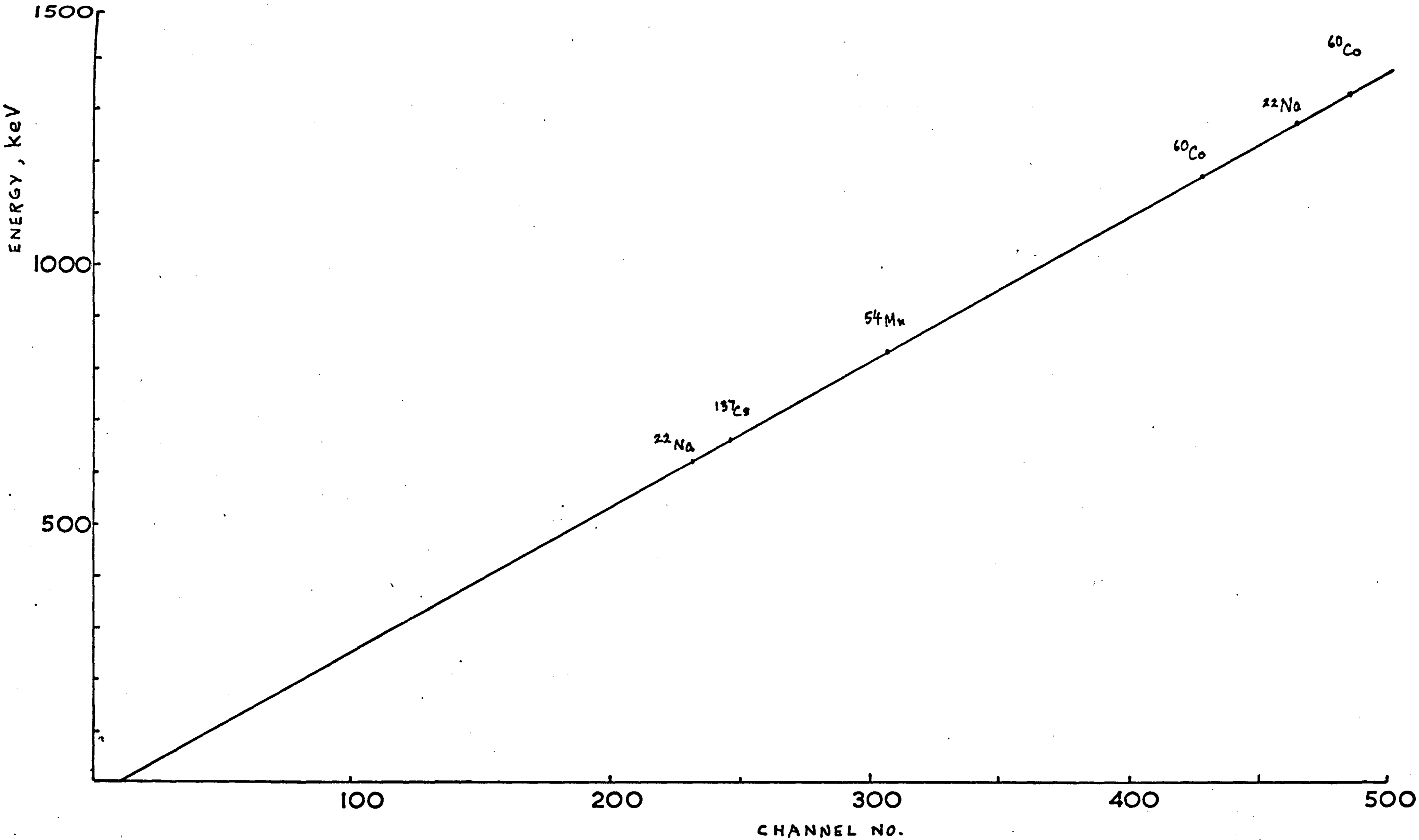


FIG. 3.2 ENERGY CALIBRATION CURVE FOR THE GE-LI DETECTOR

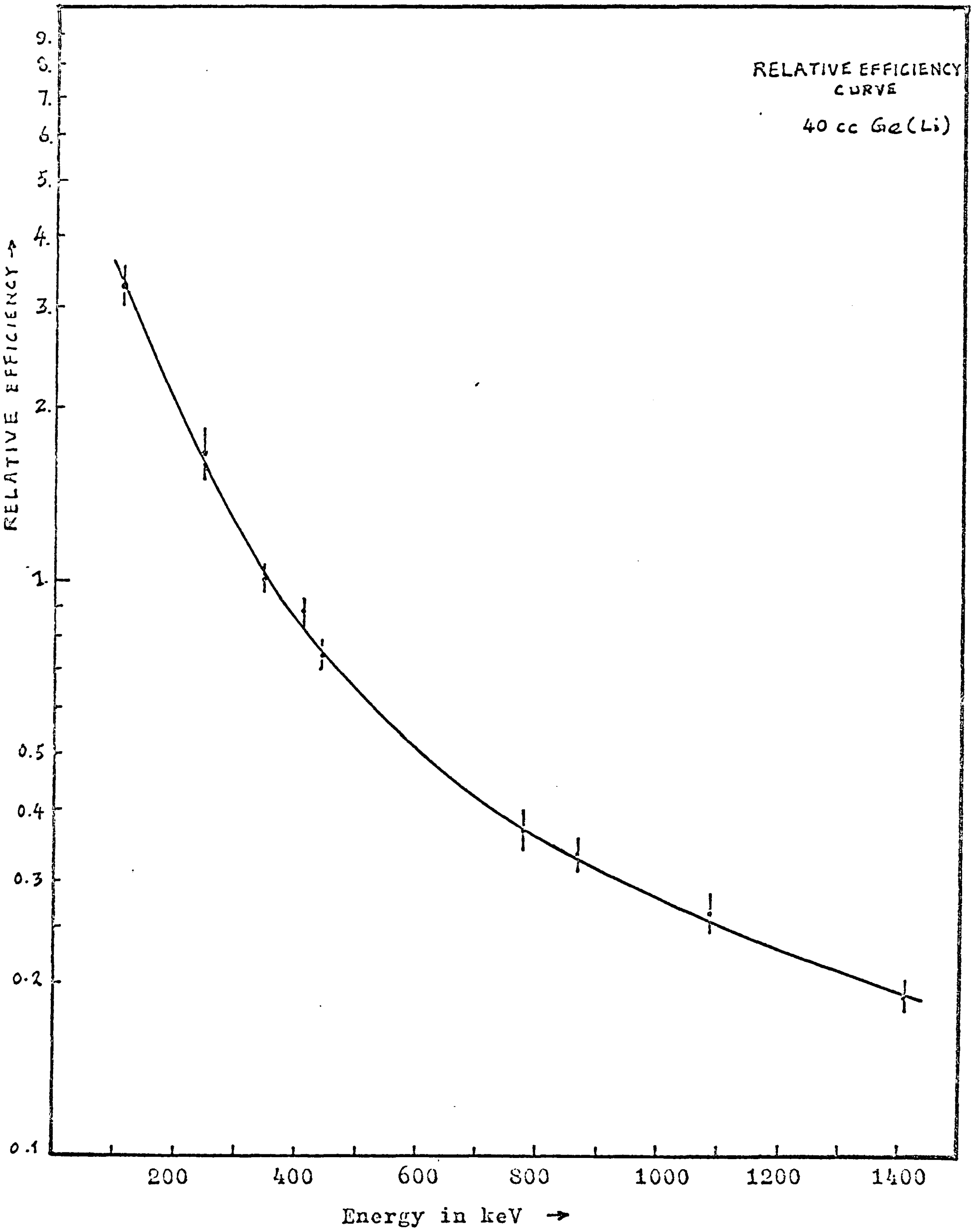


Fig. 3.3 Relative Efficiency Curve for the 40cc Ge(Li) Detector

coupled to a fast EMI 9594B fourteen stage photomultiplier tube. It was operated at an overall voltage of 2000 V. This applied EHT was constantly monitered by means of a digital voltmeter. A standard non-linear dynode chain was constructed as shown in Fig. 3.4. The cathode-to-first dynode voltage was kept constant at 300 Volts by means of two 1S 4150A zener diodes. The deflector - D1 voltage and the focus - D1 voltage were adjusted for optimum electron collection and maximum gain. They were kept fixed at 14 volts and 46 volts respectively.

A linear signal for energy selection was taken from the 8th dynode and a fast timing signal was taken from the anode.

The energy calibration for the scintillation detector was also done with sources of $^{60}$Co, $^{137}$Cs, $^{22}$Na, etc. Efficiency calibrations were not required as the NaI counter was used only to select the gating pulses.

## 3.6 The Fast-Slow Electronics

A block diagram of the fast-slow electronics is shown in Fig. 3.5. The specific units used are listed in Table 3.1. Signals from the Ge(Li) detector are allowed to register in the multi-channel analyser only if a coincident gamma ray of selected energy has been detected in the NaI(Tl) counter. The central line assesses all pulses from the two detectors to decide whether any two overlap in time. In the event of a time overlap, a pulse emerges from the fast coincidence unit. The slow coincidence unit then determines

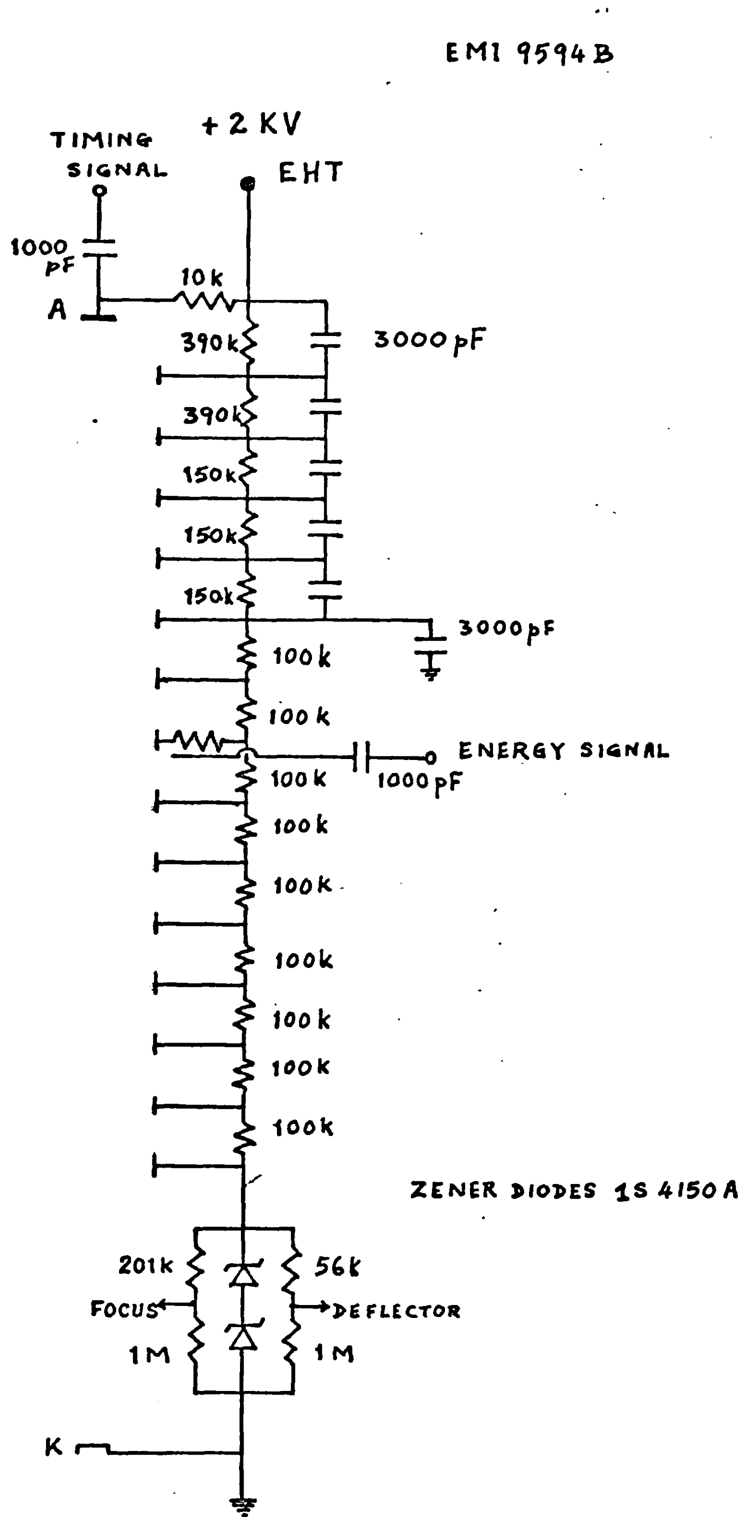


Fig. 3.4 Photomultiplier dynode chain circuit for the scintillation counter

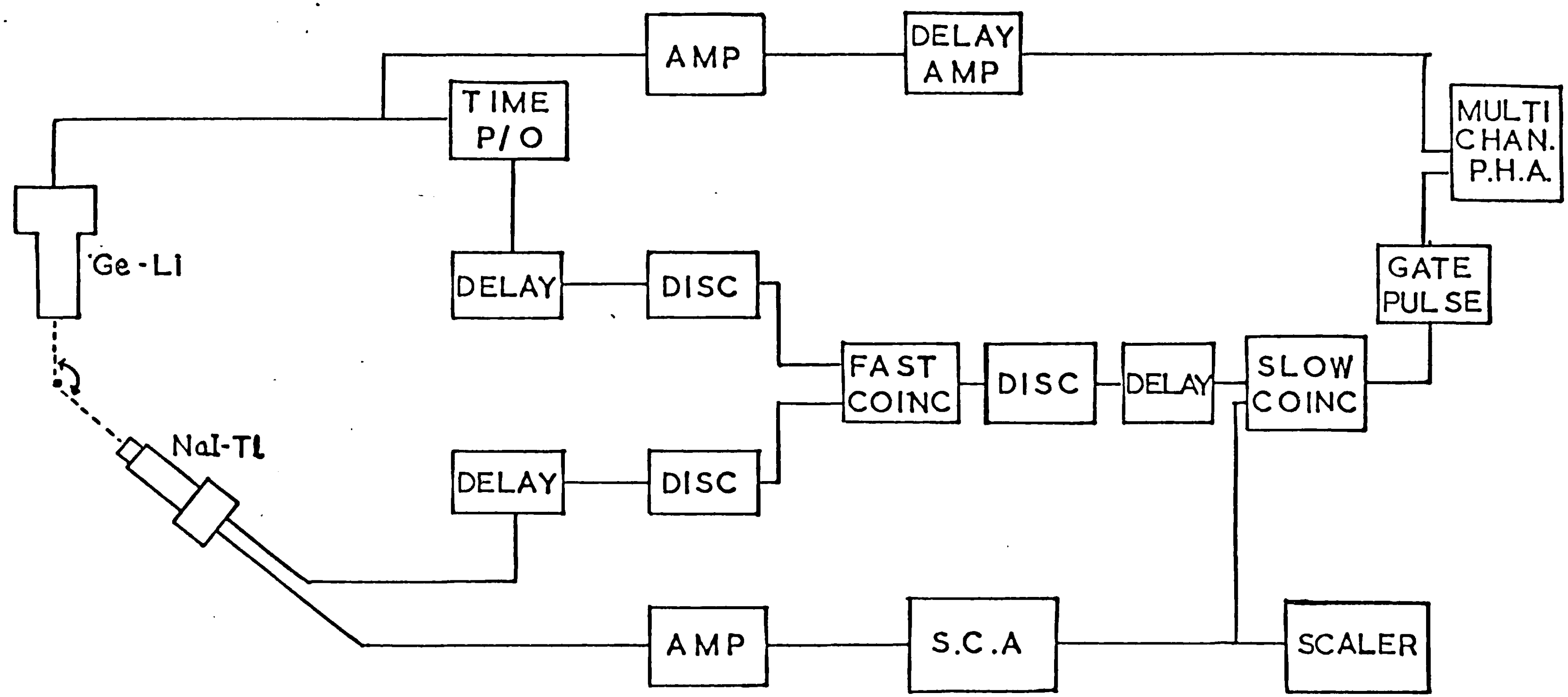


FIG. 3.5 THE FAST-SLOW ELECTRONICS SYSTEM

## TABLE 3.1 LIST OF ELECTRONICS

| | Germanium detector channel | Scintillation counter channel |
|---|---|---|
| Detector | Ge(Li) end-drifted coaxial 35mm dia., 50mm length, 12mm radial depletion depth, 13mm axial depletion depth | NaI(Tl) $1\frac{1}{2}$" diameter, 1" length |
| | | EMI 9594B photomultiplier |
| Preamplifier | NE5287A charge sensitive preamp | |
| | ORTEC 260 Time Pickoff | |
| Main amplifier | ORTEC 485 | ORTEC 485 |
| | ORTEC 427 Delay amplifier | J&P NM162 single channel analyser |
| | | J&P NM355 scaler |
| | J&P NM 622 Dual Discriminator | |
| | J&P NM 610 Fast Coincidence | |
| | J&P NM 210 Delay Coincidence | Gate Pulse Generator Type ZIN |
| Analyser | Northern Scientific NS 606, 2048 ADC, 512 channel memory | |

whether one of the pulses corresponded with a selected gamma ray as indicated by a pulse from the separate line from the NaI(Tl) detector. An output pulse from the slow coincidence system opens the gate of the multichannel analyser and permits any pulse from the Ge(Li) detector to be recorded. In this way a 512 channel spectrum results which indicates all the lines in coincidence with the selected gamma ray.

The time resolution of the coincidence system was 40 nanoseconds. A delay curve is shown in Fig. 3.6. An important part is the necessity to ensure that the gating pulse arrives at the analyser at the appropriate moment (0.7 μsecs early) and keeps the gate open long enough for the energy signal to be analysed. A gate pulse generator constructed from an integrated circuit module was used (Fig. 3.7). A linear delay amplifier, ORTEC 427, had to be inserted in the path of the signal from the germanium detector.

## 3.7 Physical Arrangement for the Directional Correlation Measurement

The physical arrangement of the counters for the directional correlation measurements is shown in Fig. 3.8. The Ge(Li) detector was stationary and the NaI (Tl) counter rotated on a radial arm about a cylindrical source placed at the axis. The experiment then consists of taking the coincident spectra at angles of 90°, 105°, 120°, 135°, 150°, 165°, 180°, etc.

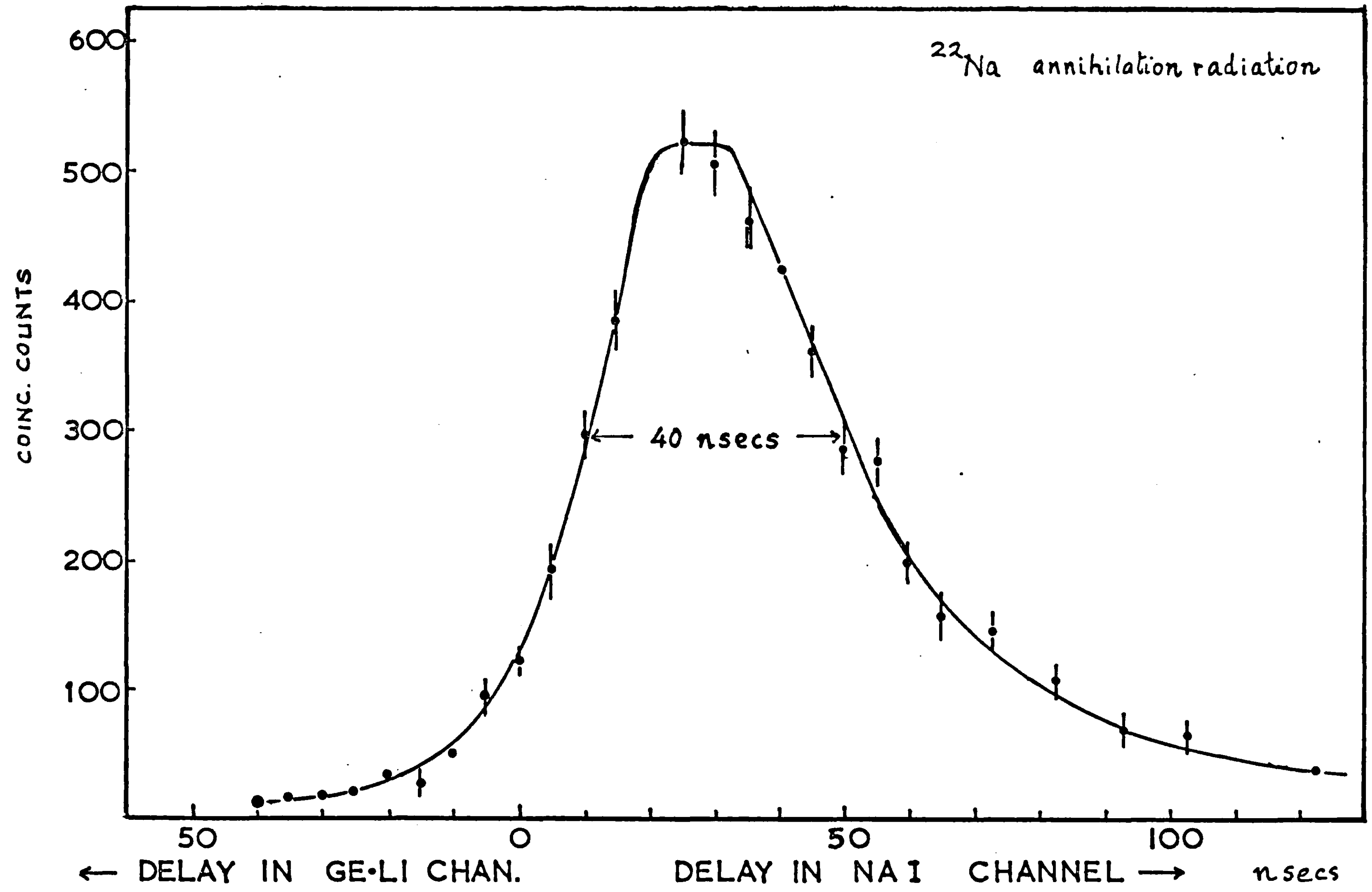


FIG. 3.6 THE DELAY CURVE

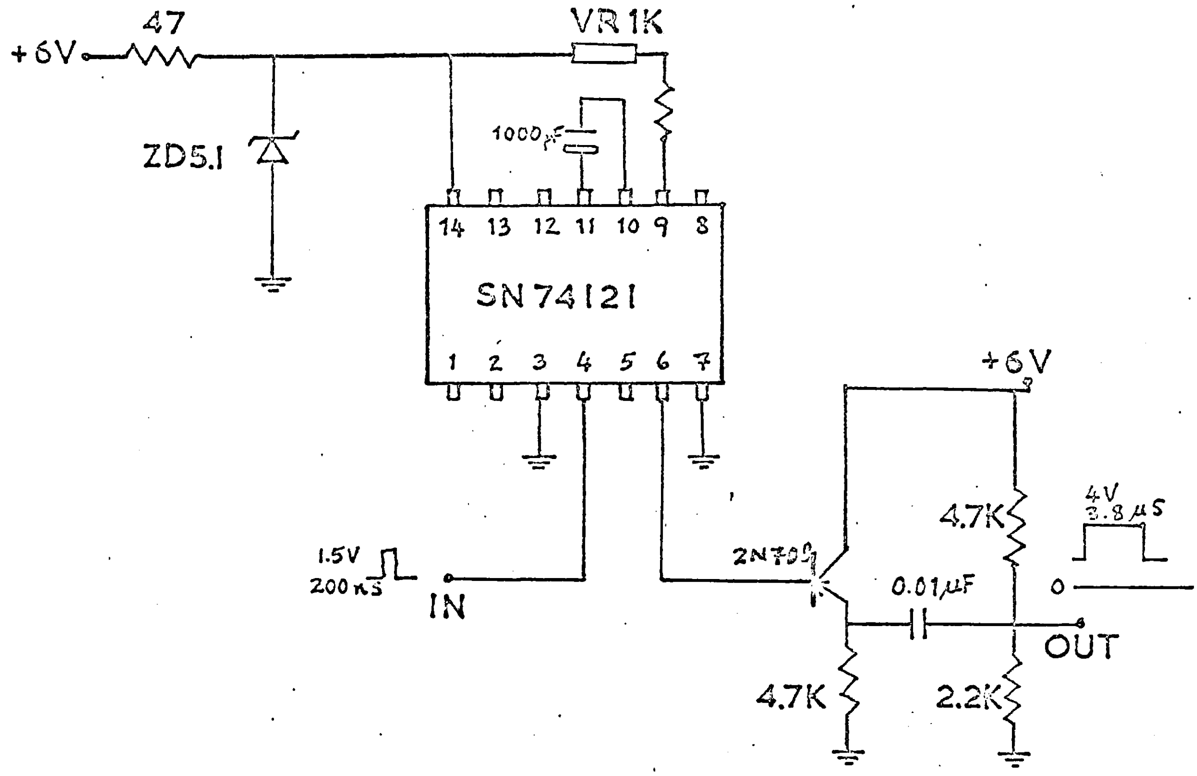


Fig. 3.7 GATE PULSE GENERATOR WITH IC MODULE SN74121

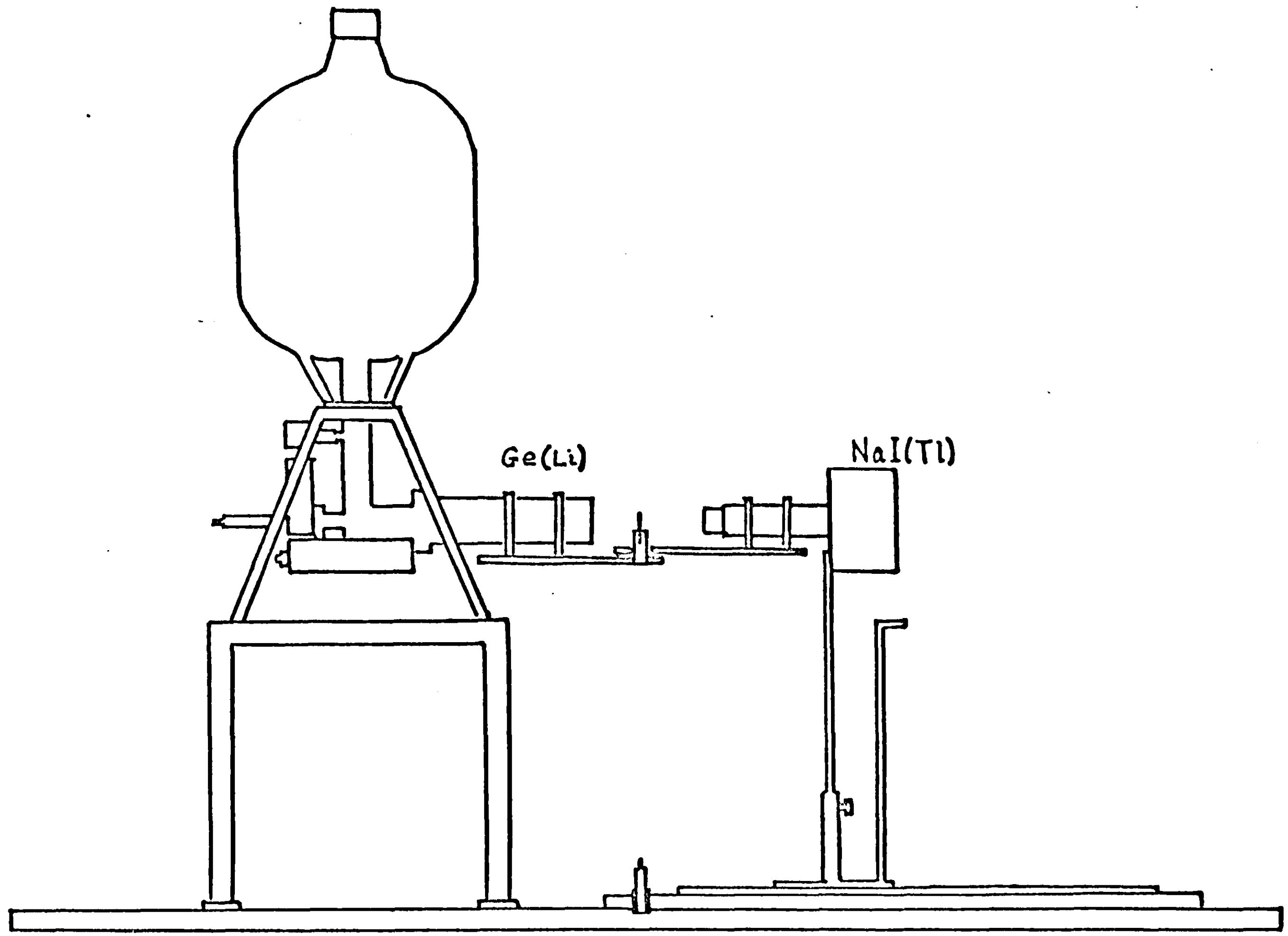


FIG. 3.8 (a) PHYSICAL ARRANGEMENT OF THE DETECTORS FOR DIRECTIONAL CORRELATION MEASUREMENTS

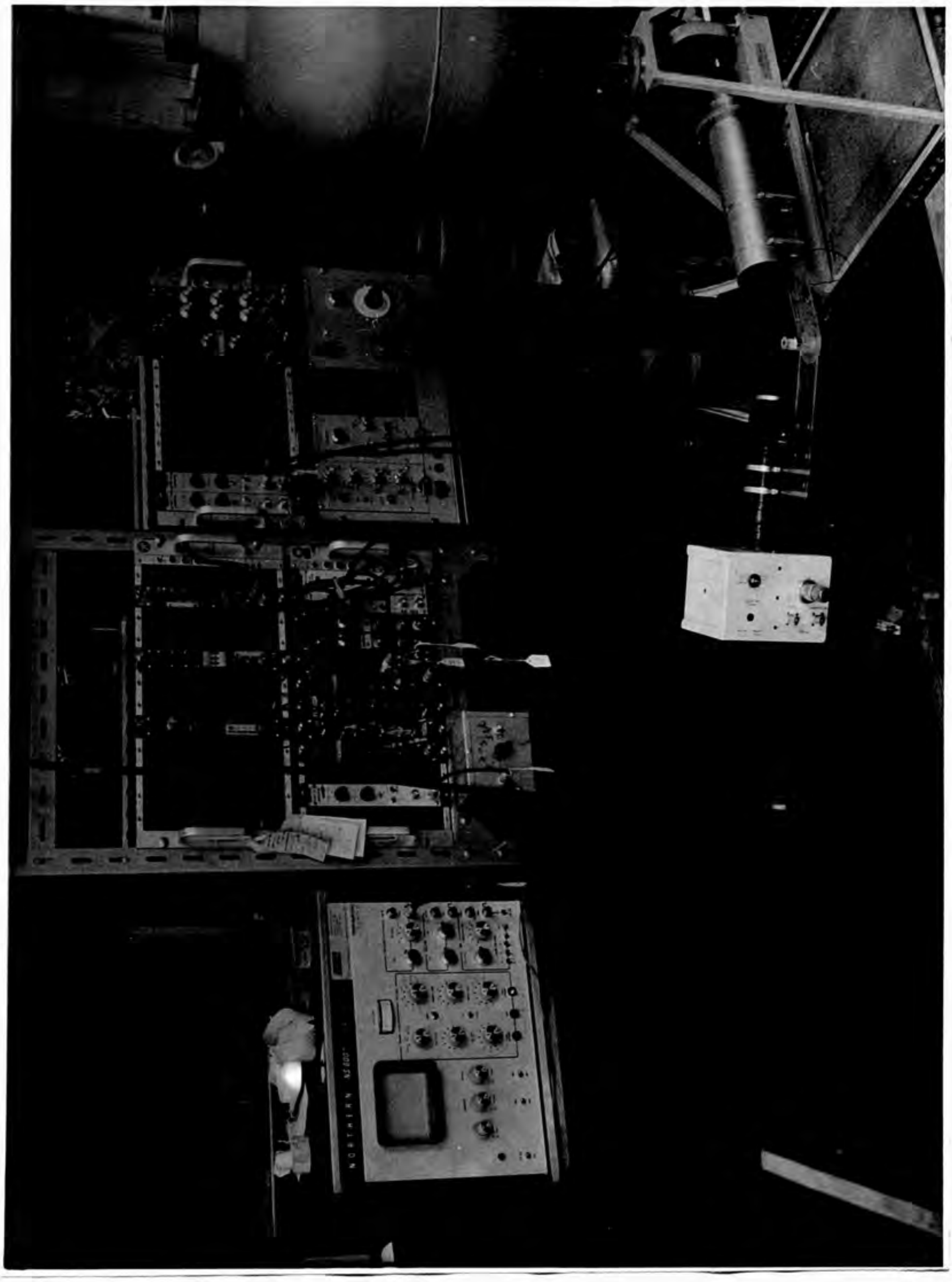

Fig. 3.8 (b) The electronics and detectors arranged for directional correlation measurements

A precaution had to be taken to correct for the effects of the strong field associated with the magnet on the Ge(Li) vacuum ion pump. It was found that the position of the gamma ray peaks from the scintillation counter varied by up to 2% according to the angular position. A C-magnet was placed under the preamplifier attached to the detector with the aim of cancelling the effect of the C-magnet on the ion pump. This was not found to be effective. Pieces of half-inch thick mild steel were used to shield the magnet on the ion pump from the scintillation counter. Although this reduced the effect on the scintillation counter it was also not found to be sufficiently effective. A mu-metal shield was next tried.This was also not effective. Finally, the correction was done by switching in a suitable resistive potential divider between the amplifier and the single channel analyser in the NaI(Tl) line for each angular position.

## CHAPTER 4 FINITE SOLID ANGLE CORRECTION FACTORS FOR THE GE(LI) DETECTOR

### 4.1 Introduction

The development of large volume lithium-drifted germanium detectors has prompted their use in gamma-gamma directional correlation experiments. Usually a Ge(Li) detector is employed in conjunction with a NaI(Tl) scintillation counter (see Fig. 3.5 and Fig. 3.8, Chapter 3), but in a few cases two Ge(Li) detectors have been used together. In these experiments a problem arises because the finite (and considerable) size of the detectors tends to smear the angular correlation. Corrections must be made for this effect.

If from a small source, excited nuclei emit two gamma rays, $\gamma_1$ and $\gamma_2$, in quick succession, the experimenter seeks the relative probability $W(\theta)\,d\Omega$ that $\gamma_2$ is emitted in the solid angle $d\Omega$ at an angle $\theta$ with respect to the direction of the first $\gamma_1$. The theoretical expression for $W(\theta)$ has been derived for most cases of interest. However, in practice it is the $\gamma_{1\ 2}$ coincidence counting rate $C(\phi)$ that is measured, and this is a function of the angle $\phi$ subtended by the axes of the two counters at the source (Fig. 4.1). Because of the finite solid angles subtended by the counters themselves, the values $C(\phi)$ are really averages of the true correlation over angles $\theta$ distributed around $\phi$. Thus the experimental correlation function $W_{expt}(\phi)$ must be corrected to yield $W_{expt}(\theta)$ which can then be compared with the theoretical expression $W(\theta)$.

For a centred point source and cylindrically symmetric

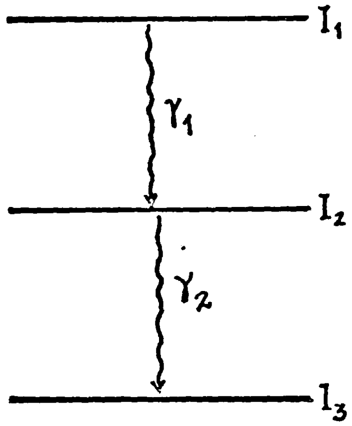


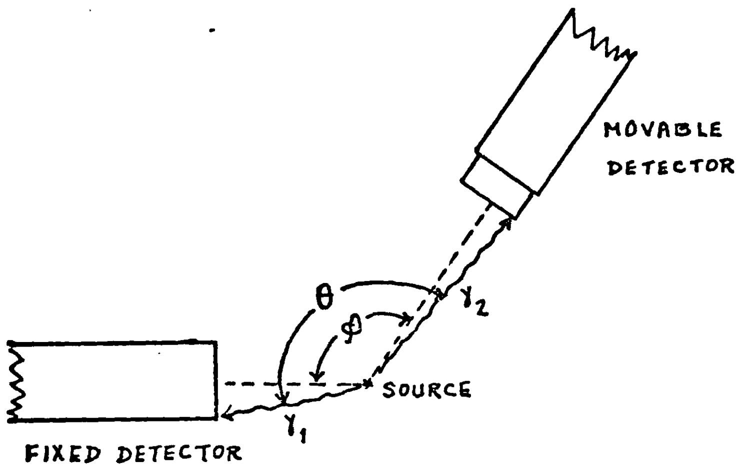


Fig. 4.1 (a) A gamma-gamma cascade, (b) directional correlation measurement of the gamma-gamma cascade

detectors, the theoretical correlation function can be written.

$$W(\theta) = 1 + A_2P_2(\cos\theta) + A_4P_4(\cos(\theta)) + \ldots$$

where $P_2(\cos\theta)$, $P_4(\cos\theta)$ etc., are Legendre polynomials. Experimentally the measured correlation is given by

$$N(\phi) = \text{const}\left[1 + A_2^{\text{expt}}P_2(\cos\phi) + A_4^{\text{expt}}P_4(\cos\phi) + \ldots\right]$$

The experimental and theoretical coefficients are related by the solid angle correction factor $Q_k$ :

$$A_k = A_k^{\text{expt}}/Q_k \quad \text{where } k = 2,4.$$

The correction factor $Q_k$ must include corrections for both detectors. They are given by

$$Q_k = Q_k^A(\gamma_1)\, Q_k^B(\gamma_2)$$

where detectors A and B observe $\gamma_1$ and $\gamma_2$ respectively.

The solid angle correction factors for cylindrical NaI(Tl) crystals have been given by Yates (1968). For coaxial germanium detectors they have been calculated by several investigators and empirically estimated by others. The most extensive treatment has been that of Camp and van Lehn (1969,1970). Using both theoretical and experimental absorption cross-sections they employed Monte Carlo type calculations to take account of multiple Compton scattering.

Camp and van Lehn tabulated their values of $Q_k$ for various detector geometries. However, the variety of available detector sizes is large and so interpolation and extrapolation is often necessary. Considerable uncertainty is thus introduced since several parameters are involved. To overcome this limitation Krane (1972) developed a simpler method of calculation and published a computer program for general use. Because the program is limited solely to coaxial detectors, we have extended Krane's work to calculate the correction factors for end-drifted coaxial detectors which are commonly encountered in laboratories. In fact the detector used in our experiment has this end drifted coaxial geometry.

## 4.2 Theoretical Procedure

The values for $Q_k$ have been calculated with the method of Rose (1953).

$$Q_k(\gamma) = J_k(\gamma)/J_o(\gamma)$$

Here

$$J_k(\gamma) = \int P_k(\cos\beta)(1 - e^{\tau(\gamma)x(\beta)}) \sin\beta \; d\beta$$

where $\tau(\gamma)$ is the gamma absorption coefficient; $\beta$ is the angle between the path of the gamma ray and the symmetry axisof the detector; and $x(\beta)$ is the path length through the active volume of the detector.

The integration is performed by dividing the end-drifted detector into four regions as shown in Fig. 4.2. The limits of integration and the path lengths in each region are as follows

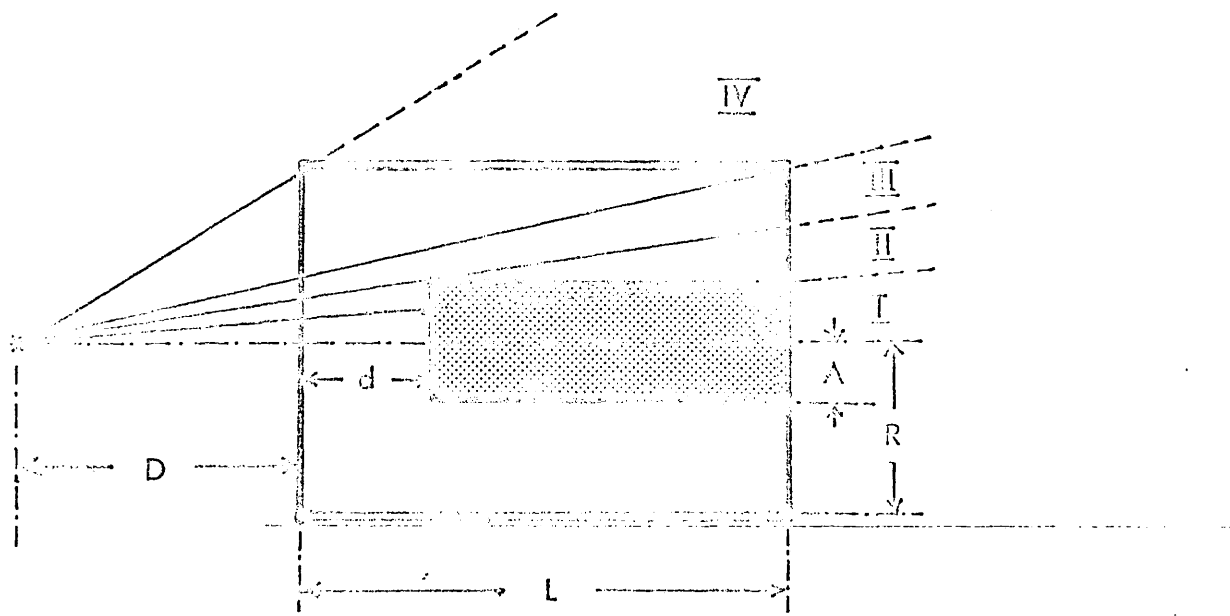


Fig. 4.2 Geometrical division of the detector into regions for computation

I $\quad 0 \leq \beta \leq \tan^{-1}[A/(D+L)]$

$$x(\beta) = d/\cos\beta$$

II $\quad \tan^{-1}[A/(D+L)] \leq \beta \leq \tan^{-1}[A/(D+d)]$

$$x(\beta) = [(D+L+d)/\cos\beta] - (A/\sin\beta)$$

III $\quad \tan^{-1}[A/(D+d)] \leq \beta \leq \tan^{-1}[R/(D+L)]$

$$x(\beta) = L/\cos\beta$$

IV $\quad \tan^{-1}[R/(D+L)] \leq \beta \leq \tan^{-1}(R/D)$

$$x(\beta) = (R/\sin\beta) - (D/\cos\beta)$$

In region II an additional factor is introduced into the integrand of the expression for $J_k(\gamma)$ to take into account the attenuation of the gamma ray in the inactive p-type core of the detector. This factor is given by

$$K(\beta) = \exp\left[-J(\gamma)\, x'(\beta)\right]$$

where $x'(\beta)$ is the path length through the dead core, i.e.

$$x'(\beta) = (A/\sin\beta) - [(D+d)/\cos\beta]$$

The modified integrand for region II is then given by

$$J_k(\gamma) = \int P_k(\cos\beta)\left[(1 - e^{-\tau(\gamma)x_1(\beta)}) + (1-e^{-\tau(\gamma)x_2(\beta)})e^{-\tau(\gamma)x'(\beta)}\right] \sin\beta\, d\beta$$

where $x_1(\beta)$ is the path length in the end-drifted part of the detector and $x_2(\beta)$ is the extra path length for gamma rays that have penetrated the inactive part of the detector.

The absorption coefficient $\tau(\gamma)$ has to be computed at each energy. Camp and van Lehn carried out Monte Carlo type computations to take into account the effects of multiple Compton scattering. As $Q_k$ is not particularly sensitive (Camp and van Lehn 1969), to the $\tau(\gamma)$ used we follow the method of Krane and consider only single Compton scatters.

In the energy region for which pair production is not important, we may write down for the absorption coefficient:

$$\tau(\gamma) = \tau_{pe}(\gamma) + P_{pe}(\gamma_c)\,\tau_c(\gamma)$$

where $\tau_{pe}(\gamma)$ and $\tau_c(\gamma)$ are the attenuation coefficients for photoelectric interactions and for Compton scattering; and $P_{pe}(\gamma_c)$ is the probability that a Compton scattered photon $\gamma_c$ will be photoelectrically absorbed. Following the discussion of Camp and van Lehn (1969) and Krane (1972), we determine $P_{pe}$ by computing $J_o(\gamma_c)$ using $\tau_{pe}(\gamma_c)$ only. As the absolute efficiency (intrinsic efficiency times solid angle) is nearly equal to $\frac{1}{2}\, J_o$ we put

$$P_{pe}(\gamma_c) \simeq \tfrac{1}{2} \quad J_o(\gamma_c)\,\Omega^{1}$$

where $\Omega$ is the solid angle substended by the detector. The coefficients $\tau_{pe}(\gamma)$ and $\tau_c(\gamma)$ were obtained from the report by Storm and Israel (1967). For each gamma energy there is a continuous distribution of Compton scattered photons, but in the computation only the average energy of the scattered photons was used. This was taken to be

$$(\gamma_c)_{av} = \gamma\, \frac{e^{\sigma}{}_s}{a^{\sigma}}$$

where ${}_e\sigma_s$ is the Klein-Nishina scattering and ${}_a\sigma$ is the Compton absorption (Evans, 1955).

The computations were carried out on a CDC 6600 computer. The FORTRAN IV program was written in a subroutine form and it is presented in the appendix.

## 4.3 Results

The program gives the correction factor $Q_k$ as a function of the incident gamma energy $E_\gamma$, the source-detector distance, and the detector geometry.

The correction factors $Q_2$ and $Q_4$ for our end-drifted coaxial detector have been calculated. The detector has a sensitive volume of 40 $cm^3$ with a length of 5 cm, a radial depletion depth of 11 mm, and an axial depletion depth of 13 mm.

Fig. 4.3 shows the dependence of $Q_2$ on $E_\gamma$ (keV) for source-detector distances of 3.5, 5.0, 7.0 and 10.0 cm. Fig. 4.4 shows the variation of $Q_4$ with $E_\gamma$ (keV) for the same source-detector distances. The numerical values of $Q_2$ and $Q_4$ obtained in the calculation are tabulated in Table 4.1. These results will be used in the analysis of the gamma-gamma directional correlation experiments on $^{74}$Ge and $^{147}$Pm.

It is instructive to gauge the importance of applying the appropriate correction factors. In Fig. 4.5 a comparison is shown of the factors calculated by our program for an end-drifted

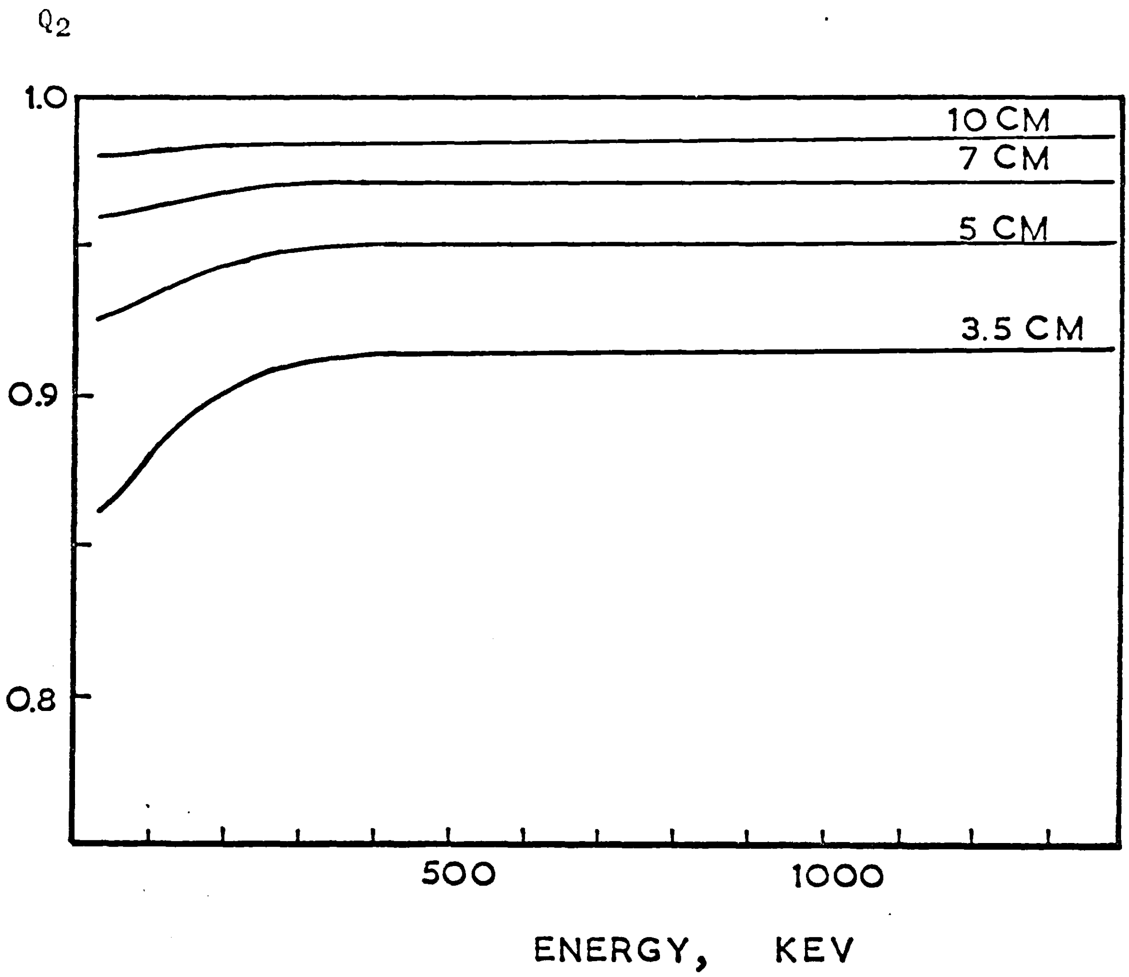


Fig. 4.3 Variation of $Q_2$ for our end-drifted detector with energy for different source-detector distances.

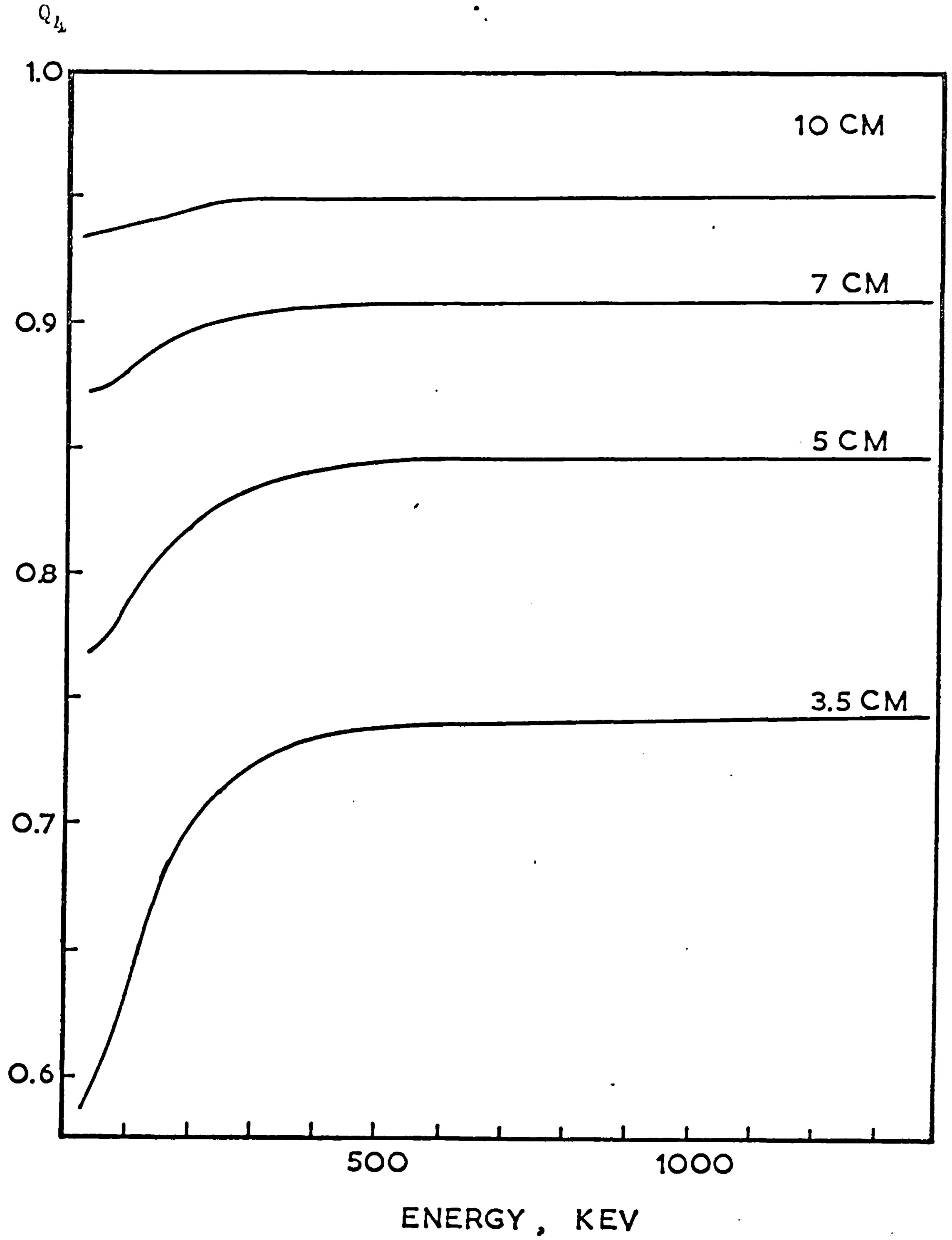


Fig. 4.4 Variation of $Q_4$ with energy for our end-drifted detector for different source-detector distances.

TABLE 4.1

Solid angle correction factors for an end-drifted coaxial Ge(Li) detector of 40 $cm^3$ with dimensions, length = 5cm, radial depletion depth = 11mm, axial depletion depth = 13mm. The variables are the gamma ray energy in keV and source-to-crystal distance in cm.

| | $Q_2$ | | | |
|---|---|---|---|---|
| E | D=3.5 | 5.0 | 7.0 | 10.0 |
| 30 | 0.86236 | 0.92611 | 0.96051 | 0.98014 |
| 40 | 0.86328 | 0.92655 | 0.96069 | 0.98021 |
| 50 | 0.86485 | 0.92723 | 0.96098 | 0.98031 |
| 60 | 0.86706 | 0.92821 | 0.96138 | 0.98047 |
| 80 | 0.87276 | 0.93076 | 0.96248 | 0.98089 |
| 100 | 0.87908 | 0.93366 | 0.96374 | 0.98137 |
| 150 | 0.89231 | 0.93991 | 0.96655 | 0.98247 |
| 200 | 0.90115 | 0.94427 | 0.96858 | 0.98329 |
| 300 | 0.91044 | 0.94891 | 0.97078 | 0.98421 |
| 400 | 0.91363 | 0.95050 | 0.97154 | 0.98452 |
| 500 | 0.91519 | 0.95128 | 0.97191 | 0.98467 |
| 600 | 0.91584 | 0.95160 | 0.97206 | 0.98473 |
| 800 | 0.91658 | 0.95197 | 0.97223 | 0.98481 |
| 1000 | 0.91682 | 0.95209 | 0.97229 | 0.98483 |
| 1500 | 0.91704 | 0.95220 | 0.97234 | 0.98485 |

TABLE 4.1 continued

| | | $Q_4$ | | |
|---|---|---|---|---|
| E | D=3.5 | 5.0 | 7.0 | 10.0 |
| 30 | 0.58967 | 0.76780 | 0.87241 | 0.93483 |
| 40 | 0.59238 | 0.76910 | 0.87297 | 0.93503 |
| 50 | 0.59657 | 0.77114 | 0.87386 | 0.93538 |
| 60 | 0.60249 | 0.77403 | 0.87515 | 0.93587 |
| 80 | 0.61794 | 0.78168 | 0.87860 | 0.93724 |
| 100 | 0.63531 | 0.79038 | 0.88258 | 0.93881 |
| 150 | 0.67227 | 0.80930 | 0.89142 | 0.94235 |
| 200 | 0.69738 | 0.82258 | 0.89787 | 0.94503 |
| 300 | 0.72407 | 0.83682 | 0.90487 | 0.94800 |
| 400 | 0.73328 | 0.84171 | 0.90727 | 0.94901 |
| 500 | 0.73779 | 0.84409 | 0.90843 | 0.94957 |
| 600 | 0.73967 | 0.84509 | 0.90892 | 0.94971 |
| 800 | 0.74182 | 0.84622 | 0.90947 | 0.94994 |
| 1000 | 0.74252 | 0.84659 | 0.90965 | 0.95002 |
| 1500 | 0.74315 | 0.84692 | 0.90981 | 0.95009 |

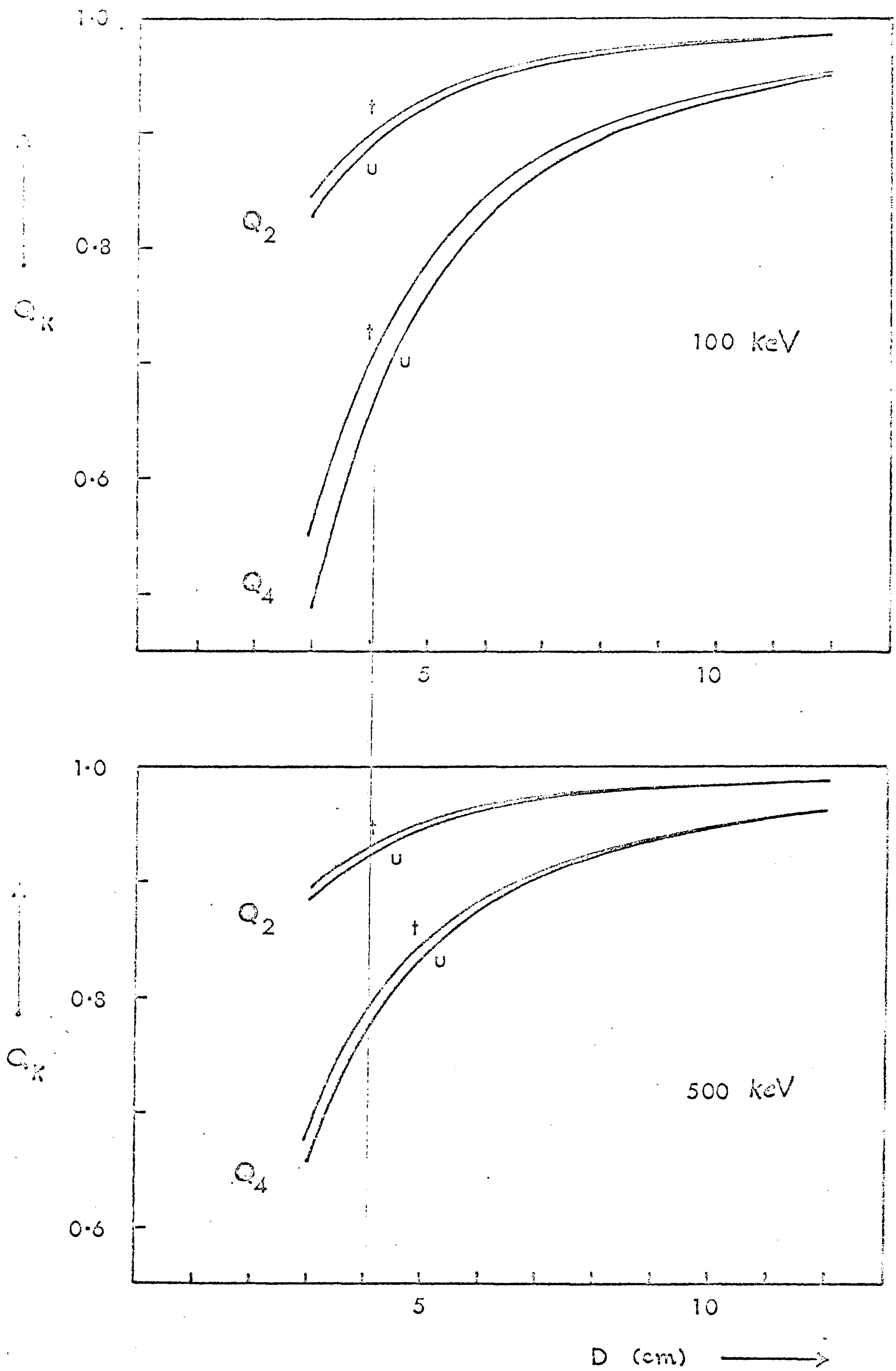


Fig.4.5 Comparison of presently calculated values of $Q_k$ for an end-drifted detector (t) with those of Krane(1972) for a coaxial detector of the same external dimensions (u).

coaxial detector, with the factors obtained with Krane's program for a coaxial detector of the same length and diameter. Although the difference in the two cases is negligible at larger distances and higher energies, it becomes significant at smaller distances and energies. And it must be noted that Ge(Li) detectors often have to be used at short distances to ensure reasonable counting rates.

# CHAPTER 5 STUDIES ON THE DECAY OF COBALT - 60

## 5.1 Previous Work

The daughter nucleus resulting from the decay of $^{60}Co$ is $^{60}Ni$. The excited levels of this nucleus have aroused considerable theoretical interest for it is thought to be approximately spherical and to consist of closed shells of neutrons and protons (N = Z = 28) plus four neutrons in the ($2p_{3/2}$, $1f_{5/2}$, $2p_{1/2}$) states. The work of Rauch et.al (1969) on the positron decay of $^{60}Cu$, and Ballini et.al (1968) on the results of $^{60}Ni$ (p,p'$\gamma$) and $^{59}Co$ ($He^3$, d) scattering has established the energies and parameters of a large number of nickel states; and these have been compared with shell model calculations - e.g. Auerbach (1967), Cohen et.al (1967), and Plastino et.al (1966).

The decay properties of $^{60}Co$ have been summarised in the Nuclear Data Sheets by Raman (1968), Fig.1. The 1173 keV and 1332 keV gamma rays are well known. The presence of the 2505 keV gamma ray has been indirectly shown by Morinaga and Takahashi (1968); they measured the neutron yield from the D($\gamma$,n) reaction caused by the 2505 keV gamma ray. Evidence for the 2159 keV gamma ray comes from Wolfson's (1955) detections of a weak externally converted gamma ray of this energy. The 826 keV gamma transition from the 2159 keV level to the 1332 keV level is indicated by the measurements of Rauch et.al (1969) on the decay of $^{60}Cu$. They have measured the energies of the gamma rays deexciting this level as $826.4 \pm 0.2$ keV and $2158.9 \pm 0.2$ keV and

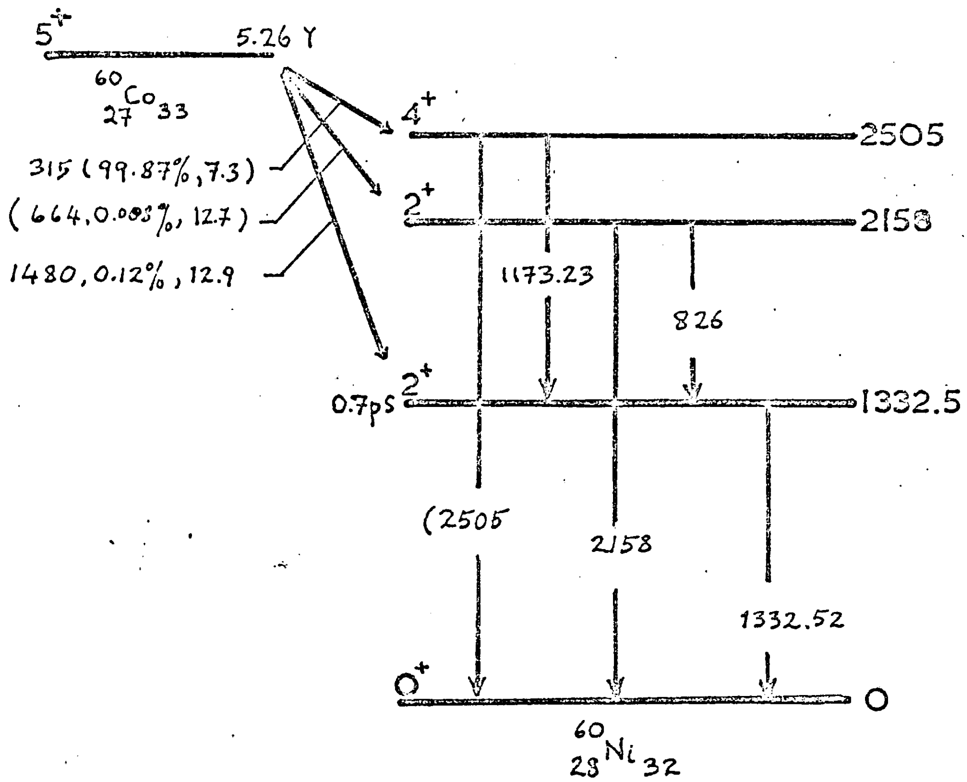


Fig. 5.1 The decay scheme of $^{60}$Co. All energies are in keV

the branching ratio as $I(826.4\gamma)/I(2158.9\gamma) = 6.5 \pm 0.5$. Raman (1969) has used Wolfson's (1955) intensity of 0.0012% for the 2158.9 keV gamma and the branching ratio of the 826.4 keV gamma to the 2158.9 keV gamma from $^{60}Cu$ decay to estimate an expected intensity of 0.007% for the 826 keV gamma transition in the decay of $^{60}Co$.

Nevertheless, uncertainty remains about the population of the nickel states by the beta decay of $^{60}Co$. Hansen and Spernol (1968) using a double focussing $\beta$- spectrometer reported evidence for a third beta transition of 670 keV to an intermediate level. In addition on the basis of a peak at 822 keV in their Ge(Li) spectrum they propose that this level should be at 2155 keV (and not 2158.9 keV). Raman (1969), however, has cast doubt on this interpretation by intimating that the 822 keV peak might be an annihilation single escape peak from the 1332 keV transition. Moreover, Hansen and Spernol's measured intensity of 0.18% for this peak together with their upper limit for the intensity of a 2155 keV gamma ray gives a branching ratio $I(822.5\gamma)/I(2155\gamma) \geq 120$ for the second excited state in $^{60}Ni$. This disagrees with the branching ratio measured by Rauch et.al (1969) from the decay of $^{60}Cu$.

The decay scheme proposed by Hansen and Spernol (1968) requires that an 0.18%, 670 keV $\beta$- group feed the $(2^+)$ 2155 keV level directly from the $5^+$ ground state of $^{60}Co$. Such a $\beta$- transition would have log ft = 11.4, which is unusually low for a second forbidden unique transition. Raman (1969) has noted, after studying some second forbidden unique ( J = 3, $\Delta\pi \rightarrow$ no) $\beta$- transitions in nuclei ranging from $^{10}$Be to $^{209}$Po, that the log ft values in such transitions are generally greater than 12.7.

The disagreements noted above prompted a study of $^{60}$Co to test whether the 822 keV peak reported by Hansen and Spernol (1968) was a genuine gamma ray or an annihilation single escape peak. At the same time we decided to search for possible weak gamma transitions.

## 5.2 Experimental Procedure

The gamma spectra have been studied with the 40 cm$^3$ Ge(Li) detector coupled to a 400 channel pulse height analyser. For this experiment the energy region from 270 keV to 1400 keV was studied by using a Nuclear Enterprises NE5259 amplifier in conjunction with a NE 5261A biased amplifier. The energy calibration was made using the prominent $^{60}$Co lines and the double escape peak at 310.5 keV. A separate energy measurement was made on the 822 keV $^{60}$Co peak using the detector coupled to a 1024 channel pulse height analyser.

An attempt was made to look for the higher energy gamma rays by taking spectra in the region 1500 keV to 2700 keV.

## 5.3 Results

The gamma spectra from $^{60}$Co decay in the region of 820 keV are shown in Figure 5.2a. It is seen that a peak clearly exists at 822.1 keV. To ascertain whether the peak is the result of single annihilation quanta escaping after pair production in the germanium crystal, isotopes of $^{46}$Sc, $^{22}$Na and $^{24}$Na were also studied. These nuclides have prominent gamma rays at 1120, 1274 and 1368 keV and might thus be expected to exhibit similar single escape peaks.

The results of this measurement are shown in Fig. 5.2b. The single escape peaks are very small and lie on high Compton backgrounds of the main gamma rays. Therefore it was found necessary to determine accurately the Compton continuum under the single escape peaks to obtain the areas of the peaks. A third degree polynomial least squares fit was made to the background choosing at least eight channels on either side of the peak. After correction for the variation of efficiency with energy, the intensities of the single escape peaks relative to the main gamma rays were calculated. Fig. 5.3 shows that the relative intensities are a smooth function of the energy. It may be seen that the intensity of the peak at 822 keV relative to the 1332 keV gamma ray in $^{60}$Co lies on this line, and we therefore conclude that the peak, suggested by Hansen and Spernol to be a gamma transition, is a single escape peak of the 1332 keV transition.

The 826 keV gamma ray could not be measured in our spectrum. The upper limit for the intensity of a gamma ray at this energy was calculated to be 0.012%.

(a)

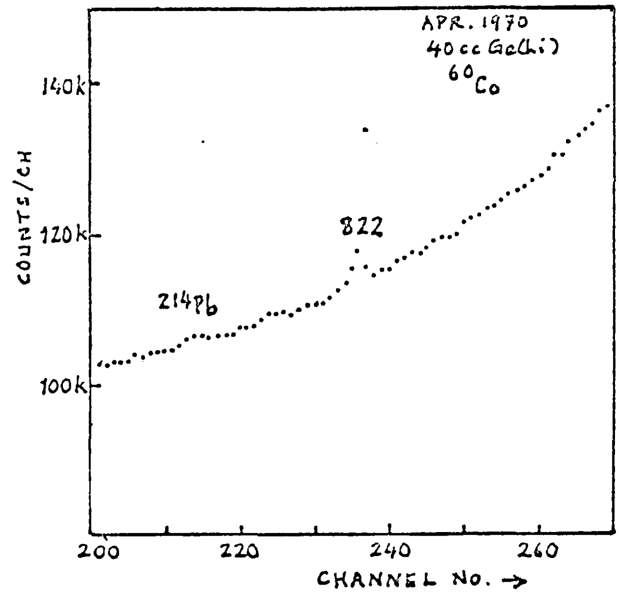


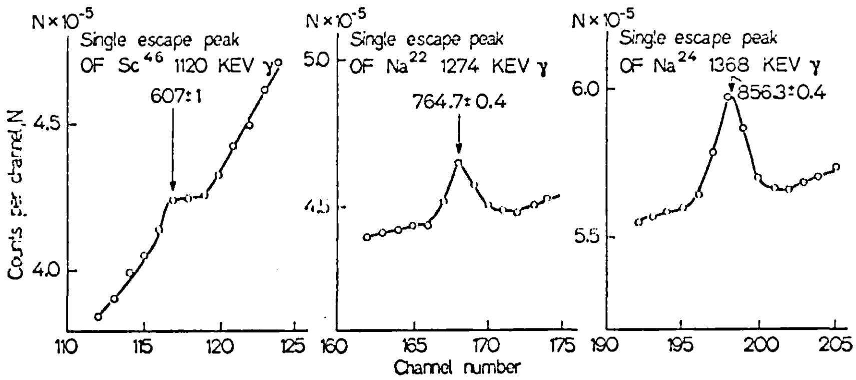


b(i)

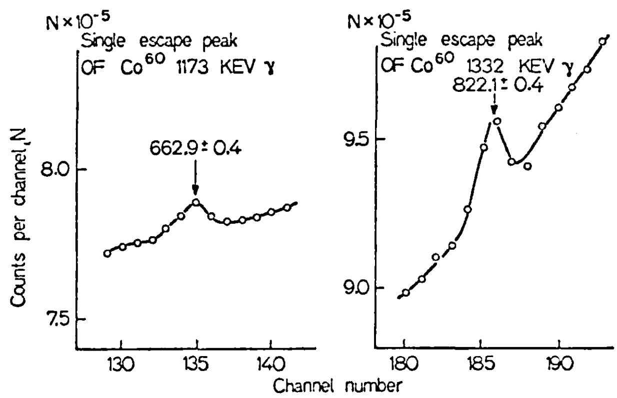


b(ii)

Fig. 5.2 Selected portions of the gamma spectra measured with the 40 cc Ge(Li) detector.(a) from $^{60}Co$ decay in the region around 820 keV. (b)(i)single escape peaks from $^{46}Sc$, $^{22}Na$, $^{24}Na$ gamma rays. (b)(ii) single escape peaks from the $^{60}Co$ gamma rays.

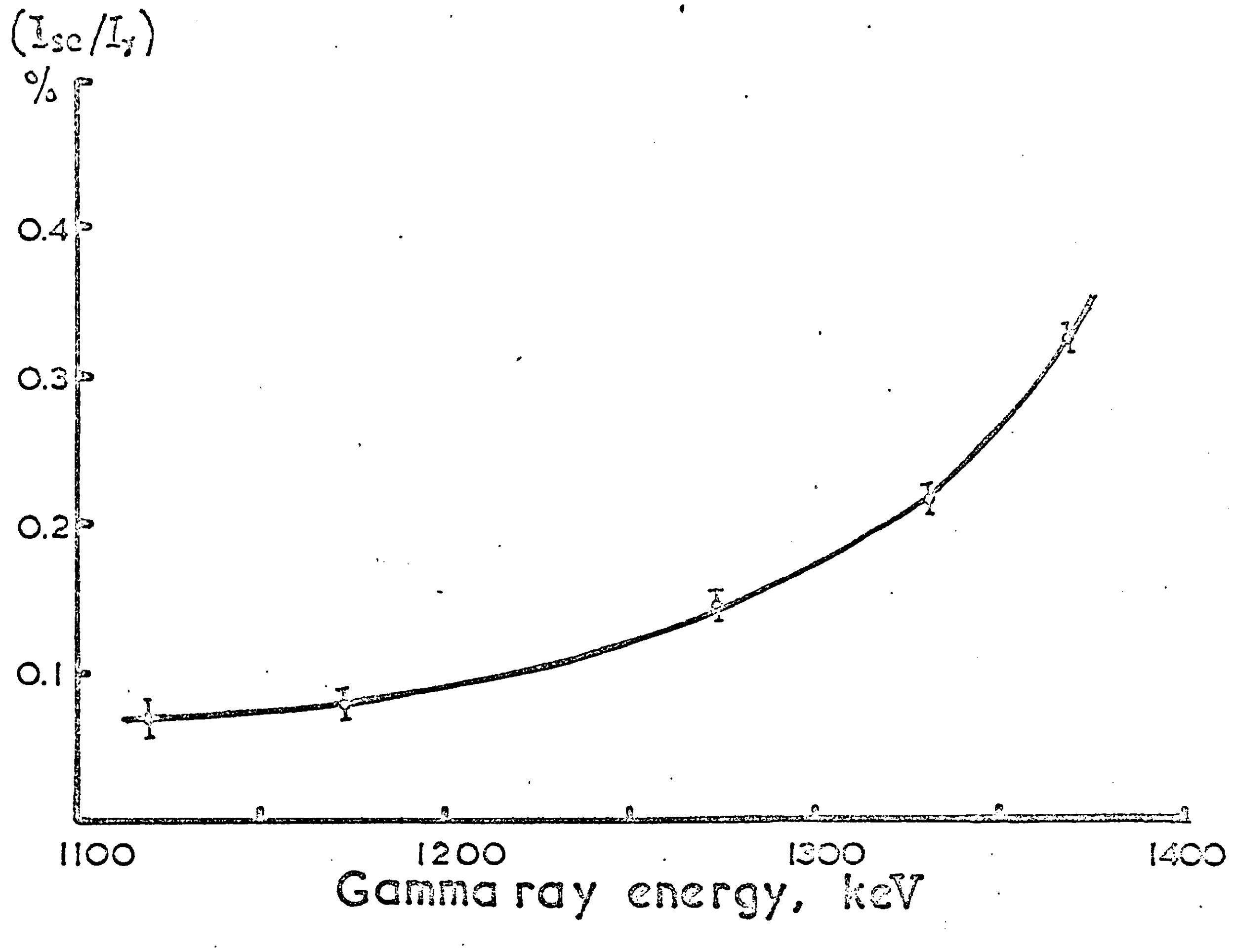


Fig. 5.3 Relative intensities of the single escape peaks shown as a function of the gamma ray energy

Fig 5.4 shows the spectra of $^{60}Co$ in the region 270 - 1200 keV. Again the 822 keV peak can be seen. The double escape peak at 310.5 keV may also be seen. An attempt was made to look for the 347 keV gamma transition from the 2505 keV level to the 2159 keV level. It was possible only to estimate an upper limit for this gamma ray as it would be located in the Compton background of the main $^{60}Co$ gamma rays in addition to lying very close to the 352 keV gamma ray of $^{214}Pb$ which forms part of the natural background. Fig. 5.5 shows the region around 350 keV. The intensity of a possible gamma ray at 346.8 keV is estimated to be (0.010 $\pm$ 0.004)% that of the 1173.2 keV gamma ray.

The spectra in the region of 1500 keV to 2700 keV shown in Fig. 5.6 A 10 microcurie source of $^{60}Co$ was placed at a distance of 5.5 cm from the Ge(Li) detector. The counting time was 10 days and $7\frac{1}{2}$ hours. The 2505 keV sum peak of the 1173.2 keV and 1332.5 keV gamma rays can be seen clearly. The gamma rays of the natural sources radium and thorium and their daughters are also identified in Fig. 5.6. A small peak may be seen at about 2159 keV. Its intensity relative to the 1332 keV peak (stored in channels 1 - 512) was estimated to be (0.93 $\pm$ 0.17) x $10^{-3}$%. This agrees with the intensity of 1.2 x $10^{-3}$% given by Wolfson (1955). Spectra were taken with another source of $^{60}Co$ of 5 millicurie strength placed at a distance of 4.8 metres from the detector. This did not improve the statistics. An absorber of

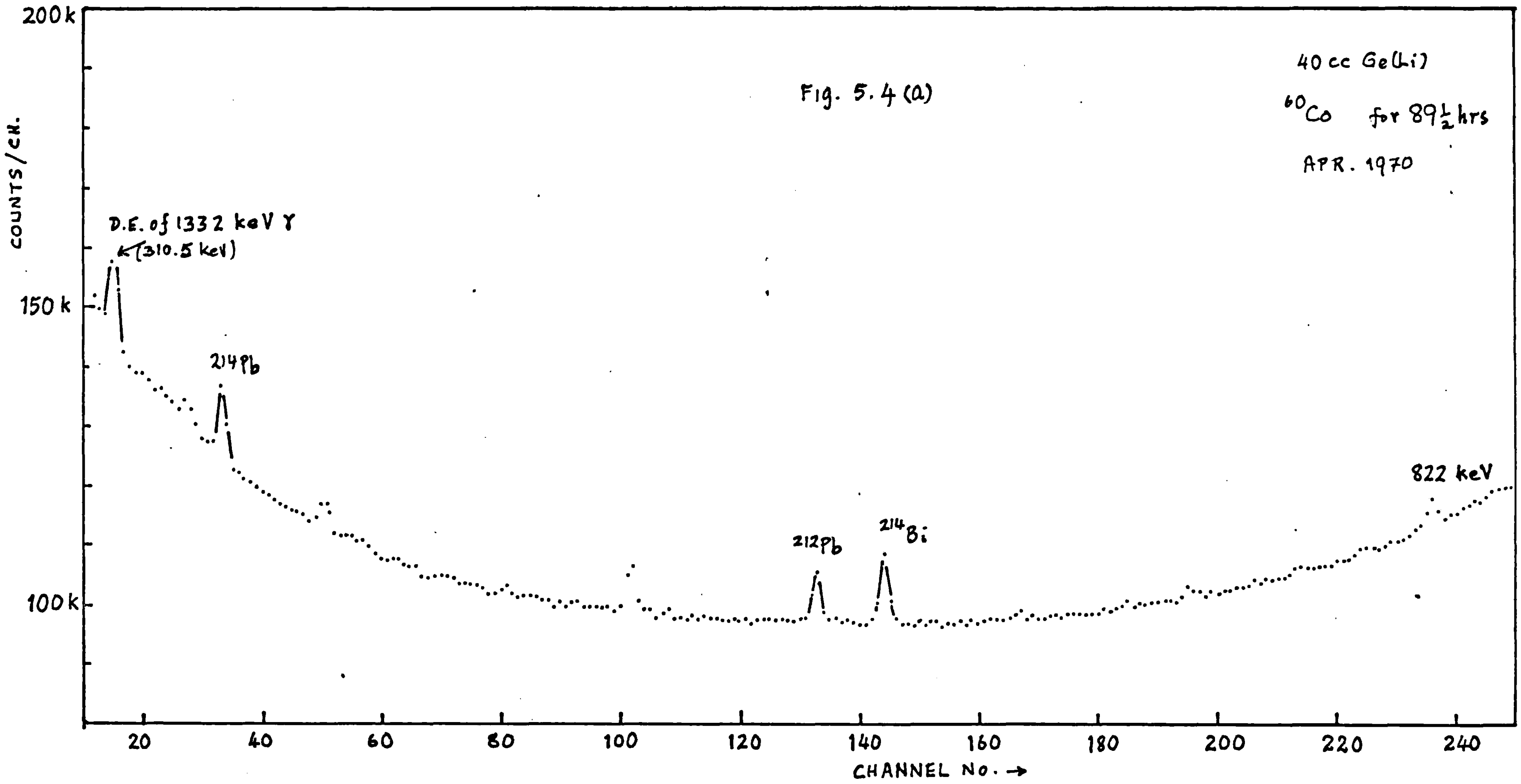


Fig. 5.4 Ge(Li) Spectra of $^{60}$Co decay in the energy region 270 - 1200 keV

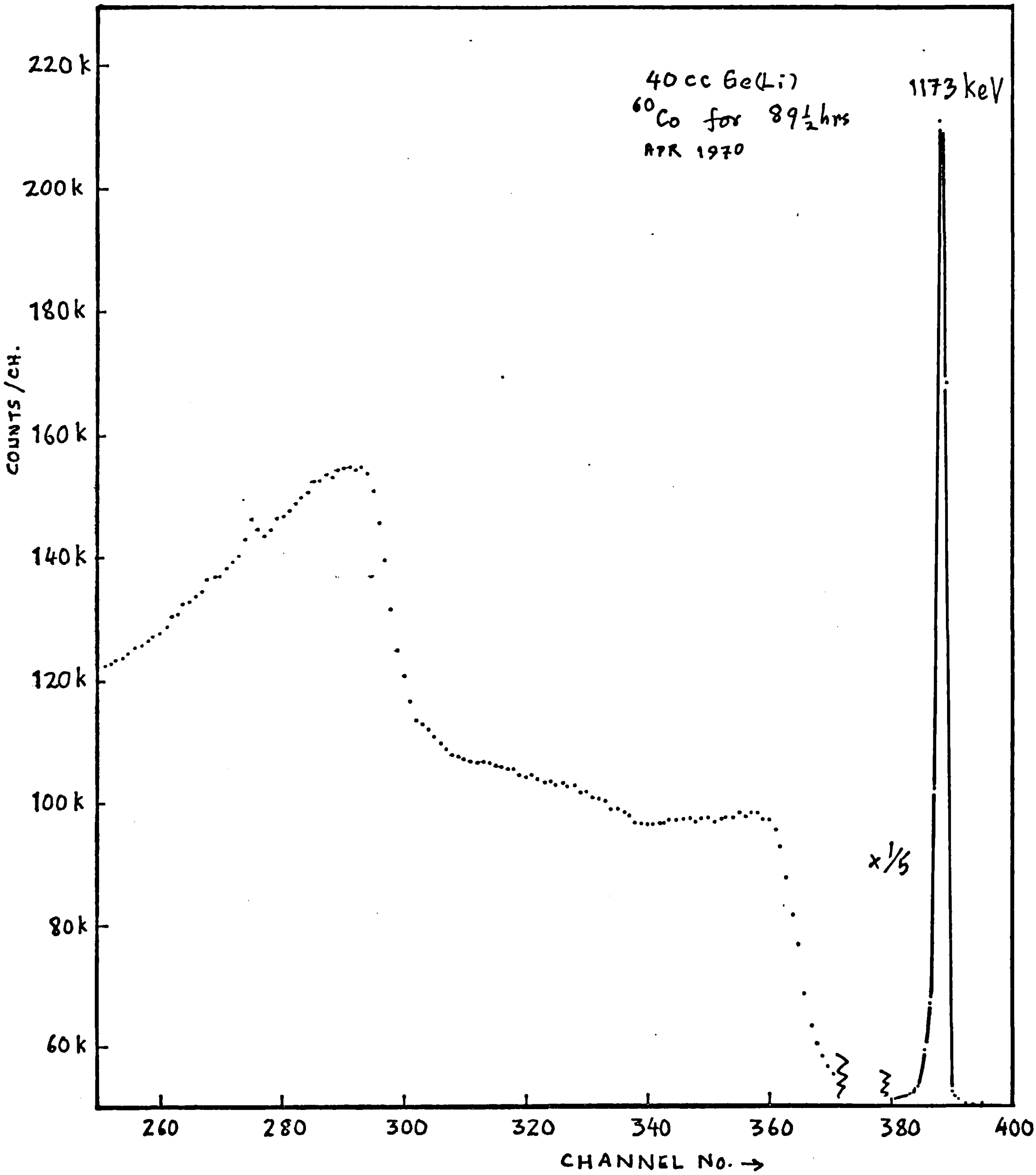

40 cc Ge(Li)
$^{60}$Co for 89½ hrs
APR 1970
1173 keV
x1/5
220 k
200 k
180 k
160 k
140 k
120 k
100 k
80 k
60 k
COUNTS / CH.
260
280
300
320
340
360
380
400
CHANNEL No. →


Fig. 5.4 (b)

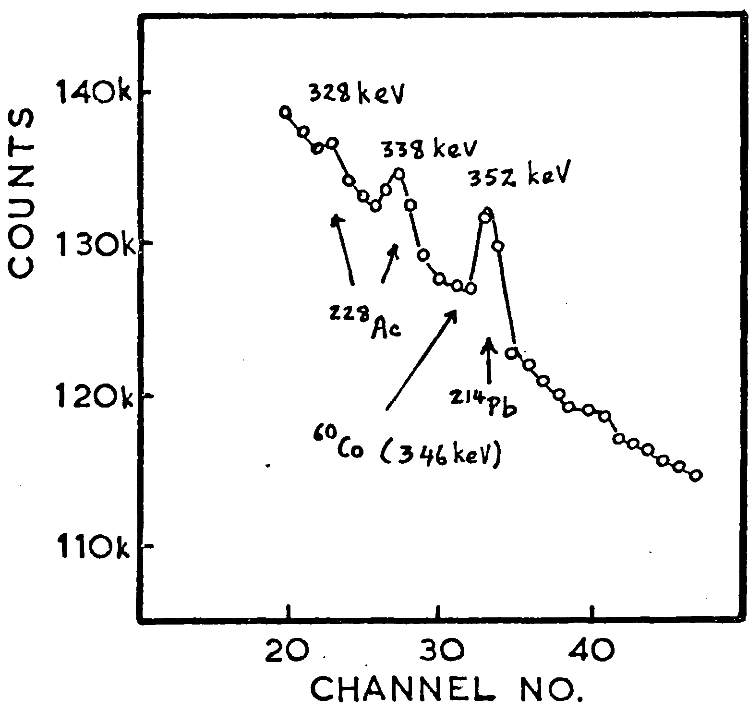


Fig. 5.5 Gamma ray spectrum of $^{60}Co$ in the energy region around 350 keV

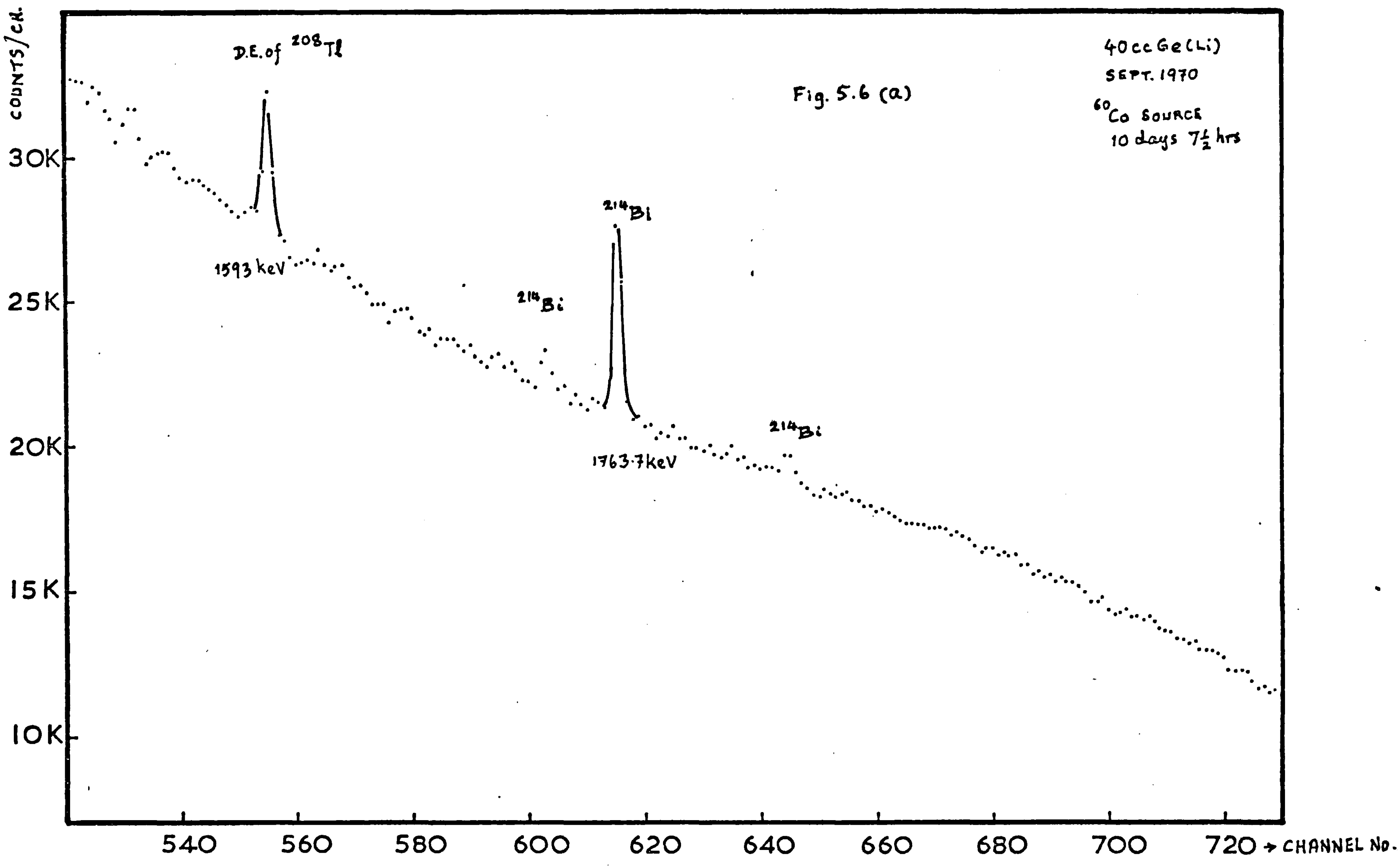


Fig. 5.6 Gamma ray spectrum of $^{60}Co$ in the energy region 1500 - 2700 keV

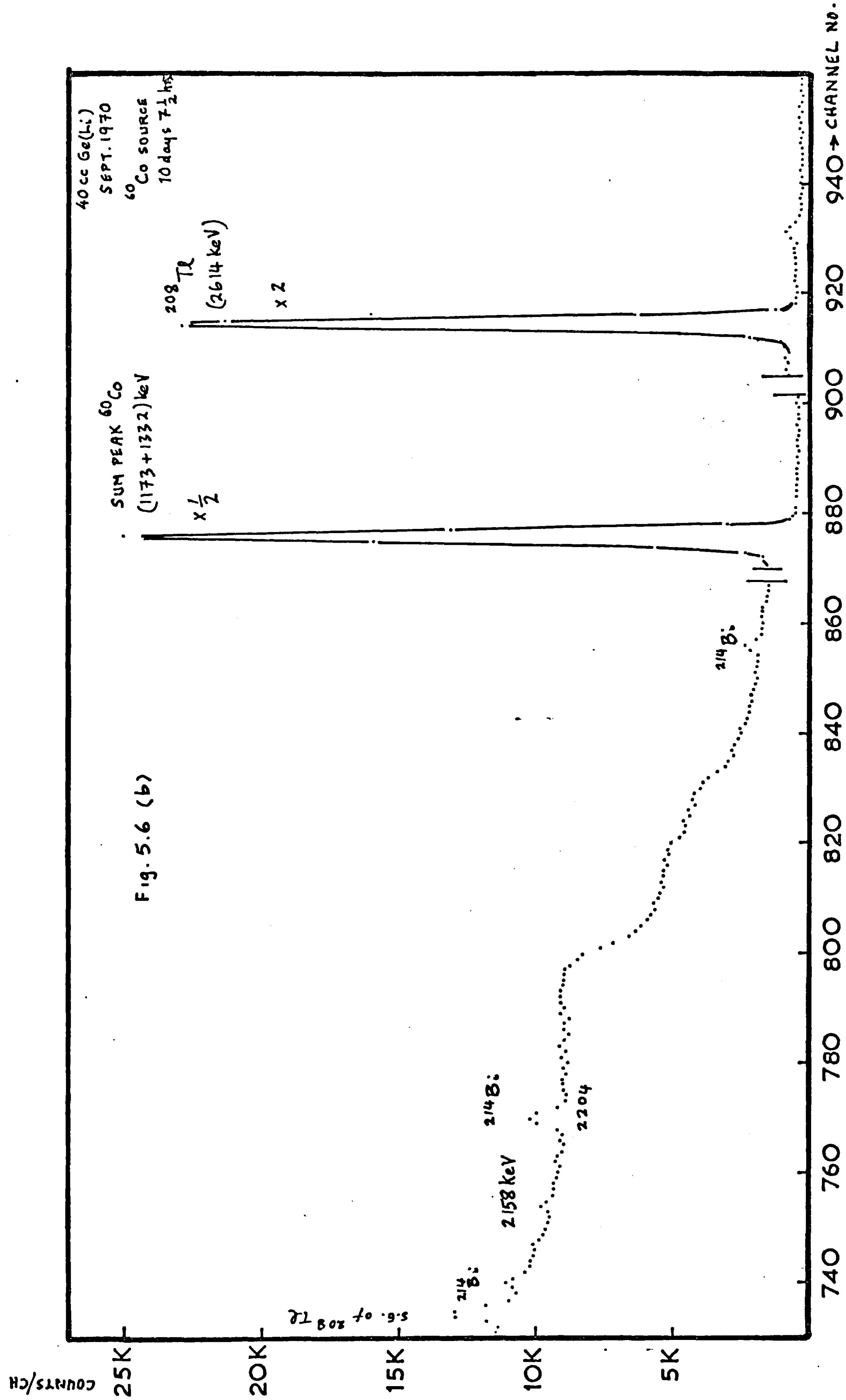
40 cc Ge(Li)
SEPT. 1970
60Co SOURCE
10 days 7½ hrs
208Tl
(2614 keV)
x 2
SUM PEAK 60Co
(1173+1332) keV
x ½
214Bi
214Bi
2204
2158 keV
214Bi
s.e. of 208Tl
COUNTS/CH
25K
20K
15K
10K
5K
740
760
780
800
820
840
860
880
900
920
940 → CHANNEL NO.

Fig. 5.6 (b)

lead of thickness 1.6 cm was placed between the source and detector to enhance the 2159 keV gamma ray and to reduce the pulse pile up due to the main gamma rays of $^{60}Co$. This also did not give us better statistics for the 2159 keV peak.

## 5.4 Discussion

It is clear that our results (Rice-Evans and Aung, 1970) discount the proposal by Hansen and Spernol (1969) for a prominent level at 2155 keV. It may be noted that although these authors presented their $\beta$-spectrum, the fact that they omitted the Fermi - Kurie analysis makes it impossible to assess the significance of their statement that three straight lines resulted, indicating a third weak beta transition to the level in question of intensity $(0.15 \pm 0.03)\%$. Our results definitely show that the 822 keV peak reported by Hansen and Spernol (1969) to be a gamma transition is an annihilation single-escape peak of the 1332 keV gamma ray of $^{60}Co$. It appears that our conclusion is corroborated by the independent work of Dixon and Storey (1970).

We have been able to estimate an upper limit of $(0.93 \pm 0.17) \times 10^{-3}\%$ for the intensity of a gamma transition of energy 2159 keV. This is in good agreement with the value of $1.2 \times 10^{-3}\%$ measured by Wolfson (1955). Dixon and Storey (1970) have looked for the 2159 keV gamma ray by studying the radiation emerging through the shielding walls of an AECL Gammacell containing about 10,000 Curies of $^{60}Co$. They estimated the intensity of the

2159 keV gamma transition to be $(0.7 \; {}^{+0.9}_{-0.4}) \times 10^{-3}\%$.

From our results, an upper limit of $(0.012 \pm 0.004)\%$ has been obtained for the intensity of a possible gamma ray at 826 keV. This result combined with Wolfsons measured value of $1.2 \times 10^{-3}\%$ of the intensity of the 2159 keV transition gives an upper value for the branching ratio of the 2159 keV level ($I(826\gamma)/(2159\gamma)$) of 10. This is very different from the value of 120 given by Hansen and Spernol (1969) but is in agreement with the 6.5 of Rauch et.al (1969).

An estimate has been made for intensity of the 346.8 keV gamma transition between the 2505.5 keV,$4_1^+$ and 2158.9,$2_2^+$ states in $^{60}$Ni, yielding the value $(0.010 \pm 0.004)\%$ that of the intensity of the 1173.2 keV transition. Van Hise and Camp (1969) using a Compton suppression spectrometer with a central Ge(Li) detector have observed this gamma transition with an intensity of 0.0078% of the 1173 keV gamma ray. They have measured the energy to be $346.95 \pm 0.10$ keV. This so-called zero-phonon transition is strictly forbidden according to the simple vibrational model. However, if this transition exists it is expected to have a relatively low intensity because of its low evergy (Van Hise and Camp, 1969), and our intensity estimate confirms this observation.

Van Hise and Camp (1969) have also detected the 826 keV (2158.9 to 1332.5 keV) transition with an intensity of 0.0055% that of the 1173.2 keV gamma. Their measurement yields a value of 826.18 $\pm$ 0.20 for the energy of this transition.

We were not able to detect the 2505 keV transition from the $4_1^+$ state because of the summing of the intense 1332.5 and 1173.2 keV gamma rays.

The results of our investigation have been reported in Z. Physik. 240 (1970) 392 - 395 and is appended at the end of this report.

# CHAPTER 6 STUDIES ON THE DECAY OF ARSENIC-74

## 6.1 Introduction

Arsenic-74 decays to Germanium-74 by $\beta^+$ and electron capture and to Selenium-74 by $\beta^-$ with a half-life of 17.9 days. Knowledge of the resulting excited states has come from scintillation counter studies (Girgis and van Lieshout, 1959; Eichler et.al, 1962), various nuclear reactions ( Darcey, 1964; Weitkamp et.al, 1966) and more recently from the groups working with Ge(Li) detectors ( Kukoc et.al, 1968; Hamilton et.al, 1969) whose decay schemes are shown in Fig.6.1. Hamilton et.al reported the existence of three new transitions but to our knowledge these have not yet been confirmed. Directional correlation measurements were done by Eichler et.al(1962) as well as by Hamilton et.al (1969).

The levels of even-even nuclei such as $^{74}$Ge are of interest because they include two-phonon vibrational modes. The relative intensities of the transitions and the multipole mixing ratios provide a basis for the comparison of the different refinements of the vibrational model (e.g. Scharff-Goldhaber and Weneser,1955; the Wilets and Jean displaced harmonic oscillator model,1956; the weak and intermediate surface interactions of Raz, 1959, etc. )

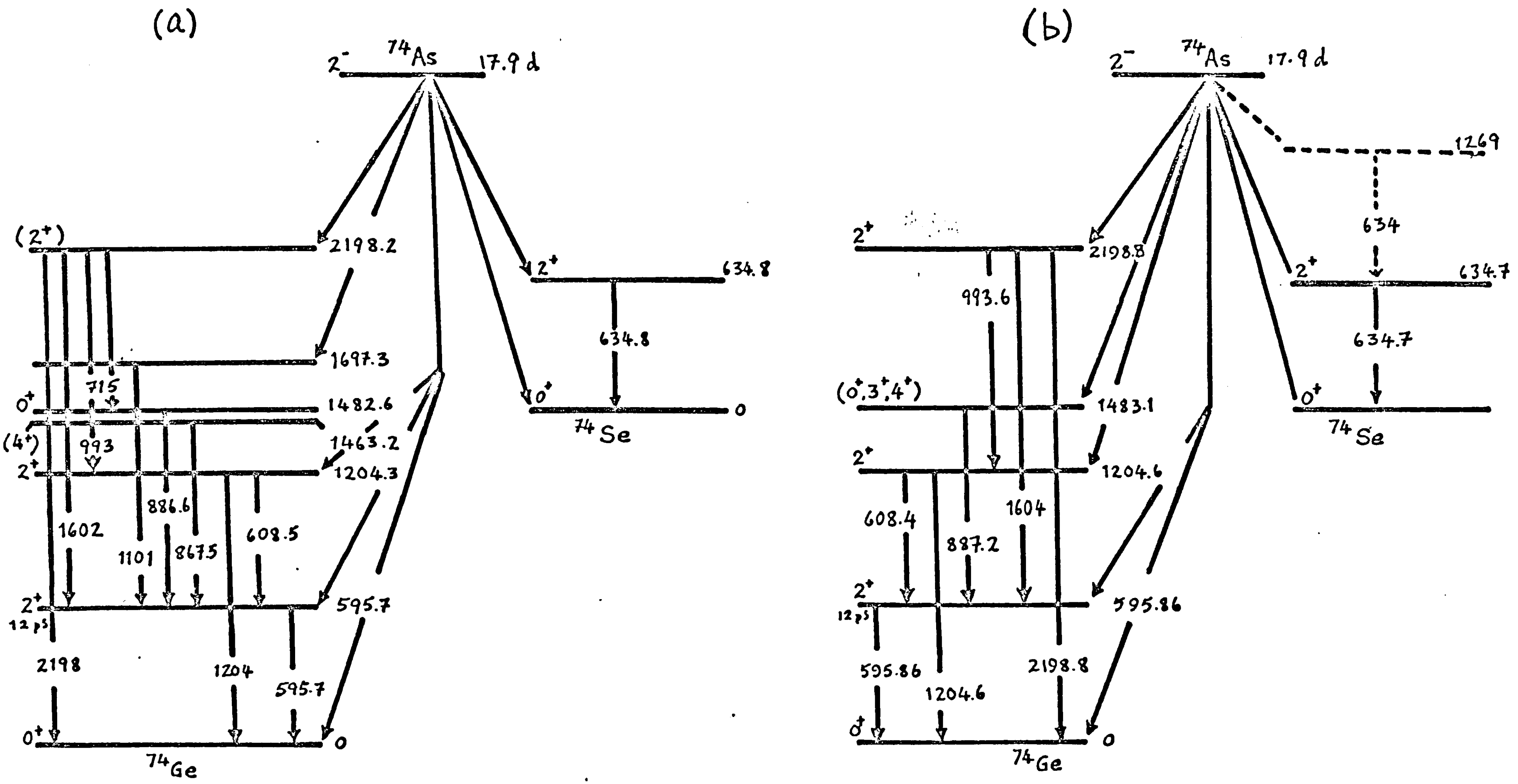


FIG. 6.1 DECAY SCHEME FOR $^{74}As$ (a) HAMILTON ET.AL (1969), (b) KUKOC ET.AL (1968)

## 6.2 Measurements of the Gamma-Ray Spectrum

The gamma spectra have been measured with the 40 cc Ge(Li) detector coupled to a 2048 channel analyser(NS.606). The $^{74}$As, obtained from the Radiochemical Centre, Amersham, was prepared by proton bombardment on natural germanium.

Singles spectra were taken with the source at a distance of 7.5 cm from the detector. Spectra with a 4 mm lead absorber between the source and the detector were also taken to enhance the high energy gammas and also to reduce the intensity of the sum peak at 1106 keV (595.6+510.8 keV). Gamma ray intensities were determined using a relative efficiency curve obtained for the detector with a $^{226}$Ra source. The intensities of the gammas from $^{226}$Ra were taken from the work of Lingemann et.al (1969).

The gamma spectra divided into regions are shown in Figures 6.2, 6.3, 6.4 and 6.5 . Fig. 6.2 shows the gamma spectrum up to 650 keV. The strong annihilation radiation at 511 keV, the strong 596 keV gamma of $^{74}$Ge and the 634 keV gamma of $^{74}$Se can be clearly seen. The 608 keV gamma of $^{74}$Ge is shown in the inset. The gamma spectrum in the region 600 keV to about 1220 keV are shown in Fig. 6.3. The weak transitions at 715 keV and 867 keV can be seen. The peak at about 867 keV includes a contribution from the 867.33 keV gamma of the impurity $^{152}$Eu. Its contribution was subtracted from the peak using the relative intensities of $^{152}$Eu gammas given by Aubin et.al (1969) after determining the intensity of the 778 keV peak of $^{152}$Eu.

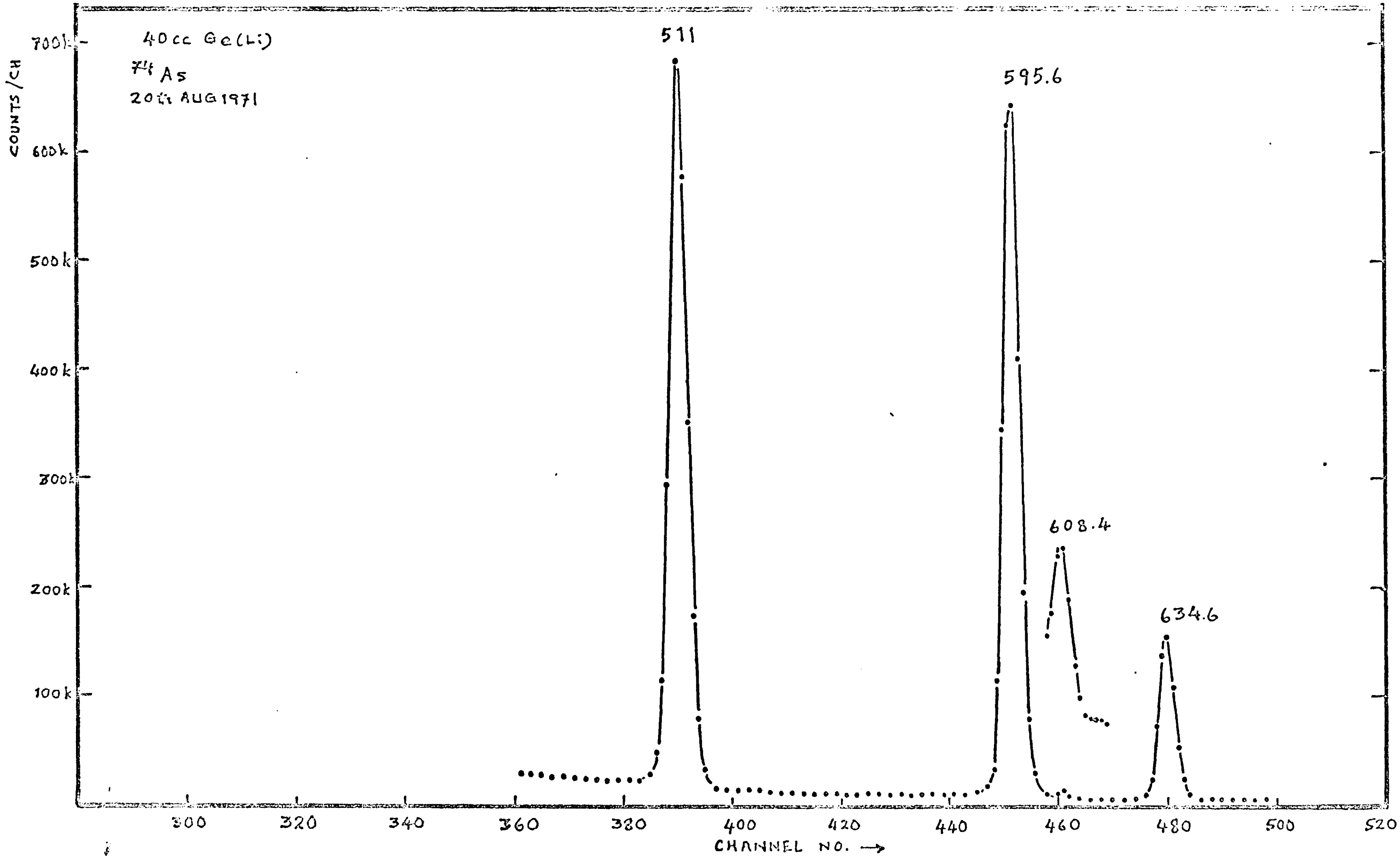


Fig. 6.2 Gamma spectrum in the decay of $^{74}$As in the energy region 400 to 650 keV

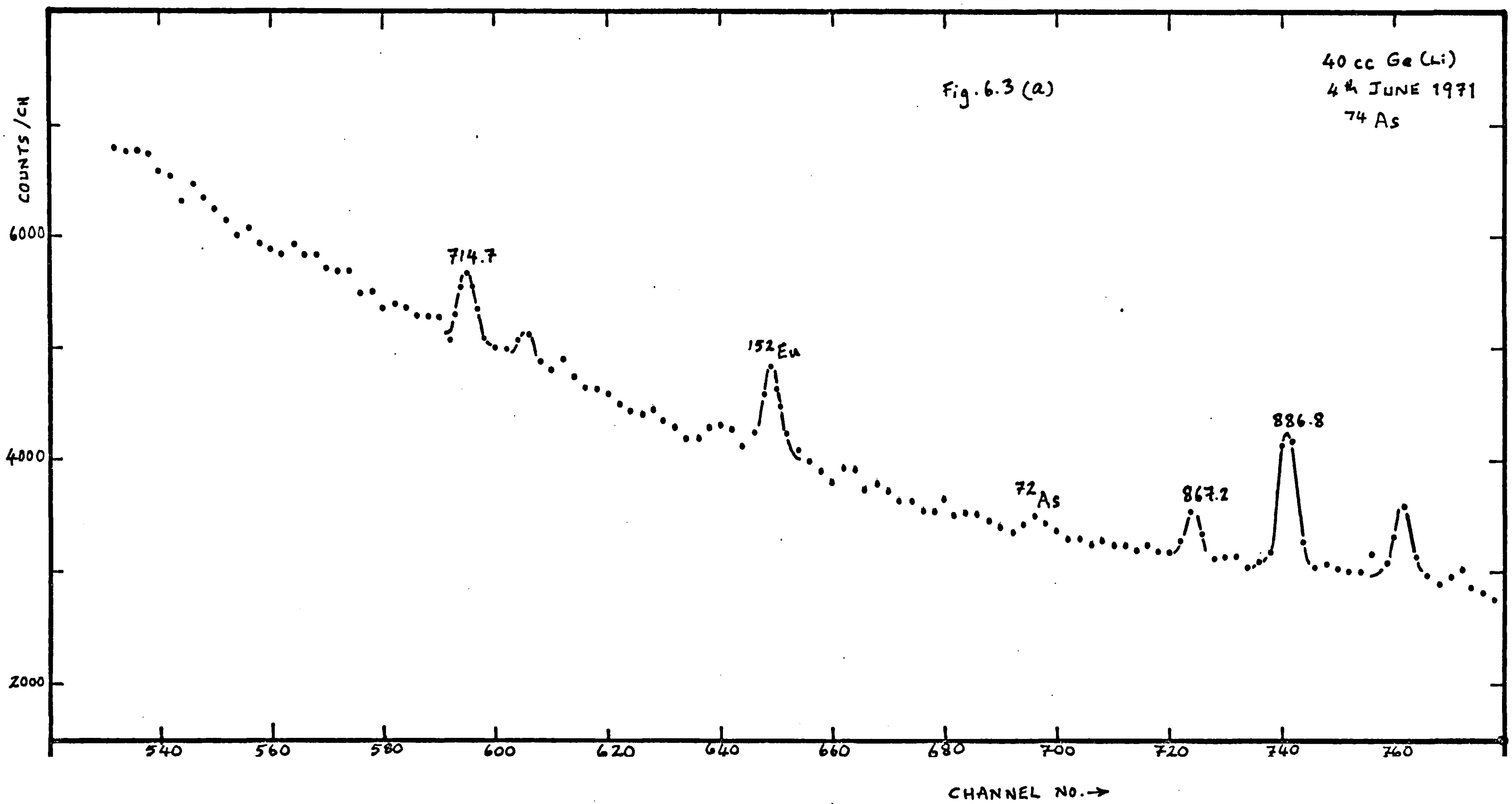


Fig. 6.3 Gamma spectrum in $^{74}$As decay - in the energy region 600 to 1220 keV

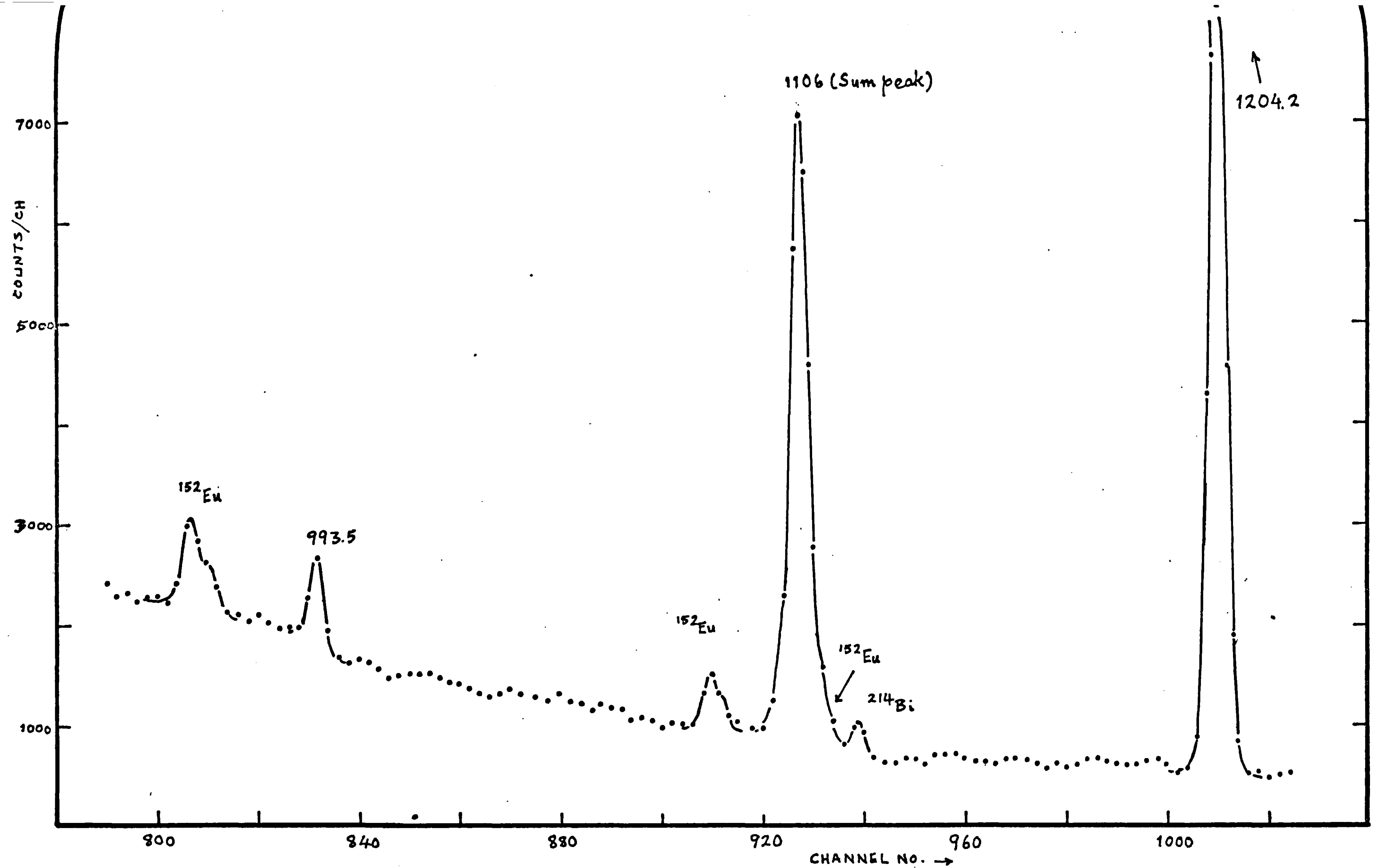
1204.2
1106 (Sum peak)
$^{152}$Eu
993.5
$^{152}$Eu
$^{152}$Eu
$^{214}$Bi
7000
5000
3000
1000
COUNTS/CH
800
840
880
920
960
1000
CHANNEL NO. →

Fig. 6.3 (b)

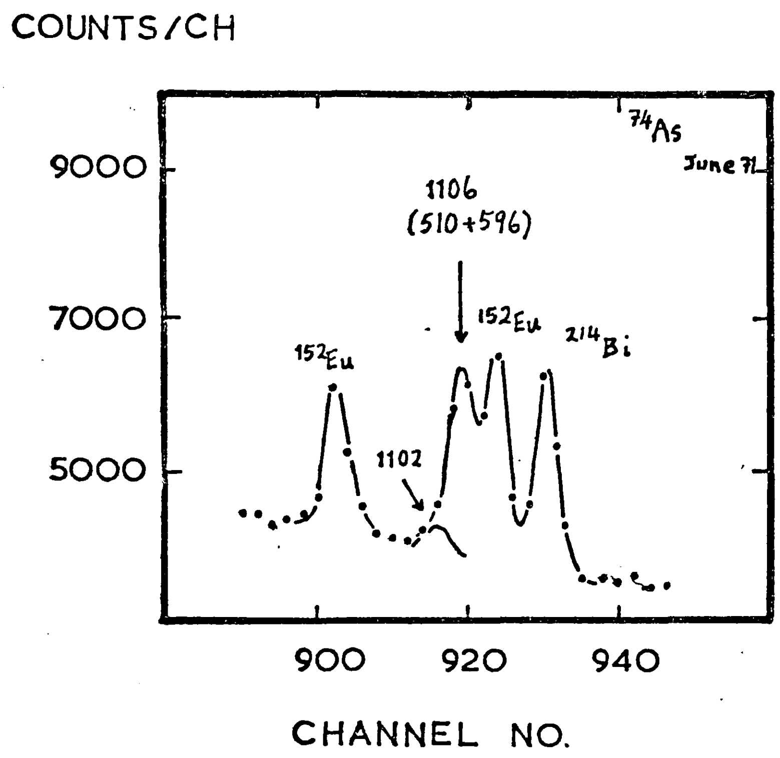


Fig. 6.4 Gamma spectrum in the energy region around 1100 keV taken with a 4 mm Pb absorber

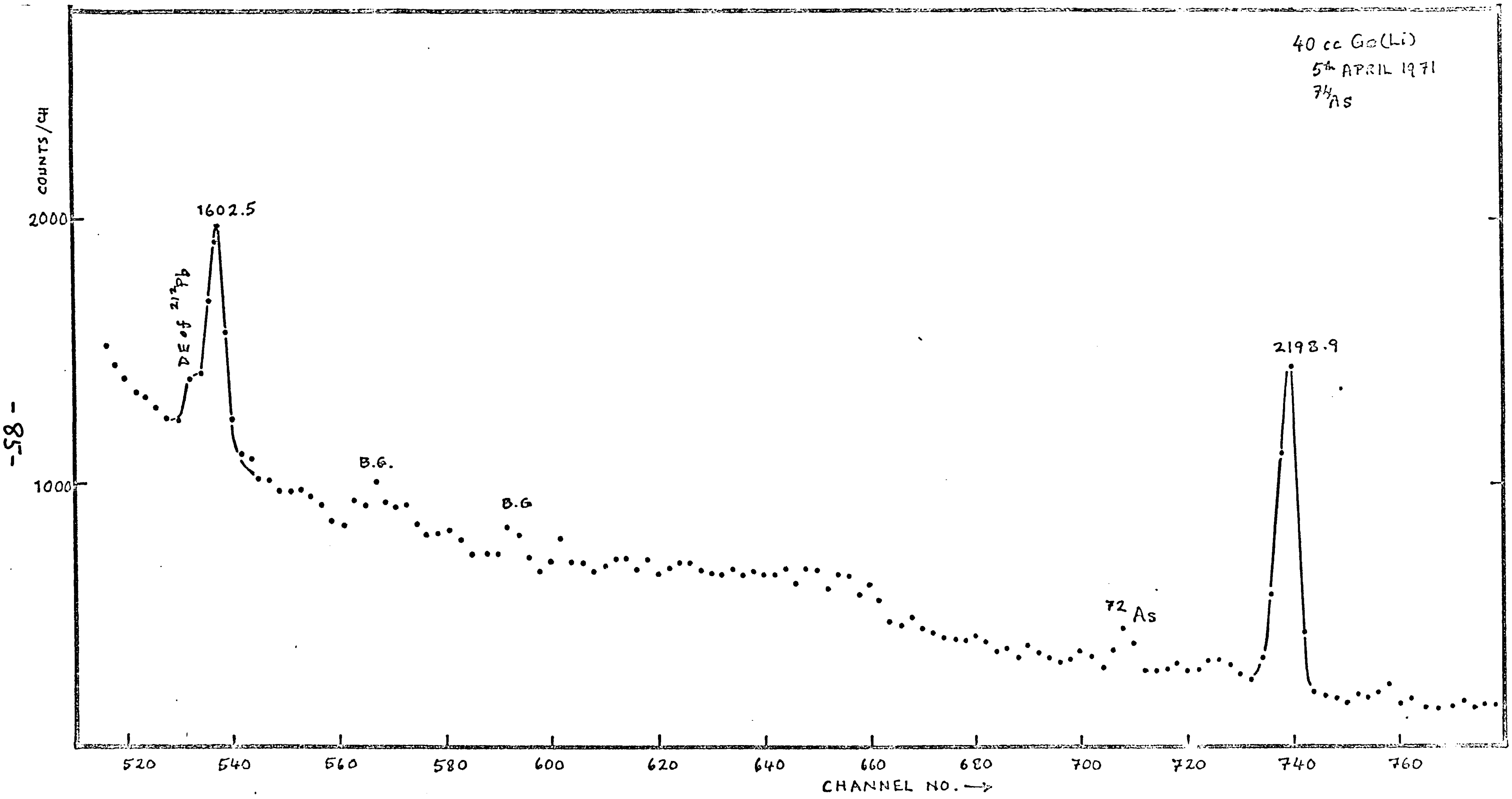


Fig. 6.5 Gamma spectrum in $^{74}$As decay - in the energy region 1550 to 2300 keV

Fig. 6.4 shows the gamma spectrum in the region of 1100 keV taken with a 4 mm lead absorber. The weak gamma ray at 1102 keV can be seen under the tail of the 1106 sum peak which is considerably reduced in intensity from that seen in Fig. 6.3 . Fig. 6.5 shows the gamma spectrum in the region 1550 to 2800 keV and shows the two gammas of $^{74}$Ge at 1602.5 keV and 2198.8 keV .

The energies and intensities of the gamma rays in the decay of $^{74}$As determined from the present work are shown in Table 6.1 together with those reported by Kukoc et.al (1968) and Hamilton et.al (1969) for comparison.

TABLE 6.1

Gamma ray energies and intensities in the decay of $^{74}As$

| Kukoc et.al (1968) $E_\gamma$ (keV) | $I_\gamma$ | Hamilton et.al (1969) $E_\gamma$ (keV) | $I_\gamma$ | Present Work $E_\gamma$ (keV) | $I_\gamma$ |
|---|---|---|---|---|---|
| 595.86±0.14 | 100.00 | 595.7±0.1 | 100.00 | 595.6±0.1 | 100.00 |
| 608.4±0.2 | 1.0 | 608.5±0.1 | 0.96±0.04 | 608.4±0.1 | 0.96±0.10 |
| 634.73±0.15 | 25.6 | 634.8±0.1 | 25.2±0.9 | 634.6±0.1 | 25.3±2.2 |
| | | 715.0±1.0 | 0.015±.005 | 714.7±1.0 | 0.013±.005 |
| | | 867.5±1.0 | 0.006±.002 | 867.2±1.0 | 0.005±.003 |
| 887.2±0.7 | 0.048 | 886.6±0.5 | 0.046±.004 | 886.8±0.2 | 0.040±.005 |
| 993.6±0.8 | 0.021 | 993.6±0.5 | 0.038±.004 | 993.5±0.2 | .033±.004 |
| | | 1101.6±1.0 | 0.013±.003 | 1102.0±1.0 | 0.011±.004 |
| 1204.6±0.4 | 0.47 | 1204.3±0.3 | 0.45±0.02 | 1204.2±0.2 | 0.44±0.05 |
| 1604.0±1.0 | 0.013 | 1602.5±0.7 | 0.012±.002 | 1602.5±1.0 | 0.014±.003 |
| 2198.8±1.0 | 0.019 | 2198.4±1.0 | 0.027±.002 | 2198.9±1.0 | 0.029±.005 |

## 6.3 Directional Correlations in Germanium-74

The directional correlation apparatus described in Chapter 3 was used for measuring the correlations in Germanium-74. The $^{74}As$ source was dissolved in acqueous solution and this was placed inside a cylindrical perspex source holder to produce a line source of 1.5 mm diameter and 4 mm length. The Ge(Li) crystal was kept at 3.5 cm from the source and the NaI(Tl) detector was on the movable arm at a distance of 7 cm from the source. The source was centred to within 1% as indicated by observing the peak singles intensity over the range $90^{\circ}$ to $270^{\circ}$.

The NaI(Tl) detector was gated on the 596 keV gamma. This included the unresolved 608 keV gamma transition in $^{74}Ge$ as well as the 634 keV gamma transition in $^{74}Se$. The Ge(Li) spectrum on the analyser gated by the NaI(Tl) detector was taken at angles of $90^{\circ}$, $105^{\circ}$, $120^{\circ}$, $135^{\circ}$, $150^{\circ}$, $165^{\circ}$ and $180^{\circ}$, and was repeated in the other quadrant from $180^{\circ}$ to $270^{\circ}$ again in steps of $15^{\circ}$. The counting time was 24 hours at each angle and the total counts in the NaI(Tl) gate were also recorded for each position. These counts were used to normalise the peak areas obtained in the coincidence spectrum to take into account the source decay and also any errors in source centring. Altogether three series of runs were taken.

Corrections for chance coincidences were calculated from the area of the 634 keV peak of $^{74}Se$ which appeared in the coincidence spectra.

The areas of the 608 keV peak in the spectra were determined by using the computer program SAMPO. These areas, after correcting for chance coincidences and normalising by the NaI(Tl) singles gate counts were fitted by a least squares procedure to the correlation function

$$W(\theta) = A_0 + A_{22}P_2(\cos\theta) + A_{44}P_4(\cos\theta)$$

Fig. 6.6 gives the correlation curve, that is $W(\theta)$ vs $\theta$, for the 608 - 596 keV cascade.

The experimentally determined correlation coefficients were then obtained from the least squares fitting procedure by

$$A_2^{expt} = A_{22}/A_0 = -0.2279 \pm 0.0360$$

$$A_4^{expt} = A_{44}/A_0 = 0.1869 \pm 0.0479$$

These results were corrected for finite solid angle effects. Correction factors for the NaI(Tl) detector were taken from the work of Yates (1965). Correction factors for our Ge(Li) detector have been calculated as discussed in Chapter 4. Referring to Fig. 4.3 and Fig. 4.4 and Table 4.1, the correction factor for $A_2$ for a gamma ray of 608 keV at a distance of 3.5 cm is $Q_2 = 0.9158$ and that for the coefficient $A_4$ has a value of $Q_4 = 0.7397$ .

The corrected values of the directional correlation coefficients were,

$$A_2 = -0.2587 \pm 0.0409 \quad \text{and} \quad A_4 = 0.2884 \pm 0.0744$$

These values agree with the results of Eichler et.al (1962) as well as with those of Hamilton et.al (1969). Table 6.2 gives a comparison of these values.

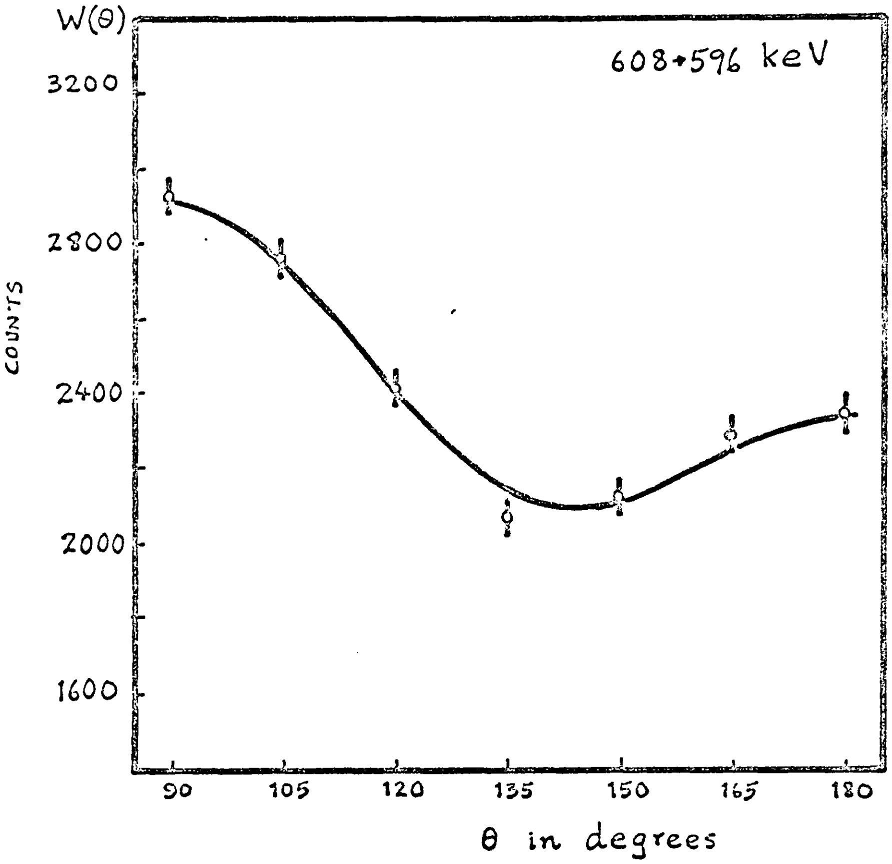


Fig. 6.6 Directional Correlation Curve for the 608 - 596 keV cascade in Germanium-74

TABLE 6.2

Values of $A_2$, $A_4$ for the 608 - 596 keV cascade in $^{74}Ge$

| $A_2$ | $A_4$ | |
|---|---|---|
| $-0.2587 \pm 0.0409$ | $0.2884 \pm 0.0744$ | Present Work |
| $-0.24 \pm 0.04$ | $0.30 \pm 0.05$ | Hamilton et.al(1969) |
| $-0.248 \pm 0.044$ | $0.251 \pm 0.070$ | Eichler et.al (1962) |

The errors in $A_2$ and $A_4$ were claculated by the method outlined in Chapter 2, Section 5.2 .

## 6.4 Multipole Mixing Ratio

The values of $A_2$ and $A_4$ determined from our experiment have been used to determine the correct spin sequence for the 608 - 596 keV cascade and the mixing ratio for the 608 keV transition. The method of Coleman (1958) has been employed in which possible values of $A_2$ and $A_4$ for particular spin sequences are plotted as a function of the mixing ratio. As the 596 keV transition is a pure multipole (electric quadrupole), the tabulated values of Taylor et.al (1971) have been used and when plotted they give the ellipses shown in Fig. 6.7 .

Our experimentally determined value of $A_2$ and $A_4$ is consistent with a spin sequence of 2 - 2 - 0 for the 608 - 596 keV cascade. The mixing ratio $\delta$ is determined to be 3.1 which gives an admixture of $(9.4^{+9.6}_{-4.6})$% M1 radiation for the 608 keV transition. Hamilton et.al (1969) obtained an M1 admixture of $(7^{+3}_{-6})$% for this transition while Eichler et.al (1963) gave a value of 9% .

The Davydov and Fillipov (1958) theory of asymmetric nuclei predicts a value for the ratio of E2/M1 multipole intensities given by

$$\delta^2(E2/M1) = 8.1 \times 10^{-5} Z^2 A^{4/3} E_\gamma^2$$

where $\delta^2(E2/M1)$ is the ratio of the intensities of the E2 and M1 components and $E_\gamma$ is in MeV. Using the values Z=32, A=74 for the 608 keV transition gives

$$\delta^2(E2/M1) = 9.538$$

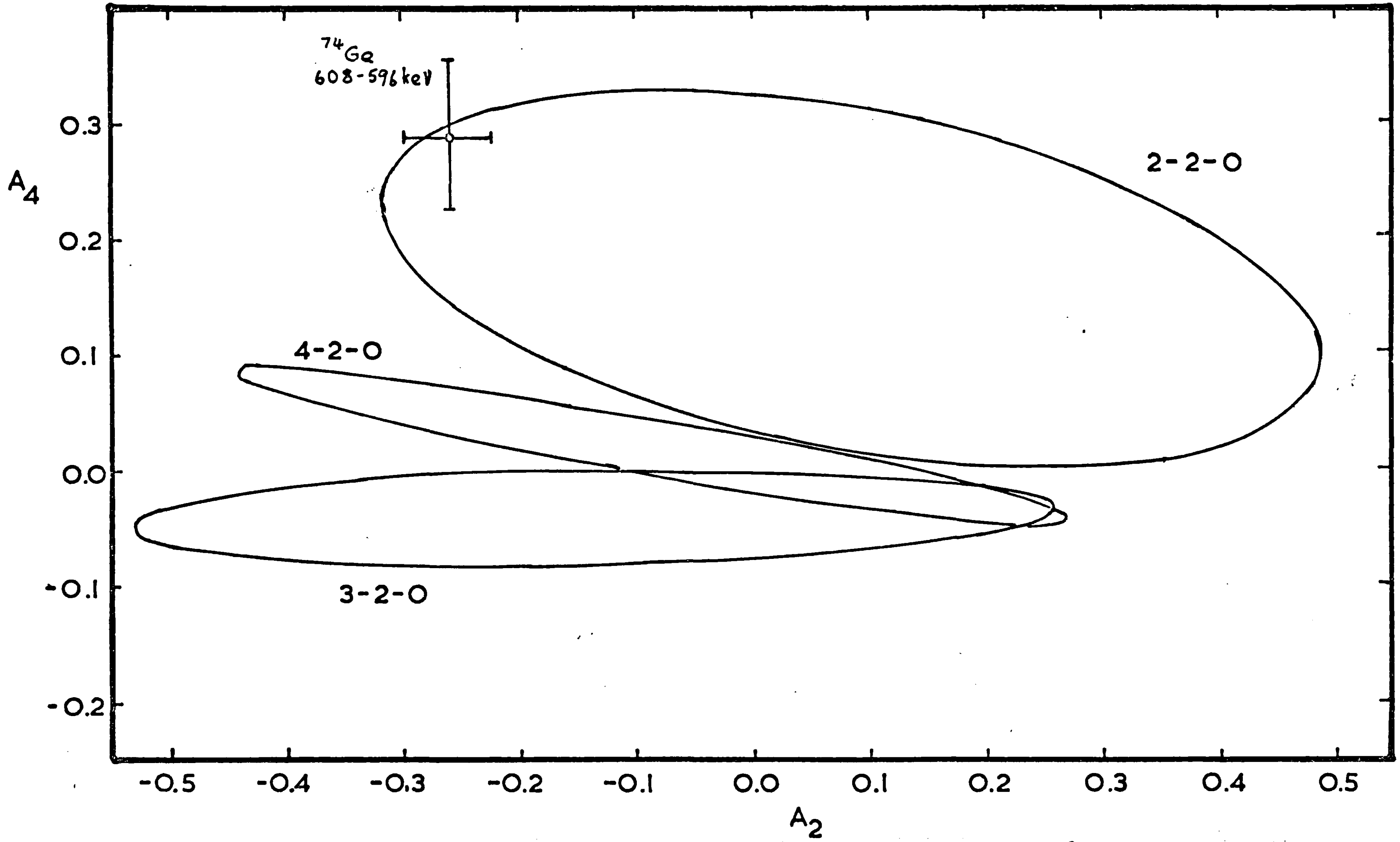


Fig. 6.7 Plot of $A_2$ vs $A_4$ as a function of the mixing parameter $\delta$ and for various I - 2 - 0 spin sequences

The mixing ratio determined from our experiment yields a value of 9.61 for $\delta^2$ which is in good agreement with the value predicted by the Davydov-Fillipov model.

Grechukhin (1963) has considered magnetic transitions in even-even nuclei with quadrupole type excitations and has given an expression for the multipole mixing ratio as follows -

$$\delta^2_{th}(E2/M1,\ I_1 \rightarrow I_2) = (441/500) \quad 1/f(I_1 I_2) \ (Z w M R_o^2/g_R)^2$$

where $f(I_1 I_2) = (I_1+I_2+3)(I_2-I_1+2)(I_1-I_2+2)(I_1+I_2-1)$, w is the transition energy in 0.511 MeV units, M is the nucleon mass equal to 1840, $R_o = 0.43\ e^2 A^{1/3}$ with $e^2 = 1/137$. $(Z/g_R)^2$ depends on the dynamics of collective motion and in the hydrodynamic model $Z/g_R = A$ ..

For the $2_2^+ \rightarrow 2_1^+$ transition in $^{74}Ge$, Grechukhin's formula predicts a value,

$$\delta^2_{th}(E2/M1, 2_2^+ \rightarrow 2_1^+) = 8.3064$$

## 6.5 Reduced Transition Probabilities

From the values of the relative intensities and the energies of the gamma transitions measured in this experiment, the following ratios of reduced transition probabilities have been calculated.*

$$\frac{B(E2;2_2^+\rightarrow 2_1^+)608\gamma}{B(E2;2_1^+\rightarrow 0^+)596\gamma} = \cancel{0.00782\pm 0.0009}\ \ 0.555 \pm 0.064$$

$$\frac{B(E2;2_2^+\rightarrow 0^+)1204\gamma}{B(E2;2_1^+\rightarrow 0^+)\ 596\gamma} = \cancel{0.00013\pm 0.00002}\ \ 0.0092 \pm 0.014$$

$$\frac{B(E2;0_1^+\rightarrow 2_1^+)887\gamma}{B(E2;2_1^+\rightarrow 0^+)596\gamma} = \cancel{(5.466\pm 0.711)\times 10^{-5}}\ \ 0.119 \pm 0.015$$

According to the simple vibrational model (Meyer,1970) the ratio of the reduced transition probabilities $B(E2;I^+\rightarrow 2_1^+)/\ B(E2;2_1^+\rightarrow 0^+)$ should equal 2 for I = 0,2,4 members of the two-phonon vibrational levels. However most of the modified models which introduce anharmonicity to the simple vibrational model predict the reduced transition probability B(E2) to have larger values for the direct transitions $2_2^+\rightarrow 2_1^+$ and $2_1^+\rightarrow 0^+$ than for the crossover transition $2_2^+\rightarrow 0^+$ (Raz,1959; Scharff-Goldhaber and Weneser,1955; Davydov and Fillipov,1958) .

In the linearised quasi-particle random phase approximation theory (Kisslinger and Sorenson, 1963) the two-phonon $2^+$ to ground state transition $(2_2^+\rightarrow 0^+)$ transition is forbidden. This is in qualitative agreement with the small $B(E2;2_2^+\rightarrow 0^+)$ value compared to the $B(E2;2_1^+\rightarrow 0^+)$ we have measured.

*N.B. Account has been taken of the population of the levels, and the effect of internal conversion has been estimated to be only ~ 0.3% of the gamma intensity and hence negligible.

McGowan and Stelson (1962) have measured the values of the reduced transition probabilities in $^{74}$Ge by Coulomb excitation methods. They obtained a value of 0.317 $e^2 \times 10^{-48}$ cm$^4$ for the excitation of the first $2^+$ state in $^{74}$Ge. That is,

$$B(E2;0^+\rightarrow 2_1^+) = 0.317\ e^2 \times 10^{-48}\ \mathrm{cm}^4 \quad .$$

The reduced transition probability in Coulomb excitation is related to the reduced transition probability in gamma emission through the following formula ( Moszkowski, 1957) ,

$B(f \rightarrow i)/\ B(i \rightarrow f) = (2I_i+1)/(2I_f+1)$ where i and f refer to the initial and final states respectively. For example, if $B(i\rightarrow f)$ refers to the reduced transition probability in a gamma transition from the state i to the state f , $B(f\rightarrow i)$ would represent the Coulomb excitation of the nucleus from the state f to the state i.

Using this relationship the reduced transition probability for emission of the 596 keV gamma ray is determined to have a value

$$B(E2;2_1^+\rightarrow 0^+)596\gamma = (0.0634\pm0.0044)\ e^2\times 10^{-48}\ \mathrm{cm}^4$$

In terms of the Weisskopf single particle units

$$B(E2;2_1^+\rightarrow 0^+)596\gamma = 34.1\pm2.4 \ \ \mathrm{spu}$$

Using the ratios of the reduced transition probabilities we have calculated, the various B(E2) values may be expressed in units of $e^2\times10^{-48}$ cm$^4$ as:-

$$B(E2;2_2^+\rightarrow 2_1^+)608\gamma = \cancel{(495.8\pm59.5)\times 10^{-6}} \quad 0.035\pm 0.004$$

$$B(E2;2_2^+\rightarrow 0^+)1204\gamma = \cancel{(8.24\pm1.45)\times 10^{-6}} \quad 0.00058 \pm 0.00008$$

$$B(E2;0_1^+\rightarrow 2_1^+)887\gamma = \cancel{(3.46\pm0.48)\times 10^{-6}} \quad 0.0075 \pm 0.0011$$

## 6.6 Discussion of the Level Scheme

The spin of the ground state of $^{74}$As is most likely to be $2^-$ although it has not been directly measured. Hamilton et.al (1969) note that the log ft values to the $2^+$ levels of $^{74}$Ge are compatible with log ft values for first forbidden non-unique transitions from the $2^-$ ground state of $^{74}$As. The transitions to the ground state, the $4^+$ state at 1463 keV and the $0^+$ state at 1483 keV of $^{74}$Ge have log ft values which are in the range of first forbidden unique transitions for the $2^-$ state of $^{74}$As. The negative parity is also supported by the $\beta$-$\gamma$ angular correlation work of Habib et.al (1966).

The energies and spins of the $2^+$ levels at 595.6, 1204.2 and 2198.8 keV in $^{74}$Ge are well established by previous work (Kukoc et.al, 1968; Hamilton et.al, 1969) as well as by the present measurements.

The energy of the 1483 keV level is also well established. Darcey (1964) from his (t,p) work predicts zero spin for this level. The directional correlation measurement of Hamilton et.al (1969) has established the spin of this level to be $0^+$. The nuclear photo excitation work of Moreh and Shahal (1970) also gives a $0^+$ spin assignment to this level.

Our detection of the weak transitions of 867.2 keV and 1102 keV supports the existence of levels at 1463 keV and 1697 keV proposed by Hamilton et.al (1969). The 1463 keV level has also been observed in nuclear reaction studies of Weitkamp et.al (1966), Darcey (1964) and Brown et.al (1967). It was also seen in the decay of $^{74}$Ga by Camp et.al (1971). Because of the absence of any significant crossover transition to the ground state a spin assignment of $0^+$ or $4^+$ to this level is possible, but as the 1483 keV level has been established to have a $0^+$ spin (Hamilton et.al, 1969) the spin assignment of $4^+$ is favoured for the 1463 keV level. The $2^+$, 1204 keV level, the $0^+$, 1483 keV level and the $(4^+)$, 1463 keV level could be the two-phonon triplet predicted by the vibrational model.

The level at 1697 keV was proposed on the observation of the weak 1102 keV gamma ray seen in the decay of $^{74}$As. A level at about this energy was also observed in the $(n,\gamma)$ work of Weitkamp et.al (1966) and in the $^{74}$Ga decay studies of Eichler et.al (1962) and Camp et.al (1971). As the log ft value to the 1697 keV level indicates a first forbidden unique transition, a spin of $0^+$ or $4^+$ is favoured.

A relatively strong gamma ray observed at 634.6 keV is due to the transition from the first excited $2^+$ state in $^{74}$Se. We are, however, unable to confirm the existence of a 1269 keV level in $^{74}$Se tentatively proposed by Kukoc et.al (1968).

## 6.7 Conclusions

The results of this experiment confirm the existence of the three new gamma transitions in $^{74}$Ge reported by Hamilton et.al (1969) and support their proposal that the 1697 keV level is populated in the decay of $^{74}$As. Our result on the ratio of the E2/M1 multipole intensities agrees with the value predicted by the Davydov-Fillipov theory of asymmetric nuclei. The reduced transition probabilities have been calculated for the gamma transitions in $^{74}$Ge. These values together with the energies and spins of the levels indicate that the $^{74}$Ge nucleus can be represented by the collective model. Our measurements are in agreement with the general qualitative predictions made by the various refinements of the basic collective-vibrational model.

It appears that the independent work of van Hise and Paperiello (1972) also confirms the existence of the gamma transitions of 715 keV, 867 keV and 1102 keV. Their measured values of the intensities for these transitions are 0.014, 0.0088 and 0.01 respectively. Using a Compton suppression spectrometer with a central Ge(Li) detector these authors have also reported two additional gamma transitions of energy 734.2 keV (0.0059) in $^{74}$Ge and 1269.6 keV (0.0031) in $^{74}$Se. This latter transition appears to confirm the proposal of Kukoc et.al (1968) for the existence of a level at 1269 keV in $^{74}$Se.

Van Hise and Papierello (1972) have considered the low lying levels of $^{74}$Ge to be separable into a quasi ground rotational band and quasi $\beta$- and $\gamma$-vibrational bands in analogy with similar bands found in highly deformed nuclei. This appears to be a qualitatively good approach but on comparison with the levels of neighbouring $^{70}$Ge and $^{72}$Ge nuclei the trend is found to be imperfect. Van Hise and Papierello (1972) conclude that this is not surprising since the rotational formalism is bound to suffer in the region of traditionally spherical nuclei. However, it is possible that the low lying levels of $^{74}$Ge could be explained equally well by both the vibrational and rotational formalisms of the collective model.

## CHAPTER 7 STUDIES ON THE DECAY OF NEODYMIUM - 147

### 7.1 Introduction

The beta decay of 11.1 day neodymium - 147 to excited states of promethium - 147 has been studied by many investigators and different decay schemes have been suggested. Excited levels at 91.1, 410.5, 489.3, 531.0 and 685.9 keV above the ground state in $^{147}$Pm have been established by recent work with Ge(Li) detectors. Hill and Weidenbeck (1967) used a 2 metre curved crystal spectrometer as well as a Ge(Li) detector and have introduced an additional level at 680.4 keV. The work of Canty and Conner (1967), Jacobs et.al (1967), using Ge(Li) detectors, also support the existence of this level.

Gunye, Jambunathan, and Saraf (1961) and Spring (1963) from studies with scintillation detectors have proposed a level at 720 keV depopulating to the 410 keV level through a 310 keV gamma transition. This gamma ray was, however, not detected in the work of Hill and Weidenbeck (1967), Canty and Conner (1967) and Jacobs et.al (1967). More recently Singh et.al (1971) using a Ge(Li) detector have proposed a level at 723 keV depopulating via a 312 keV transition to the 411 keV level. These authors also detected the 590 and 680 keV gamma transitions depopulating the 680 keV level proposed by Hill and Weidenbeck (1967). In addition they reported another gamma ray of 299.7 keV which was assigned to $^{147}$Pm but not placed in the decay scheme.

The Ge(Li) - NaI(Tl) coincidence studies of Jacobs et.al (1967) suggest the existence and location of a 78 keV gamma (489 - 410keV) and a 154 keV gamma (686 - 531 keV). These gamma rays were not detected by Hill and Weidenbeck (1967) and Canty and Conner (1967).

Additional levels have been proposed at 182 keV by Wendt and Kleinheinz (1960), Sastry et.al (1964) and Rajput and Sehgal (1967), and at 230 keV by P.R. Evans (1958). Recent measurements with Ge(Li) detectors fail to support the existence of these levels.

Directional correlations of the gamma transitions in $^{147}$Pm were studied by Bodenstedt et.al (1960), Arya (1961), Saraf et.al (1961), Spring (1963), and Gopinatham (1966). All these measurements employed scintillation detectors. Recently, Blaskovich and Arya (1970) used a 10 cc Ge(Li) detector in conjunction with a 2" x 2" NaI(Tl) crystal to measure the gamma-gamma directional correlations in $^{147}$Pm.

The spin of the $^{147}$Nd ground state has been established as $5/2^-$ by the paramagnetic-resonance studies of Kedzie et.al (1957) and by Cabezas et.al (1960) who employed the atomic beam magnetic resonance method.

The ground state spin of $^{147}$Pm has been measured to be $I = 7/2^+$ by Klinkenberg and Tomkins (1960) from their optical hyperfine structure studies. This corresponds to the $g_{7/2}$ shell-model state. Cabezas et.al (1960) also obtained the same spin value for this state.

The spin of the 91 keV first excited level of $^{147}Pm$ has been determined to be $5/2^+$. From measurements of subshell ratios the 91 keV gamma is known to be a mixture of M1 and E2 radiation. This limits the spin of the 91 keV level to 5/2, 7/2 or 9/2 with positive parity. The nuclear orientation experiments of Westenberger and Shirley (1961) excluded a 7/2 spin assignment. The log ft value of 7.4 for the 807 keV beta transition from the ground state of the $5/2^-$ $^{147}Nd$ (Jacobs et.al, 1967) eliminates the spin 9/2 possibility. Therefore the 91 keV level is assigned a spin of $5/2^+$.

In previous $\gamma$-$\gamma$ directional correlation studies Bodenstedt et.al (1960) obtained a spin of $5/2^+$ for the 410 keV level while Arya (1961) determined it to be $7/2^+$ and Saraf et.al (1961) favoured an assignment of $7/2^+$ while they do not rule out the $3/2^+$ and $5/2^+$ possibilities. The recent measurements of Blaskovich and Arya (1970) favour a $3/2^+$ spin assignment to this level. Hill and Weidenbeck (1967) from their measurements of relative photon intensities with a Ge(Li) detector list $3/2^+$ and $7/2^+$ as the possible spin choices. Westenberger and Shirley (1961) from their nuclear orientation studies were also only able to limit the spin choices to $3/2^+$ or $7/2^+$.

Hill and Wiedenbeck (1967) were not able to eliminate possible spin choices of $3/2^+$, $5/2^+$, $7/2^+$ for the 489 keV level. Bodenstedt et.al (1960) favour a $5/2^+$ spin with $7/2^+$ being listed as possible choice also. Saraf et.al (1961) favour the spin $7/2^+$ although retaining $5/2^+$ as a possible choice. Blaskovich and Arya (1970) affixes a value $5/2^+$ Canty and Conner (1967) favour a spin of $7/2^+$ for this level.

The spin of the 531 keV level is assigned a value $5/2^+$ by most investigators (Ewan et.al, 1961; Spring, 1963; Canty and Conner, 1967; Hill and Weidenbeck, 1967; Blaskovich and Arya, 1970). Only Bodenstedt (1960) favours $3/2^+$ spin while listing $7/2^+$ as another possibility.

Ewan et.al (1961) suggested spin values of $5/2^+$ or $3/2^+$ for the 686 keV level. Westenberger and Shirley (1961) propose $5/2^+$ or $7/2$ while Hill and Weidenbeck (1967) favour $5/2^+$ with $7/2^+$ as a possible choice also. Saraf et.al (1961), Arya (1961), Spring (1963), Canty and Conner (1967), Blaskovich and Arya (1970) all agree on the choice of spin $5/2^+$ for this level.

Hill and Weidenbeck (1967) suggest the spin of their proposed level at 680 keV to be either $5/2^+$ or $7/2^+$.

The discrepancies reported in the number of gamma transitions, the nuclear energy levels and the spin assignments prompted this study of the gamma transitions and their directional correlations in $^{147}Pm$.

## 7.2 Experimental Procedure

The radioactive sources were prepared by irradiating 99.9% pure (spec-pure) neodymium oxide ($Nd_2O_3$) in the thermal neutron flux of the University of London Reactor. The sources were used in the powder form in sealed cylindrical polythene containers for singles spectra.

A source was also purchased from the Radiochemical Centre, Amersham. This was in the form of neodymium chloride in dilute hydrochloric acid.

The sources were allowed to decay for about two weeks to permit the short lived $^{149}$Nd and $^{151}$Nd to die. Singles spectra were measured with the sources 5 cms from the 40 cc Ge(Li) detector.

## 7.3 Analysis of Ge(Li) Singles Spectra

The gamma spectra obtained with the Ge(Li) detector were analysed by using the computer program SAMPO Fig. 7.1 shows the complete gamma spectrum contained within the energy region 0-780 keV. The main gamma rays of $^{147}$Nd are indicated by their energies in keV. Peaks due to naturally occurring radioactivity ($^{226}$Ra and daughters) are identified by isotope. The decay of $^{147}$Nd was followed over a period of two months, that is over 5 lifetimes. A peak at about 155 keV was detected by SAMPO. The statistical significance of this peak was around 3.8

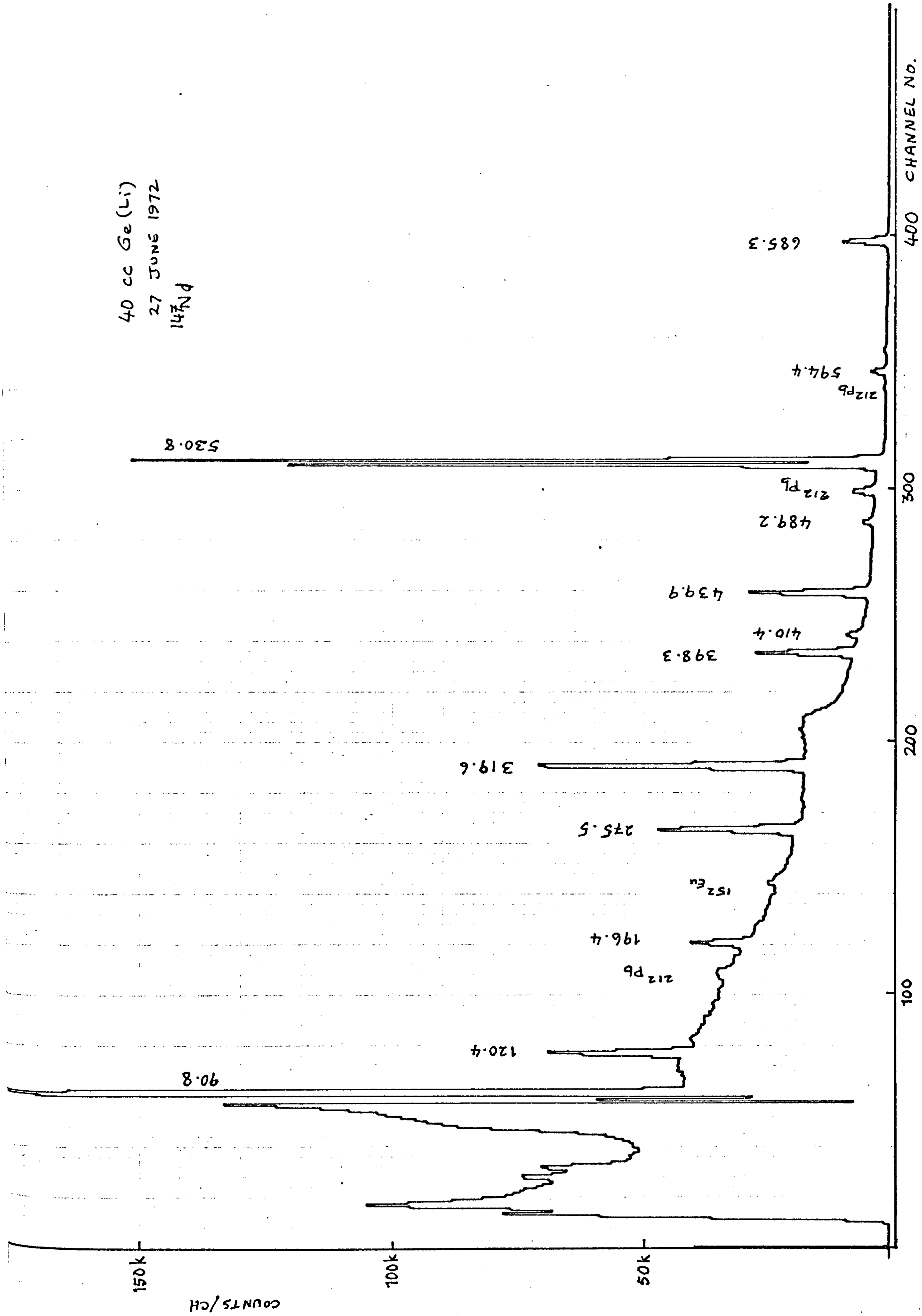


Fig. 7.1 Complete gamma spectrum in the decay of $^{147}$Nd in the energy region 0 - 780 keV

in most of the runs.

The statistical significance of a potential peak in channel is measured as

$$ss_i = dd_i / sd_i$$

where the generalised second-difference expression

$$dd_i = \sum_{j=-k} c_j \; n_{i+j}$$

is divided by its standard deviation

$$sd_i = \left[ \sum_{j=-k}^{k} c_j^2 \; n_{i+j} \right]^{\frac{1}{2}}$$

The expressions of $dd_i$ and $sd_i$ are obtained by summing over 2k+1 channels the counts per channel $n_i$, multiplied by the coefficient $c_j$. The $c_j$ 's define a weighting function which is designed to enhance the detection of real photopeaks and to discriminate against statistical fluctuations and spurious peaks.

The 155 keV peak corresponds to the gamma transition from the 686 keV level to the 531 keV level. The existence of this gamma transition was previously reported from coincidence data by Jacobs et.al (1967) although it was not directly seen in their Ge(Li) spectra.

The gamma ray of 310 keV reported by Blaskovich and Arya (1970) and proposed by some earlier investigations (Gunye et.al, 1961; Spring, 1963) was not found in this experiment. The search was made down to a statistical significance of 2.00. However a peak at 307.7 keV started appearing in the gamma spectra taken about two months after the production of the source. The lifetime of this peak was estimated from the values of its intensity relative to the 91 keV gamma of $^{147}$Nd taken at an interval of 120 days. Its value was found to be (29 $\pm$ 5) days. It has been identified as a gamma transition in the impurity $^{169}$Yb which has a half-life of 32 days. Other gamma rays of $^{169}$Yb (109.5, 130.6, 177 and 197 keV) were also identified. This conclusion is in conflict with that of Blaskovich and Arya (1970) who, having found the lifetime of the transition to be "comparable" with that of $^{147}$Nd, proceeded to assign the transition to this isotope.

The 299.7 keV gamma ray reported by Singh et.al (1971) was not detected in this experiment. The 78 keV gamma transition suggested by Jacobs et.al (1967) was also not observed.

The 589 keV and 680 keV gamma rays first reported by Hill and Weidenbeck (1967) were detected in this investigation. These gamma rays were not completely resolved from the nearby 594 keV and 686 keV peaks but were analysed by SAMPO as shown in Fig. 7.2 and Fig.7.3.

In both figures the presence of the weak transitions at the lower tails of the stronger peaks can be seen in the first analysis by SAMPO. A second analysis taking into account the presence of the weak transitions gives the excellent agreement between data and fit seen in these figures.

The energies and intensities of the gamma transitions

CHAN. DEV. CONTINUUM YMIN= 1.803E+03 IIIIIIIIIIIII SEMILOGARITHMIC SCALE IIIIIIIIIIIII YMAX= 1.774E+04

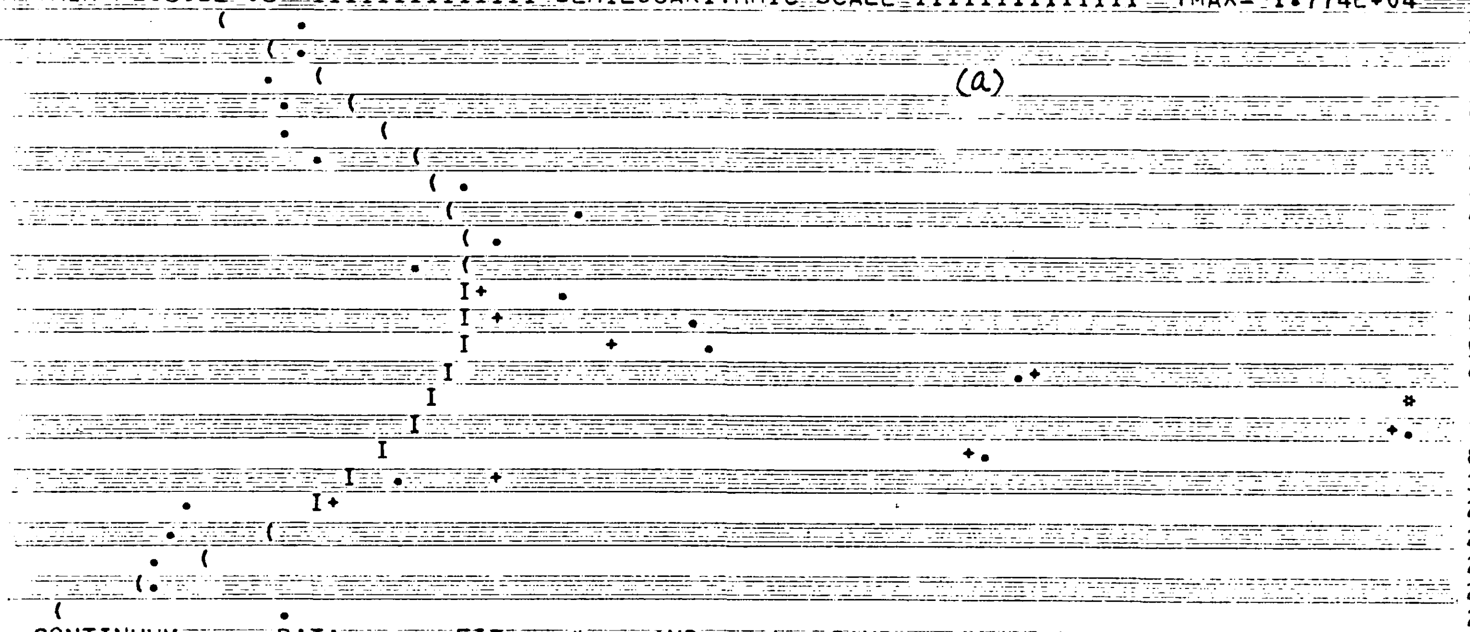


| CHAN. | DEV. | CONTINUUM | DATA | FIT |
|---|---|---|---|---|
| 378 | 7.2 | 2.37E+03 | 2.750E+03 | 2.373E+03 |
| 379 | 2.5 | 2.61E+03 | 2.747E+03 | 2.614E+03 |
| 380 | -4.1 | 2.83E+03 | 2.621E+03 | 2.830E+03 |
| 381 | -6.4 | 3.02E+03 | 2.688E+03 | 3.021E+03 |
| 382 | -10.2 | 3.19E+03 | 2.662E+03 | 3.186E+03 |
| 383 | -10.0 | 3.33E+03 | 2.798E+03 | 3.326E+03 |
| 384 | 2.9 | 3.44E+03 | 3.615E+03 | 3.440E+03 |
| 385 | 12.5 | 3.53E+03 | 4.357E+03 | 3.529E+03 |
| 386 | 3.9 | 3.59E+03 | 3.835E+03 | 3.593E+03 |
| 387 | -5.5 | 3.63E+03 | 3.318E+03 | 3.633E+03 |
| 388 | 9.4 | 3.64E+03 | 4.278E+03 | 3.663E+03 |
| 389 | 20.1 | 3.63E+03 | 5.228E+03 | 3.773E+03 |
| 390 | 10.4 | 3.59E+03 | 5.380E+03 | 4.615E+03 |
| 391 | -3.4 | 3.53E+03 | 9.121E+03 | 9.449E+03 |
| 392 | -2.4 | 3.44E+03 | 1.742E+04 | 1.774E+04 |
| 393 | 2.9 | 3.32E+03 | 1.741E+04 | 1.703E+04 |
| 394 | 2.5 | 3.18E+03 | 8.633E+03 | 8.400E+03 |
| 395 | -10.3 | 3.02E+03 | 3.220E+03 | 3.804E+03 |
| 396 | -12.3 | 2.82E+03 | 2.283E+03 | 2.871E+03 |
| 397 | -9.0 | 2.61E+03 | 2.185E+03 | 2.608E+03 |
| 398 | -4.0 | 2.36E+03 | 2.178E+03 | 2.364E+03 |
| 399 | 1.6 | 2.10E+03 | 2.170E+03 | 2.096E+03 |
| 400 | 16.7 | 1.80E+03 | 2.662E+03 | 1.803E+03 |

SYMBOLS I = CONTINUUM . = DATA + = FIT * = .AND+ ( = IAND+ ) = IAND. £ = IAND+AND.

CHAN. DEV. CONTINUUM YMIN= 2.137E+03 IIIIIIIIIIIII SEMILOGARITHMIC SCALE IIIIIIIIIIIII YMAX= 1.755E+04

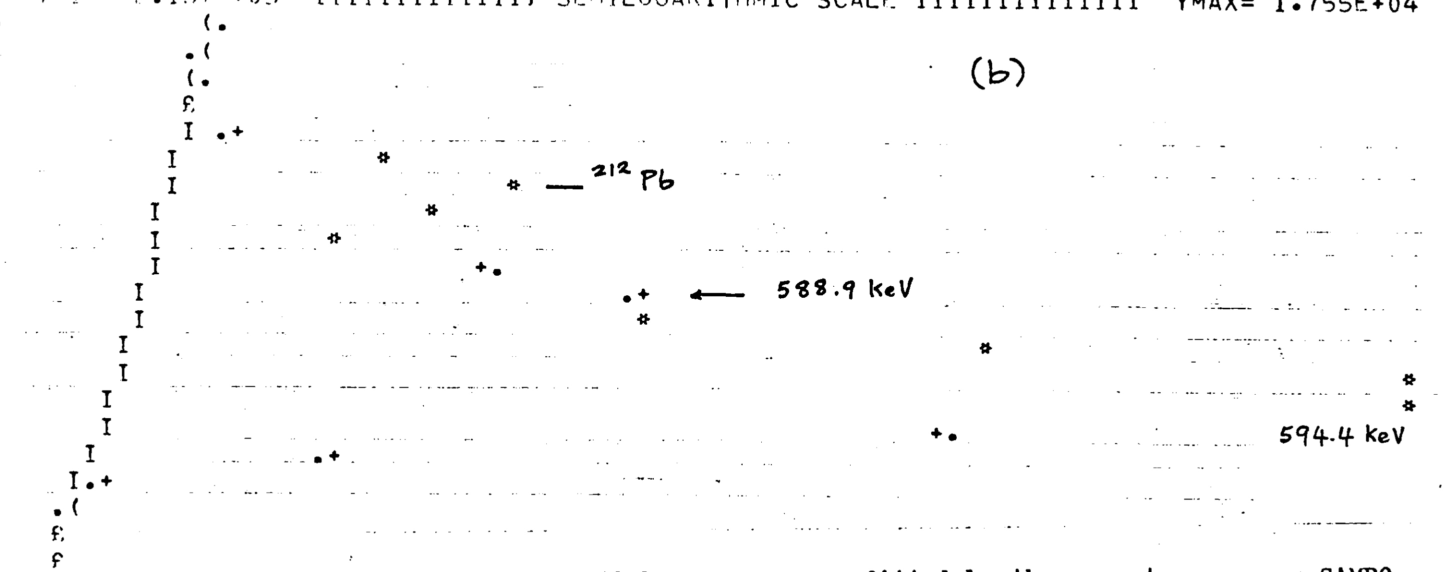


| CHAN. | DEV. | CONTINUUM | DATA | FIT |
|---|---|---|---|---|
| 379 | .9 | 2.70E+03 | 2.747E+03 | 2.701E+03 |
| 380 | -1.2 | 2.68E+03 | 2.621E+03 | 2.681E+03 |
| 381 | .5 | 2.66E+03 | 2.688E+03 | 2.664E+03 |
| 382 | -.1 | 2.64E+03 | 2.662E+03 | 2.667E+03 |
| 383 | -.8 | 2.62E+03 | 2.798E+03 | 2.842E+03 |
| 384 | .4 | 2.59E+03 | 3.615E+03 | 3.591E+03 |
| 385 | .1 | 2.57E+03 | 4.357E+03 | 4.349E+03 |
| 386 | -.5 | 2.54E+03 | 3.835E+03 | 3.867E+03 |
| 387 | .6 | 2.52E+03 | 3.318E+03 | 3.284E+03 |
| 388 | 1.2 | 2.49E+03 | 4.278E+03 | 4.198E+03 |
| 389 | -1.7 | 2.46E+03 | 5.228E+03 | 5.354E+03 |
| 390 | 1.0 | 2.43E+03 | 5.380E+03 | 5.308E+03 |
| 391 | 1.4 | 2.40E+03 | 9.121E+03 | 8.991E+03 |
| 392 | -1.0 | 2.37E+03 | 1.742E+04 | 1.755E+04 |
| 393 | -.8 | 2.34E+03 | 1.741E+04 | 1.752E+04 |
| 394 | 2.0 | 2.31E+03 | 8.633E+03 | 8.451E+03 |
| 395 | -1.1 | 2.28E+03 | 3.220E+03 | 3.280E+03 |
| 396 | -.6 | 2.24E+03 | 2.283E+03 | 2.310E+03 |
| 397 | -.6 | 2.21E+03 | 2.185E+03 | 2.211E+03 |
| 398 | .1 | 2.17E+03 | 2.178E+03 | 2.174E+03 |
| 399 | .7 | 2.14E+03 | 2.170E+03 | 2.137E+03 |

SYMBOLS I = CONT

**Fig. 7.2 The unresolved 589+594 keV gamma rays fitted by the computer program SAMPO**

**(a) first run (b) second run**

CHAN. DEV. CONTINUUM YMIN= 1.298E+03 IIIIIIIIIIIII SEMILOGARITHMIC SCALE IIIIIIIIIIIII YMAX= 4.802E+04

| CHAN. | DEV. | CONTINUUM | DATA | FIT |
|---|---|---|---|---|
| 444 | -9.9 | 2.11E+03 | 1.705E+03 | 2.113E+03 |
| 445 | -6.1 | 2.06E+03 | 1.801E+03 | 2.059E+03 |
| 446 | 4.4 | 2.00E+03 | 2.234E+03 | 2.024E+03 |
| 447 | 12.3 | 1.94E+03 | 2.778E+03 | 2.131E+03 |
| 448 | 8.8 | 1.88E+03 | 3.787E+03 | 3.243E+03 |
| 449 | 4.2 | 1.82E+03 | 1.167E+04 | 1.122E+04 |
| 450 | -3.4 | 1.77E+03 | 3.424E+04 | 3.486E+04 |
| 451 | -2.1 | 1.71E+03 | 4.756E+04 | 4.802E+04 |
| 452 | 1.1 | 1.65E+03 | 2.757E+04 | 2.738E+04 |
| 453 | 4.2 | 1.59E+03 | 7.638E+03 | 7.269E+03 |
| 454 | -1.4 | 1.54E+03 | 1.970E+03 | 2.032E+03 |
| 455 | -.5 | 1.48E+03 | 1.474E+03 | 1.495E+03 |
| 456 | -2.2 | 1.42E+03 | 1.340E+03 | 1.420E+03 |
| 457 | -1.8 | 1.36E+03 | 1.298E+03 | 1.362E+03 |

SYMBOLS I = CONTINUUM . = DATA + = FIT * = .AND+ ( = IAND+ ) = IAND. £ = IAND+AND.

CHAN. DEV. CONTINUUM YMIN= 1.287E+03 IIIIIIIIIIIII SEMILOGARITHMIC SCALE IIIIIIIIIIIII YMAX= 4.761E+04

| CHAN. | DEV. | CONTINUUM | DATA | FIT |
|---|---|---|---|---|
| 442 | -.4 | 1.73E+03 | 1.718E+03 | 1.733E+03 |
| 443 | 1.7 | 1.75E+03 | 1.820E+03 | 1.748E+03 |
| 444 | -1.4 | 1.75E+03 | 1.705E+03 | 1.764E+03 |
| 445 | -.7 | 1.76E+03 | 1.801E+03 | 1.832E+03 |
| 446 | 1.2 | 1.75E+03 | 2.234E+03 | 2.179E+03 |
| 447 | -.6 | 1.74E+03 | 2.778E+03 | 2.807E+03 |
| 448 | -.4 | 1.72E+03 | 3.787E+03 | 3.811E+03 |
| 449 | 2.4 | 1.70E+03 | 1.167E+04 | 1.141E+04 |
| 450 | -1.3 | 1.67E+03 | 3.424E+04 | 3.448E+04 |
| 451 | -.2 | 1.63E+03 | 4.756E+04 | 4.761E+04 |
| 452 | -.2 | 1.59E+03 | 2.757E+04 | 2.760E+04 |
| 453 | 1.8 | 1.54E+03 | 7.638E+03 | 7.478E+03 |
| 454 | -1.4 | 1.49E+03 | 1.970E+03 | 2.034E+03 |
| 455 | .7 | 1.43E+03 | 1.474E+03 | 1.447E+03 |
| 456 | -.6 | 1.36E+03 | 1.340E+03 | 1.360E+03 |
| 457 | .3 | 1.29E+03 | 1.298E+03 | 1.287E+03 |

SYMBOLS I = CONTINUUM . = DATA + = FIT * = .AND+ ( = IAND+ ) = IAND. £ = IAND+AND.

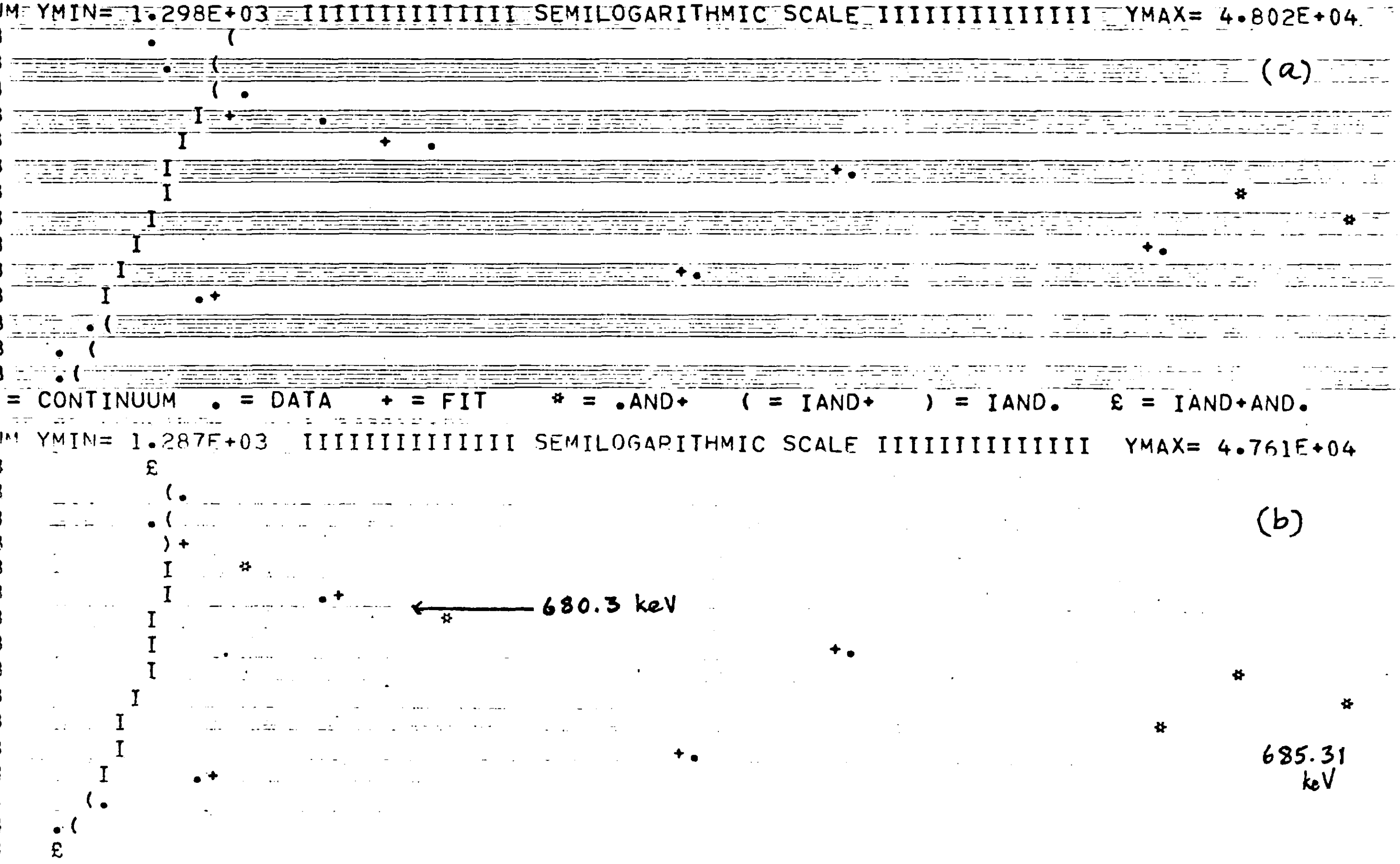


**Fig. 7.3 The unresolved 680+686 keV gamma rays fitted by the computer program SAMPO**

**(a) first run (b) second run**

measured in this work are shown in Table 7.1 together with those of Canty and Conner (1967) and Hill and Weidenbeck (1967) for comparison.

## 7.4 Directional Correlations of the Gamma Transitions in Promethium - 147

The sources used in the directional correlation measurement were prepared by neutron irradiation of specpure $Nd_2O_3$ at the University of London Reactor. Measurements were started about 3 weeks after irradiation to allow the short lived impurities to decay. The irradiated $Nd_2O_3$ was dissolved in 0.1N HCl solution and placed in small cylindrical perspex holders to produce a line source of 2 mm diameter by 5 mm length.

Directional correlation of ~~transitions~~ cascades involving the 91 keV transition were measured. The NaI(Tl) detector selected the 91 keV gamma rays and after processing in the fast-slow coincidence system (See Chapter 3) provided the gating signal to the multichannel analyser. The resulting Ge(Li) spectrum which is in coincidence with the 91 keV gamma rays was observed on the multichannel analyser. The NaI(Tl) crystal was at a distance of 7 cm from the source and the Ge(Li) crystal was at a distance of 5 cm from the source. The source was centred on the directional correlation apparatus in such a way that the singles counting rate in the movable detector arm (i.e. the NaI(Tl)) was constant to within 1% at each angular position. Coincidence spectra were taken with the NaI(Tl)

TABLE 7.1

Energies and intensities of gamma transitions in $^{147}Pm$

| Canty and Conner (1967) | | Hill and Weidenbeck (1967) | | Present Work | |
|---|---|---|---|---|---|
| E (keV) | I | E (keV) | I | E (keV) | I |
| 91.0 | 211±20% | 91.105±0.0016 | 227±35 | 90.8±0.2 | 224±31 |
| 120.6 | 2.5±20% | 120.49±0.009 | 3.3±0.5 | 120.38±0.21 | 2.2±0.3 |
| | | | | 155.0±1.0 | 0.03±0.01 |
| 196.6 | 1.3±10% | 196.66±0.03 | 1.5±0.6 | 196.96±0.13 | 1.52±0.24 |
| 275.1 | 6.5±20% | 275.42±0.02 | 6.8±1.4 | 275.55±0.11 | 6.29±0.91 |
| 319.3 | 14.2±10% | 319.41±0.03 | 16.3±2.4 | 319.58±0.11 | 14.99±1.06 |
| 397.8 | 6.4±10% | 398.22±0.07 | 6.8±1.1 | 398.26±0.11 | 6.62±0.94 |
| 409.6 | 1.3±10% | 410.3±0.4 | 1.2±0.5 | 410.43±0.21 | 1.04±0.16 |
| 439.4 | 9.2±10% | 439.85±0.08 | 9.3±1.1 | 439.87±0.11 | 9.23±0.97 |
| 488.5 | 1.5±50% | 489.31±0.35 | 1.1±0.5 | 489.18±0.12 | 1.15±0.18 |
| 530.7 | 100 | 531.01±0.07 | 100 | 530.81±0.10 | 100 |
| 589.0 | 0.40 | 589.3±0.7 | 0.31±0.14 | 588.95±0.50 | 0.29±0.06 |
| 594.4 | 2.2±10% | 594.7±0.4 | 1.9±0.4 | 594.36±0.15 | 1.83±0.31 |
| 680.0 | 0.28 | 679.4±1.5 | 0.23±.16 | 680.3±0.8 | 0.16±0.08 |
| 686.1 | 6.6±10% | 685.8±0.35 | 5.9±1.0 | 685.31±0.26 | 6.33±0.91 |

detector at angles ranging from $90^{\circ}$ to $270^{\circ}$ from the Ge(Li) detector in steps of $15^{\circ}$. The counting time at each position was about 24 hours. The total counts recorded in the NaI(Tl) gate at each position were used to normalise the peak areas obtained in the coincidence spectra. Three series of measurements were taken.

The areas of the peaks in the Ge(Li) spectrum in coincidence with the 91 keV transition were determined by using the computer program SAMPO. These areas after correcting for chance coincidences and normalising by the NaI(Tl) singles gate counts were fitted by a least squares procedure to the directional correlation function.

$$W(\theta) = A_0 + A_{22} P_2 (\cos \theta) + A_{44} P_4(\cos \theta)$$

Figs. 7.4, 7.5, 7.6, and 7.7 give the correlation curves for the 319 - 91 keV, 398 - 91 keV, 439-91 keV and 595 - 91 keV cascades respectively. The values of the correlation coefficients resulting from the fitting procedure for each cascade are tabulated in Table 7.2. These have not been corrected for finite solid angle effects. These coefficients were then corrected for finite solid angle affects. The correction factors for the NaI(Tl) detector were taken from the work of Yates (1968). Those for the Ge(Li) detector have been calculated as outlined in Chapter 4

The corrected correlation coefficients for each cascade studied in this work are shown in Table 7.3. The values obtained by

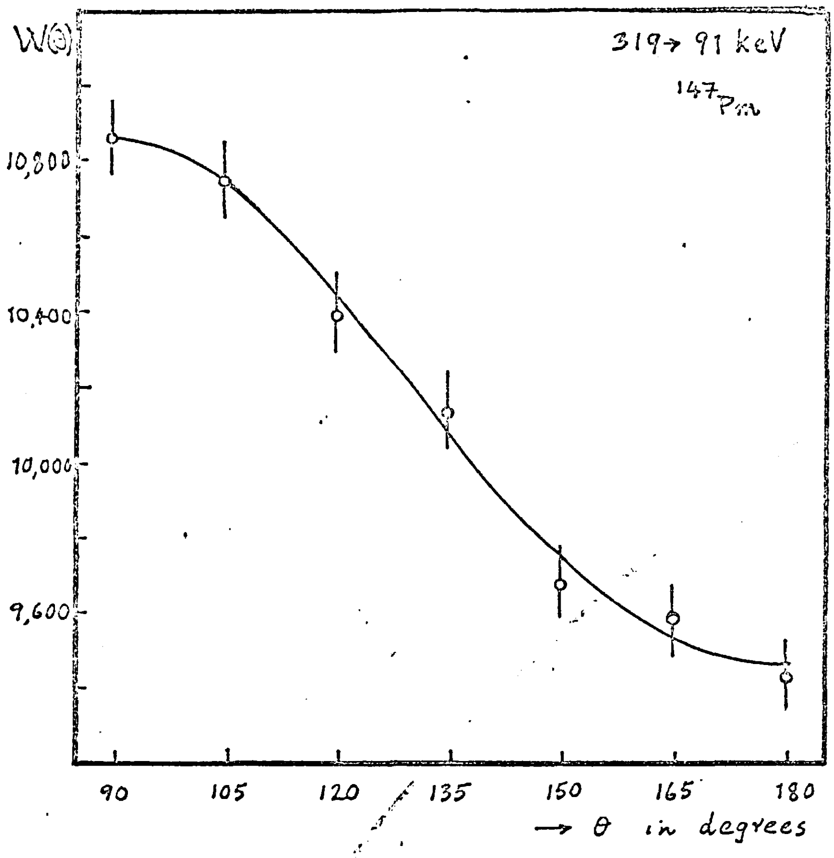


Fig. 7.4 The directional correlation curve for the 319 - 91 keV cascade in $^{147}$Pm

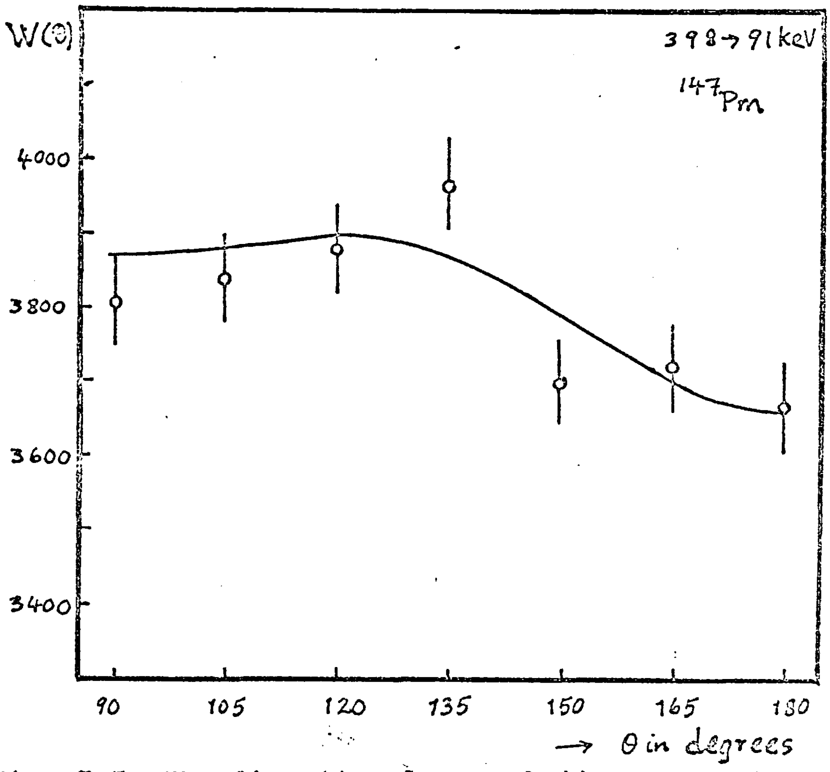


Fig. 7.5 The directional correlation curve for the 398 - 91 keV cascade in $^{147}$Pm

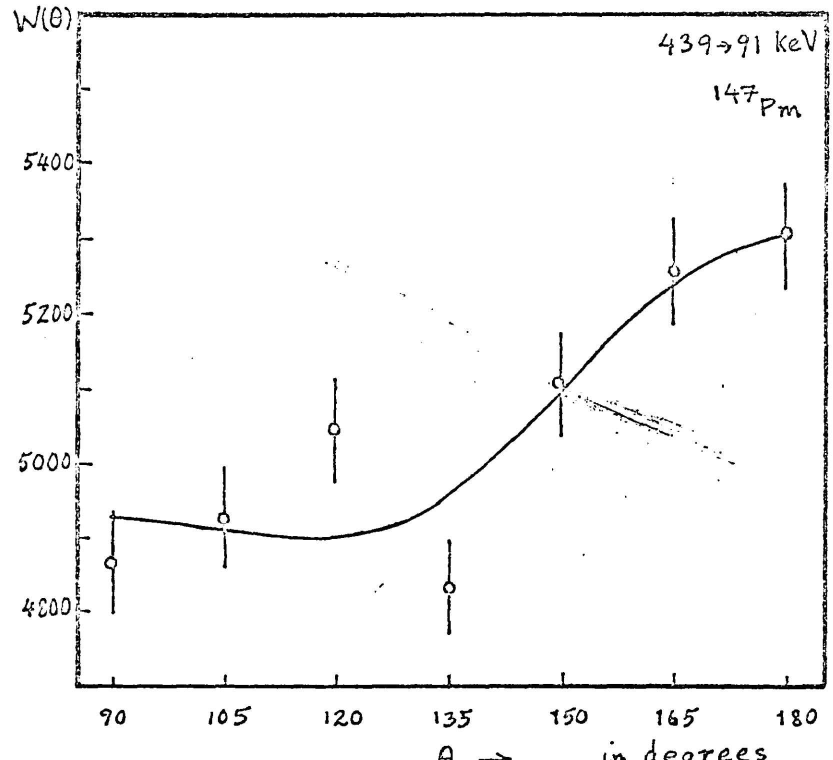


Fig. 7.6 The directional correlation curve for the 439 - 91 keV cascade in $^{147}$Pm

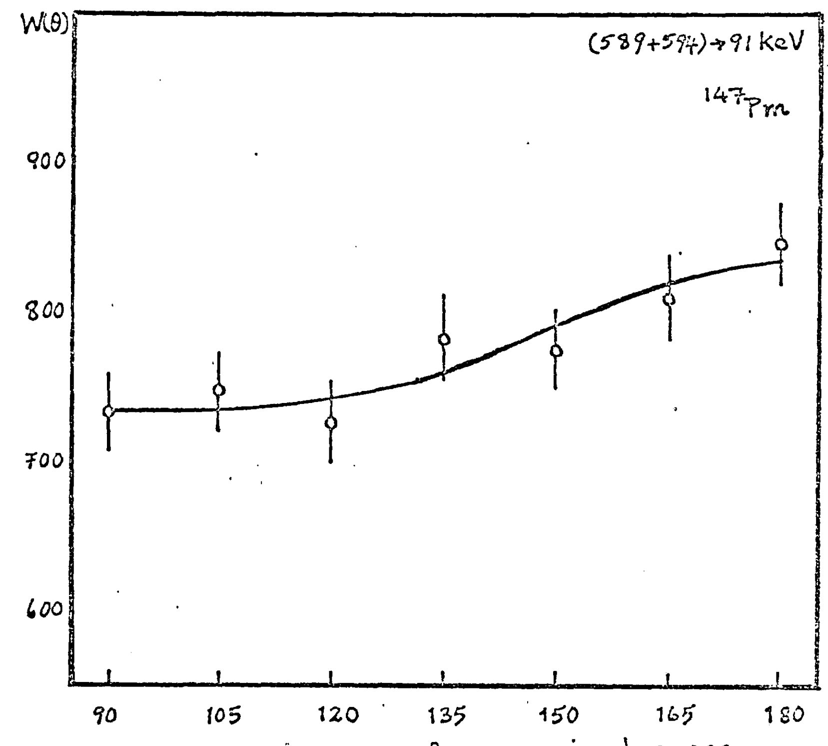


Fig. 7.7 The directional correlation curve for the (589+594) - 91 keV cascade in $^{147}$Pm .

TABLE 7.2

Directional Correlation Coefficients (not corrected for solid angle effects) for gamma-gamma cascades in $^{147}$Pm measured in this experiment.

| Cascade (keV) | $A_2^{expt}$ | $A_4^{expt}$ |
|---|---|---|
| 319 - 91 | $-0.0930\pm0.0069$ | $-0.0103\pm0.0075$ |
| 398 - 91 | $-0.0264\pm0.0156$ | $-0.0260\pm0.0193$ |
| 439 - 91 | $+0.3933\pm0.1582$ | $+0.0288\pm0.0189$ |
| (589+594)-91 | $+0.0167\pm0.0045$ | $+0.0079\pm0.0063$ |

TABLE 7.3

Directional Correlation Coefficients for gamma-gamma cascades in $^{147}Pm$. The coefficients have been corrected for finite solid angle effects.

| Cascade (keV) | $A_2$ | $A_4$ |
|---|---|---|
| 319 - 91 | | |
| Present Work | $-0.1033\pm0.0077$ | $-0.0146\pm0.0106$ |
| Blaskovich & Arya(1970) | $-0.085\pm0.011$ | $-0.014\pm0.015$ |
| Arya(1961) | $-0.1030\pm0.0298$ | $+0.0107\pm0.0099$ |
| Bodenstedt et.al(1960) | $-0.087\pm0.008$ | $-0.001\pm0.003$ |
| 398 - 91 | | |
| Present Work | $-0.0293\pm0.0173$ | $-0.0368\pm0.0273$ |
| Blaskovich & Arya(1970) | $-0.074\pm0.019$ | $-0.019\pm0.023$ |
| Bodenstedt et.al(1960) | $-0.022\pm0.008$ | $-0.002\pm0.009$ |
| 439 - 91 | | |
| Present Work | $+0.0435\pm0.0175$ | $+0.0408\pm0.0268$ |
| Blaskovich & Arya(1970) | $+0.054\pm0.018$ | $+0.016\pm0.024$ |
| Bodenstedt et.al(1960) | $-0.065\pm0.010$ | $-0.010\pm0.015$ |
| Saraf et.al(1961) | $+0.065\pm0.020$ | $-0.035\pm0.025$ |
| (589+594)- 91 | | |
| Present Work | $+0.019\pm0.005$ | $+0.01\pm0.008$ |
| Spring(1963) | $-0.02\pm0.05$ | $-0.02\pm0.07$ |
| Saraf et.al(1961) | $+0.06\pm0.03$ | $-0.05\pm0.03$ |

previous investigators are also shown for comparison.

The correlation coefficients measured in this experiment were then used to obtain the multipole mixing ratios and to deduce the correct spin assignments as discussed in the next section.

## 7.5 Determination of Multipole Mixing Ratios

The spins of the ground states of $^{147}$Nd and $^{147}$Pm have been established to be $5/2^-$ and $7/2^+$ respectively. The beta transitions to the excited levels of $^{147}$Pm have been classified as first forbidden (Jacobs et.al, 1967) with a spin change of 0 or 1 and a change in parity. The excited levels of $^{147}$Pm must therefore have even parity with spins of 3/2, 5/2 or 7/2. Consequently the gamma transitions in $^{147}$Pm consist of mixtures of E2 and M1 multipolarities.

The spin of the 91 keV first excited state of $^{147}$Pm is known to be $5/2^+$. Barrett and Shirley (1969) undertook new nuclear orientation measurements on the decay of $^{147}$Nd and also reanalysed old data (Westenberger and Shirley, 1961) in the light of a revised temperature scale for neodymium ethyl sulphate. They determined the quadrupole content of the 91 keV transition to be $(0.8 \pm 0.1)\%$ E2 with an admixture of $(99.2 \pm 0.1)\%$ M1 radiation. This corresponds with a mixing ratio for this transition of $\delta$ = $0.089 \pm 0.005$ which is in agreement with the value $|\delta| = 0.084$ found in the internal conversion studies of Ewan et.al (1961).

Barrett and Shirley's (1969) value of the mixing ratio for the 91 keV transition has been used in the analysis of the results of our directional correlation measurements on $^{147}$Pm.

Because the 91 keV transition is of mixed multipolarity, the method of Arns and Weidenbeck (1958) was used to determine the mixing ratios and the correct spin sequences of the gamma-gamma cascades investigated. In this method, $A_2$ and $A_4$ are plotted against $a = \delta^2/(1+\delta^2)$ for various spin sequences and the experimental points compared to the theoretical values.

For a gamma-gamma cascade in which both transitions are mixed the directional correlation function is of the form

$$W(\theta) = 1 + \sum_{k=2,4} A_k(\gamma_1)\, A_k(\gamma_2)\, P_k\,(\cos\theta)$$

That is,

$$W(\theta) = 1+A_2(\gamma_1)A_2(\gamma_2)P_2(\cos\theta) + A_4(\gamma_1)A_4(\gamma_2)P_4(\cos\theta)$$

The constant $A_k(\gamma_1)$ is determined only by the parameters of the first transition, i.e. by $I_1$ $I_2$ and $L_1$ , $L_1'$. Similarly $A_k(\gamma_2)$ depends on the parameters of the second transition only.

Specifically

$$A_k(\gamma_1) = \frac{1}{1+\delta_1^2}\left[F_k(L_1L_1I_1I_2)+(-1)^{L_1-L_1'}\, 2\,\delta_1 F_k(L_1L_1'\,I_1I_2) + \delta_1^2 F_k(L_1'L_1'I_1I_2)\right]$$

and

$$A_k(\gamma_2) = \frac{1}{1+\delta_2^2}\left[F_k(L_2L_2I_3I_2) + 2\delta_2\, F_k(L_2L_2'I_3I_2) + \delta_2^2\, F_k(L_2'L_2'I_3I_2)\right]$$

$A_k(\gamma_1)$ and $A_k(\gamma_2)$ are related to the experimentally measured coefficients $A_k$ in the following way

$$A_k(\gamma_1)\, A_k(\gamma_2) = A_k \pm \sigma_k$$

where $\sigma_k$ is the experimental error in $A_k$.

As the errors in the experimental coefficient $A_4$ are usually large only the $A_2$ coefficients are used in the analysis. The set of values of $A_2(\gamma_1)$ and $A_2(\gamma_2)$ satisfying the relationship above were calculated and plotted to give the equilateral hyperbolae. The effect of the error is to produce a band of uncertainty along each hyperbola.

Values of $A_2(\gamma)$ for different values of the mixing ratio were calculated from the formulae given above using the values of the F. coefficients tabulated by Ferentz and Rosenzweig (1955). These calculations were done for the spin sequences 7/2 - 5/2, 5/2 - 5/2 and 3/2 - 5/2.

When the $A_2$ coefficients were plotted against $Q = \delta^2/(1+\delta^2)$ the ellipses in Fig 7.8 resulted.

These single transition mixture curves were then placed with scales to coincide with the $A_2(\gamma_1)$, $A_2(\gamma_2)$ axes of the

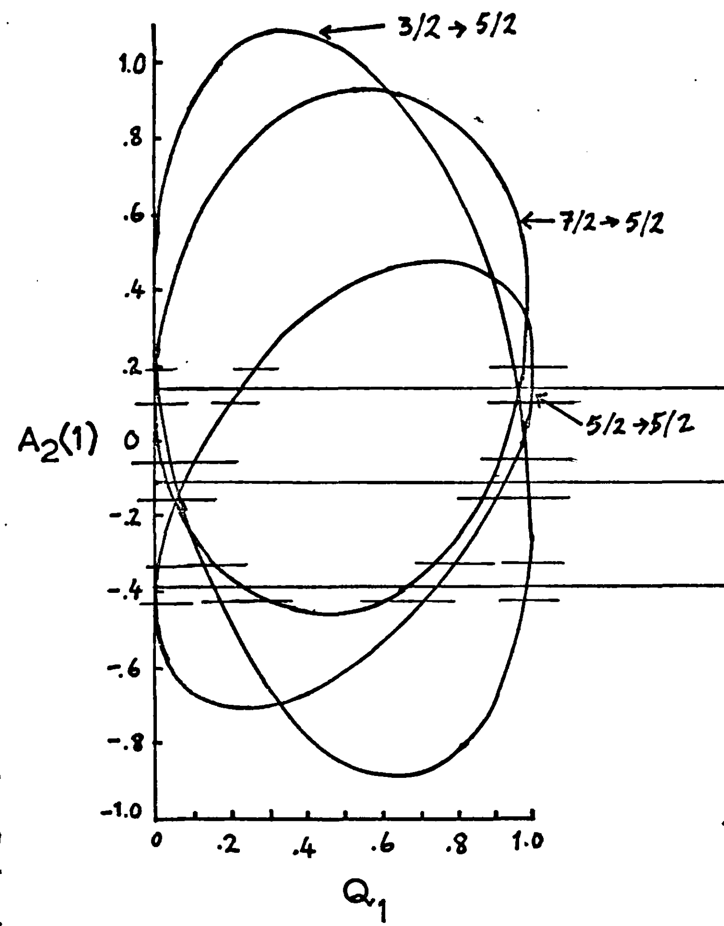


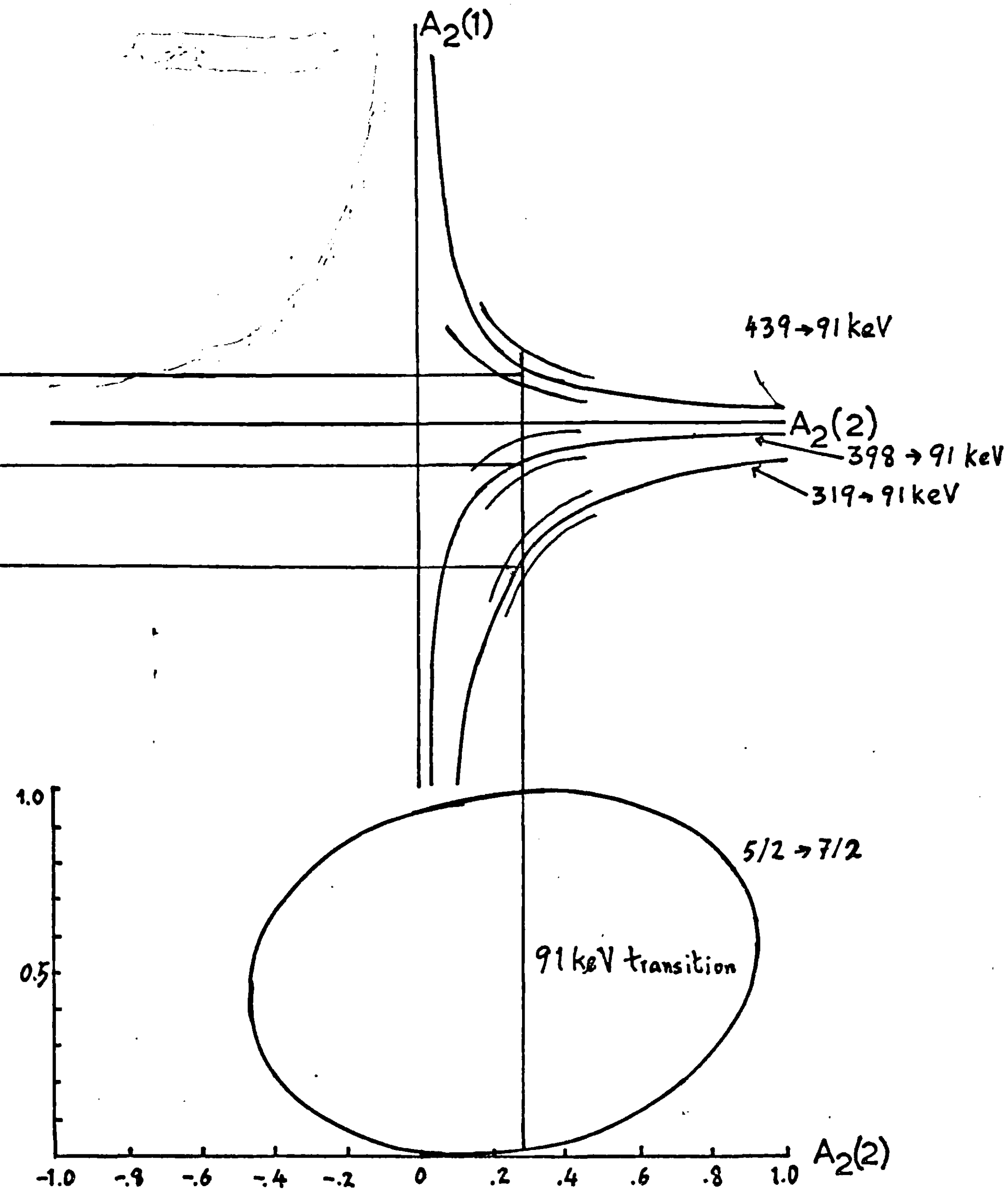


Fig. 7.8 Plots of $A_2$ vs $Q = \delta^2/(1+\delta^2)$ and $A_2^{expt} = A_2(\gamma_1)\, A_2(\gamma_2)$ for the analysis of cascades in which both transitions are of mixed multipolarity

experimental graph, as shown in Fig. 7.8. Then a range of $Q_1$ consistent with the first transition will correspond to a range of values of $Q_2$ for the second transition required by the experimental graph and vice versa. To obtain unique spin assignments, additional information from internal conversion data, nuclear orientation measurements or other directional correlation studies must be used. As noted in the beginning of this section we have utilised information from nuclear orientation measurements to analyse the results of our directional correlation measurements.

The 319 - 91 keV cascade

In this cascade the 410.5 keV level deexcites to the 91 keV level which subsequently depopulates by a 91 keV transition to the ground state. Using the multipole mixing ratio of the 91 keV transition from the nuclear orientation measurement of Barrett and Shirley (1969), the contribution of the 319 keV gamma ray to the experimentally measured correlation coefficients was determined. The quadrupole content of the 319 keV gamma transition has been found to be (23 $\pm$ 3)% E2 from nuclear orientation measurements (Barrett and Shirley,1969) and 20% E2 from the internal conversion studies of Ewan et.al (1961). A spin assignment of 5/2 to the 410.5 keV level results in a quadrupole content of $(76.4 \pm^{1.2}_{3.3})$% E2 which is inconsistent with the results from nuclear orientation and internal conversion data. A 7/2 spin assignment results in a multipole mixture of $(21.3 ^{+4.5}_{-2.6})$% E2 with the mixing ratio

$\delta = -0.52\,^{+0.07}_{-0.04}$. The quadrupole content is consistent with nuclear orientation and internal conversion data but the sign obtained is in disagreement with that obtained by Westenberger and Shirley (1961) and Barrett and Shirley (1969).

A $3/2^+$ spin assignment results in a quadrupole content of $(16.2\,^{+3.2}_{-2.0})$ % E2 and a mixing ratio of $\delta = +0.44\,^{+0.05}_{-0.04}$ which is in agreement with the nuclear orientation results $\delta = +0.55 \pm 0.05$ .

Thus our measurement and analysis affixes the spin of the 410.5 keV level as $3/2^+$

The 398 - 91 keV cascade

The 489 keV level deexcites via a 398 keV transition to the 91 keV level which then decays to the ground state by emitting a 91 keV gamma ray. Using a similar procedure the contribution of the 398 keV gamma transition is determined. The quadrupole content of this transition has been determined to be $(2 \pm 1)$% E2 from nuclear orientation studies (Westenberger and Shirley, 1961; Barrett and Shirley, 1969). An attempt to assign a spin of $3/2^+$ to the 489 keV level results in an admixture of $(6.1\,^{+1.4}_{-1.6})$% E2 with $\delta = +0.255\,^{+0.030}_{-0.037}$ . A spin assignment of $5/2^+$ permits an admixture of $(7.3\,^{+3.1}_{-1.8})$% E2 with $\delta = -0.28\,^{+0.04}_{-0.06}$. Finally a spin assignment of $7/2^+$ results in a quadrupole content of $(3.3\,^{+2.6}_{-1.6})$% E2 which is in agreement with that found by nuclear orientation studies.

Thus our measurement and analysis of the 398 - 91 keV cascade affixes the spin of the 489.3 keV level as $7/2^+$.

The 439 - 91 keV cascade

In this cascade the 531 keV level deexcites by the emission of the 439 keV gamma ray to the first excited state which then deexcites to the ground state by emitting the 91 keV gamma ray. The contribution of the 439 keV transition to the experimentally measured correlation $A_2$ coefficient was determined to be $A_2$ (439 $\gamma$) = $+ 0.167 \pm 0.067$. If a spin of $3/2^+$ is assigned to the 531 keV level, analysis through Fig. 7.8 allows an admixture of $(1.2 \pm 0.7)$% E2 with $\delta = + 0.11 {}^{+0.3}_{-0.4}$. A spin assignment of 5/2 results in an admixture of $(24.5 \pm {}^{6.5}_{4.5})$% E2 with $\delta = - 0.57 {}^{+0.07}_{-0.10}$. A 7/2 spin assignment permits a quadrupole content of 0.1% E2. The quadrupole content of the 439 keV transition has been determined to be $(33 \pm 6)$% E2 by nuclear orientation methods (Barrett and Shirley, 1969). Consequently our data is in agreemnet with the spin assignment of $5/2^+$ for the 531 keV level.

The 594 - 91 keV cascade

The 594 keV gamma ray is not resolved from the 589 keV gamma which deexcites the 680 keV level. As the multipole mixing and the directional correlation of the 589 keV gamma is not known no attempt was made to determine the mixing ratio for this cascade.

## 7.6 Conclusions

The decay scheme resulting from the measurements of this experiment is shown in Fig. 7.9 . The spin assignments arising from the analysis of the directional correlation measurements of this work are shown in Table 7.4 together with those of other investigators. The spins of the ground state and first excited state of $^{147}$Pm have been established as $7/2^+$ and $5/2^+$ respectively.

Although Arya(1961) favoured $7/2^+$ and Bodenstedt et.al (1960) favoured $5/2^+$ for the spin of the 410 keV level, other directional correlation measurements (Spring,1963; Blaskovich and Arya,1970) agree on $3/2^+$. The present investigation also results in a $3/2^+$ spin assignment which is in agreement with the assignment from nuclear orientation studies (Westenberger and Shirley,1961; Barrett and Shirley,1969) as well as with those from beta decay studies (Beekhuis et.al, 1966) .

Concerning the 489 keV level most of the investigations have been unable to provide a unique spin assignment. Nuclear orientation studies of Westenberger and Shirley (1961) and Barrett and Shirley (1969) favour a spin of $7/2^+$. Recent directional correlation studies with a Ge(Li) - NaI(Tl) system (Blaskovich and Arya, 1970) favoured a spin assignment of $5/2^+$. However, in contradiction to this assignment our measurements, also with a Ge(Li) - NaI(Tl) system, indicate a spin $7/2^+$ assignment.

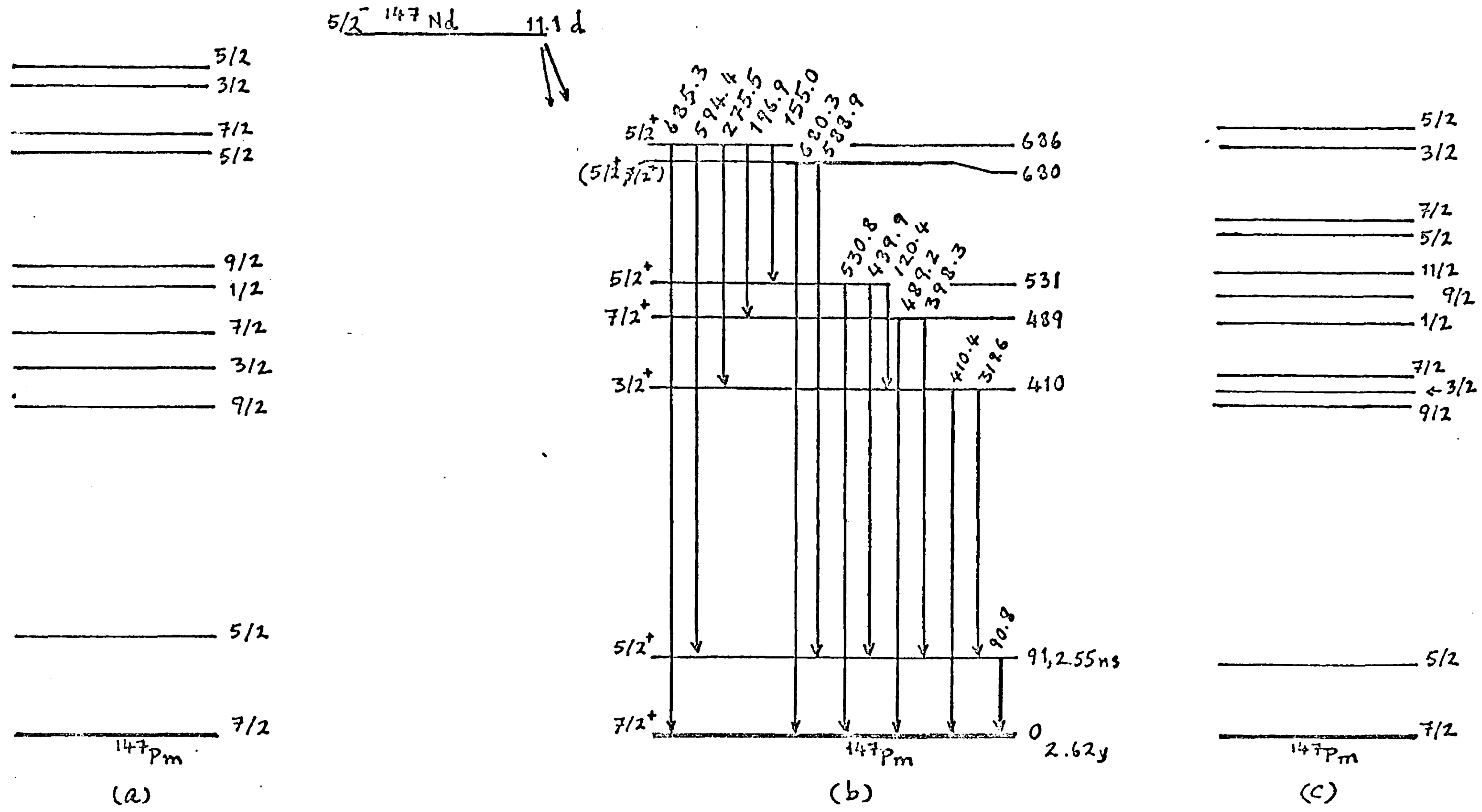


Fig. 7.9 Energy levels in $^{147}$Pm. (a) calculated by Heyde and Brussard (1967)
(b) $^{147}$Nd decay scheme consistent with our experimental results, and
(c) as calculated by Choudhury and O'Dwyer (1967)

TABLE 7.4 Spin assignments of the levels in $^{147}Pm$

| Level (keV) | Canty & Conner (1967) | Hill & Weidenbeck (1967) | Barrett & Shirley (1969) | Bodenstedt et.al (1960) | Saraf et. al (1961) | Arya (1961) | Spring (1963) | Blaskovich & Arya (1970) | Present Work |
|---|---|---|---|---|---|---|---|---|---|
| 686 | $(5/2^+)$ | $(5/2^+)$ | $5/2^+$ | - | $5/2^+$ | $(5/2^+)$ | $5/2^+$ | $5/2^+$ | $5/2^+$ |
| 680 | - | $(5/2^+,7/2^+)$ | - | - | - | - | - | - | $(5/2^+,7/2^+)$ |
| 531 | $5/2^+$ | $5/2^+$ | $5/2^+$ | $3/2^+,(7/2^+)$ | $5/2^+$ | - | $5/2^+$ | $5/2^+$ | $5/2^+$ |
| 489 | $(5/2^+,7/2^+)$ | $3/2^+,5/2^+,7/2^+$ | $(7/2^+)$ | $5/2^+,(7/2^+)$ | $7/2^+,(5/2^+)$ | - | - | $5/2^+$ | $7/2^+$ |
| 410 | $(3/2^+)$ | $3/2^+,7/2^+$ | $3/2^+$ | $5/2^+$ | $7/2^+,(3/2^+, 5/2^+)$ | $7/2^+$ | $3/2^+$ | $3/2^+$ | $3/2^+$ |
| 91 | $5/2^+$ | $5/2^+$ | $5/2^+$ | $5/2^+$ | $5/2^+$ | $5/2^+$ | $5/2^+$ | $5/2^+$ | $5/2^+$ |
| 0 | $7/2^+$ | $7/2^+$ | $7/2^+$ | $7/2^+$ | $7/2^+$ | $7/2^+$ | $7/2^+$ | $7/2^+$ | $7/2^+$ |

The spin of the 530 keV level has been assigned a value of $5/2^+$ by all previous work with the exception of Bodenstedt et.al (1960) who favoured a $3/2^+$ assignment. The results of this investigation confirm the assignment of spin $5/2^+$ to this level.

The beta decay to the 680 keV level has a log ft value of 8.9 which limits the spin of this level to 7/2, 5/2 or 3/2 . The approximate equality of the intensities of the 589 and 680 keV gamma rays depopulating this level indicates that the spin choice of 5/2 or 7/2 is more probable.

Our measurements do not permit us to make a unique spin assignment for the 686 keV level. The log ft value of 7.0 for the 211 keV beta transition from the $5/2^-$ ground state of $^{147}Nd$ limits the choice of spin of the 686 keV level to 3/2, 5/2 or 7/2 . From internal conversion measurements (Ewan et.al, 1961) the 686 keV gamma transition is known to consist of mainly M1 radiation which rules out the spin choice 3/2. Only the spin choice of 5/2 is consistent with nuclear orientation measurements (Barrett and Shirley, 1969) and previous directional correlation measurements (Saraf et.al, 1961; Blaskovich and Arya, 1970) and hence the spin assignment of $5/2^+$ to this level is favoured.

The level scheme for $^{147}Pm$ has been theoretically calculated by Choudhury and O'Dwyer (1967) and also by Heyde and Brussard (1967). Their results are shown in Fig. 7.9 alongside the decay scheme consistent with the results of our measurements. The calculations in both cases followed the intermediate coupling approach in the unified model. The $^{147}Pm$ nucleus is treated as a coupled system consisting of a doubly even core which can undergo quadrupole vibrations plus the odd proton which has available to it the $1g_{7/2}$ and $2d_{5/2}$ single particle shell model states. The three parameters used in the calculation are the phonon energy of core vibrations $\hbar w$, the strength of coupling $\xi$ between single particle motion and core vibrations, and the energy spacing between the single particle states $\Delta \equiv |E_{g7/2} - E_{d5/2}|/\hbar w$. Choudhury and O'Dwyer (1967) used $\hbar w$ = 455 keV, $\xi$ = 3.5 and $\Delta$ = 100 keV while Heyde and Brussaard (1967) used $\hbar w$ = 492 keV, $\xi$ = 3.76 and $\Delta$ = 114 keV. Both calculations give reasonably fair reproductions of the level scheme, but the calculations give a larger number of levels than have been experimentally observed so far.

The calculated levels of Heyde and Brussaard (1967) give a better agreement with energies and spins that have been experimentally determined. The only serious discrepancy is in the spin of the 530 keV level, the experimental value of which is $5/2^+$ while the possible calculated level has a spin of 1/2 or at a slightly higher energy a spin of 9/2. Their calculation provides a level of spin 7/2 which can be identified with the 489 keV level for which we have assigned a spin of 7/2.

Choudhury and O'Dwyer (1967) used a smaller value of the energy spacing and obtained good matches for the $5/2^+$, 91 keV level and $3/2^+$, 410 keV level. However, the spin of the calculated level corresponding to the $7/2^+$, 489 keV level has a value of 1/2. Although there are two calculated levels of spin 9/2 and 11/2 in the region of 530 keV, it is probable they are not excited in the present decay scheme. Finally, the $5/2^+$, 686 keV level may be matched with a calculated level with spin $5/2$.

## Acknowledgements

I wish to express my sincere appreciation to my supervisor, Dr. Peter Rice-Evans, for the guidance and help extended by him during the course of this research.

I also wish to thank Professor H.O.W. Richardson, Mr. R.N. Thomas, Dr. Ruth Thomas and Dr. P. Pal for their help and interest, and Messrs. W.A.G. Baldock, F.A. Grimes, A.K. Betts and A.H. King for technical assistance.

I wish to thank the Government of the Union of Burma for the award of a scholarship, and the British Council for an Overseas Students Fees Award. I am also grateful to the Arts and Science University of Rangoon for granting me leave of absence.

My thanks also go to Miss M. McKeaney for her patience in typing the thesis.

## REFERENCES


Arns,R.G., and Weidenbeck,M.L., 1958. Phys.Rev.111, 1631

Arya,A.P., 1961. Phys.Rev.122, 1226

Aubin,G., Barrette,J., Barrette,M., and Monaro,S., 1969. Nucl.Instr.Meth.76, 93

Auerbach,N., 1967. Phys.Rev.163, 1203

Ballini,R.,Blair,A.G., Cindre,N., Delauny,J., and Fouan,J.P., 1968. Nucl.Phys.A111, 147

Barrett,P.H., and Shirley,D.A., 1969. Phys.Rev.184, 1181

Becker,A.J., and Steffen,R.M., 1969. Phys.Rev.180, 1043

Beekhuis,H., Boskma,P., van Klinken,J., and de Waard,H., 1966. Nucl.Phys.79, 220

Berg,R.E., and Kashy, E., 1966. Nucl.Instr.Meth.39, 169

Biedenharn,L.C., 1960. in Nuclear Spectroscopy,Part B (ed. F.Ajzenberg-Selove) Academic Press, New York, p.732

Blaskovich,N., and Arya,A.P., 1970. Phys.Rev.C2, 1881

Bodenstedt,E., Korner,H.J., Frisius, F., Hovestadt,D., and Gerdau,E., 1960. Z.Physik 160, 33

Bohr,A., 1952. Mat.Fys.Medd.Dan.Vid.Selsk.26, no.14

Bohr,A., and Mottelson,B.R., 1953. Mat.Fys.Medd.Dan.Vid.Selsk. 27, no.16

Brown,G., Haigh,J.G., Hudson,R.R., and McGregor,A.E., 1967. Nucl.Phys.A101, 163

Cabezas,A., Lindgren,I., Lipworth,E., Marrus,R., and Rubinstein,M., 1960. Nucl.Phys.20, 509

Camp,D.C., Fielder,D.R., and Foster,B.P., 1971. Nucl.Phys.A163, 145

Camp,D.C., and van Lehn,A.L., 1969. Nucl.Instr.Meth.76, 192

Canty,M.J., and Conner,R.D., 1967. Nucl.Phys.A104, 35

Choudhury,D.C., 1954. Mat.Fys.Medd.Dan.Vid.Selsk.28, no.4

Choudhury,D.C., and O'Dwyer,T.F., 1967. Nucl.Phys.A93, 300

Cohen,S., Lawson,R.D., McFarlane,M.H., Pandys,S.P., and Soga,M., 1967. Phys.Rev.160, 903

Coleman,G.F., 1958. Nucl.Phys.5, 495

Darcey,W., 1964. Compt.rend.congr.intern.phys.nucleaire, Paris 2, 456

Davydov,A.S., and Fillipov,G.S., 1958. Nucl.Phys.8, 237

De-Shalit,A., 1961. Phys.Rev.122, 1530

Devons,S., and Goldfarb,L.J.B., 1957. in Encyclopedia of Physics 42, (ed. S.Flugge) Springer, Berlin, p.362

Dixon,W.R., and Storey,R.S., 1970. Can.J.Phys.48, 483

Eichler,E., O'Kelly,G.D., Robinson,R.L., Marinsky,J.A., and Johnson,N.R., 1962. Nucl.Phys.35, 625

Evans,P.R., 1958. Phil.Mag.3, 1061

Evans,R.D., 1955. The Atomic Nucleus, McGraw Hill, New York, p.687

Ewan,G.T., Graham,R.L., and Geiger,J.S., 1961. Bull.Am.Phys.Soc.6, 238

Ferentz,M., and Rosenzweig,N., 1955. Argonne National Laboratory Report ANL-5324

Ferguson,A.J., 1965. Angular Correlation Methods in Gamma-Ray Spectroscopy, North-Holland, Amsterdam, Chapter

Frauenfelder,H., and Steffen,R.M., 1965. in Alpha-, Beta-, and Gamma-Ray Spectroscopy (ed. K.Siegbahn) North-Holland, Amsterdam, Vol.2, p.997

Freck,D.W., and Wakefield,J., 1962. Nature 4816, 669

Girgis,R.K., and van Lieshout, R., 1959. Physica 23, 688

Gopinathan,K.P., 1966. AEET-267, 44

Grechukhin,D.P., 1963. Nucl.Phys.40, 422

Gunye,M.R., Jambunathan,R., and Saraf,B., 1961. Phys.Rev.124, 172

Habib,E., Ogata,H., and Armstrong,W., 1966. Can.J.Phys.44, 1157

Hamilton,J.H., Coffman,F.E., and Ramayya,A.V., 1969. Nucl.Phys. A132, 254

Hansen,H.H., and Spernol,A., 1968. Z.Physik 209, 111

Heath,R.L., Black,W.W., and Kline,J.E., 1966. IEEE Trans.Nucl.Sci. NS 13, 445

Heitler,W., 1936. Proc.Camb.Phil.Soc.32, 112

Heyde,K., and Brussaard,P.J., 1967. Nucl.Phys.A104, 81

Hill,J.C., and Weidebbeck,M.L., 1967. Nucl.Phys.A98, 599

Jacobs,E., Heyde,K., Dorikens,M., Demuynck,J., and Dorikens-Vanpraet,L., 1967. Nucl.Phys.A99, 411

Kedzie,R.W., Abraham, M., and Jeffries,C.D., 1957. Phys.Rev.108,54

Kisslinger,L.S., and Sorenson,R.A., 1963. Rev.Mod.Phys.35, 853

Klinkenberg,P.F.A., and Tomkins,F.S., 1960. Physica 26, 103

Krane,K.S., 1972. Nucl.Instr.Meth.98, 205

Kukoc,A.H., King,J.D., and Taylor,H.W., 1968. Nucl.Phys.A115, 625

Lawson,R.D., and Uretsky,J.L., 1957. Phys.Rev.108, 1300

Lingemann,E.W.A., Koniju,J., Polak,P., and Wapstra, , 1969. Nucl.Phys.A133, 630

McGowan,F.K., and Stelson,P.H., 1962. Phys.Rev.126, 257

Meyer,E., 1970. Am.J.Phys.38, 1202

Moreh,R., and Shahal,O., 1970. Phys.Rev.C2, 2217

Morinaga,H., and Takahashi, K., 1968. J.Phys.Soc.Japan 14, 1460

Moszkowski,S.A., 1965. in Alpha-, Beta-, Gamma-Ray Spectroscopy (ed. K.Siegbahn) North-Holland, Amsterdam, Vol.2, p.683

Moszkowski,S.A., 1957. in Encyclopedia of Physics 39 (ed. S.Flugge) Springer, Berlin, p.490

Nilsson,S.G., 1955. Mat.Fys.Medd.Dan.Vid.Selsk.29, no.16

Perlman,I., and Asaro,F., 1954. Ann.Rev.Nucl.Sci.4, 587

Plastino,A., Arvieu,R., and Moszkowski,S.A., 1966. Phys.Rev.145,837

Rajput,M.S., and Seghal, M.L., 1967. Ind.J.Phys.41, 176

Raman,S., 1968. Nuclear Data Sheets for A=60, Nucl.Data B2-5-41

Raman,S., 1969. Z.Physik 228, 387

Rauch,F., van Patter,D.M., and Hinrichsen,P.F., 1969. Nucl.Phys. A124, 145

Raz, J., 1959. Phys.Rev.114, 1116

Rice-Evans,P., and Aung,Z., 1970. Z.Physik 240, 392

Rose,M.E., 1953. Phys.Rev.91, 610

Routti,J.T., 1969. Lawrence Radiation Laboratory Report, UCRL-19452 TID-4500 UC.34 (unpublished)

Routti,J.T., and Prussin,S.G., 1969. Nucl.Instr.Meth.72, 125

Saraf,B., Jambunathan,R., and Gunye,M.R., 1961. Phys.Rev.124, 178

Sastry,V.V.G., Lakshminarayana,V., and Jnanananda,S., 1964. Ind. J.Phys.2, 307

Scharff-Goldhaber,G., 1953. Phys.Rev.90, 587

Scharff-Goldhaber,G., and Weneser,J., 1955. Phys.Rev.98, 212

Singh,H., Sethi,B., and Mukerjee,S.K., 1971. Nucl.Phys.A174, 437

Spring,E., 1963. Phys.Letters 7, 218

Steffen,R.M., 1970. in Angular Correlations in Nuclear Disintegration (eds. H.van Krugten and B.van Nooijen) Wolters-Noorhoff Publishing Co, Groningen, p.1

Storm,E., and Israel,I.H., 1967. Los Alamos Scientific Laboratory Report, LA-3753 (unpublished)

Taylor,H.W., Singh,B., Prato,F.S., and McPherson,R., 1971. Nuclear Data Tables A9, No.1

van Hise,J.R., and Camp,D.C., 1969. Phys.Rev.Lett.23, 1248

van Hise,J.R., and Paperiello,C., 1972. Nucl.Phys.A188, 148

Weitkamp,C., Michaelis,W.,Schmidt,H., and Fanger,U., 1966. Z.Physik 192, 423

Wendt,H.D., and Kleinheinz,P., 1960. Nucl.Phys.20, 169

Westenberber,G.A., and Shirley,D.A., 1961. Phys.Rev.123, 1812

Wilets,L., and Jean,M., 1956. Phys.Rev.102, 788

Wolfson,J.L., 1955. Can.J.Phys.33, 886

Yates,M.J.L., 1965. in Alpha-, Beta-, Gamma-Ray Spectroscopy (ed. K.Siegbahn) North-Holland, Amsterdam, Vol.2, p.1691

# APPENDIX

```
      SUBROUTINE GCF(XL,R,A,XD,D,TAU,K,Q)
C
C     SUBROUTINE FOR GEO.CORRECTION FACTORS 5-SIDED COAX GE-LI DETECTORS
C
      DIMENSION F(101),B(5),XJ(2)
      B(1)=0.0
      B(2)=ATAN2(A,D+XL)
      B(3)=ATAN2(A,D+XD)
      B(4)=ATAN2(R,D+XL)
      B(5)=ATAN2(R,D)
      DO 100 N=1,2
      XJ(N)=0.0
      IF(K.EQ.0.AND.N.EQ.2) GO TO 110
      KA=K*(2-N)+1
      DO 100 J=1,4
      YL=B(J)
      YU=B(J+1)
      DL=(YU-YL)/100.
      DO 90 M=1,101
      XM=YL+DL*(M-1)
      GO TO(10,20,30,40),J
   10 EX=-TAU*XD/COS(XM)
      GO TO 45
   20 EX=-TAU*XD/COS(XM)
      EY= TAU*((D+XD)*TAN(XM)-A)/SIN(XM)
      EZ= TAU*(A-(D+XL)*TAN(XM))/SIN(XM)
      GO TO 46
   30 EX=-TAU*XL/COS(XM)
      GO TO 45
   40 EX= TAU*(D*TAN(XM)-R)/SIN(XM)
   45 F(M)=SIN(XM)*(1.-EXP(EX))
      GO TO(90,50,60,70,80),KA
   46 F(M)=SIN(XM)*((1.-EXP(EX))+((1.-EXP(EZ))*EXP(EY)))
      GO TO(90,50,60,70,80),KA
   50 F(M)=F(M)*COS(XM)
      GO TO 90
   60 F(M)=F(M)*(1.5*COS(XM)**2-0.5)
      GO TO 90
   70 F(M)=F(M)*(2.5*COS(XM)**3-1.5*COS(XM))
      GO TO 90
   80 F(M)=F(M)*(4.375*COS(XM)**4-3.75*COS(XM)**2+0.375)
   90 CONTINUE
      EV=0.0
      OD=0.0
      DO 95 M=2,98,2
      EV=EV+F(M)
   95 OD=OD+F(M+1)
      FINT=DL/3.*(F(1)+4.*(EV+F(100))+2.*OD+F(101))
  100 XJ(N)=XJ(N)+FINT
  110 Q=XJ(1)
      IF(K.NE.0) Q=Q/XJ(2)
      RETURN
      END
```

Z. Physik 240, 392–395 (1970)


# On the Decay of Cobalt 60

PETER RICE-EVANS and ZIN AUNG
Physics Department, Bedford College, University of London

Received August 12, 1970

The gamma spectrum from Cobalt 60 decay has been investigated with a 40 cc Ge(Li) detector. A peak at 822 keV is shown to be not a gamma transition but a single escape peak and an upper limit of 10 is given to the branching ratio of the 2158 keV level.

## 1. Introduction

The daughter nucleus resulting from the beta decay of $Co^{60}$ is $Ni^{60}$. The excited levels of this nucleus have aroused considerable theoretical interest for it is thought to be approximately spherical and to consist of closed shells of neutrons and protons ($N=Z=28$) plus four neutrons in the ($2p_{3/2}$, $1f_{5/2}$, $2p_{1/2}$) states. The work of Rauch *et al.*[1] on the $\beta^+$ decay of $Cu^{60}$, and Ballini *et al.*[2] on the results of $Ni^{60}$ ($p, p'\,\gamma$) and $Co^{59}(He^3, d)$ scattering has established the energies and parameters of a large number of nickel states; and these have been compared with shell model calculations – e.g. Auerbach[3], Cohen *et al.*[4], and Plastino *et al.*[5].

On the basis of these experiments, the decay scheme recommended in the table of Isotopes[6] is as shown in Fig. 1. The main evidence for the excitation of the 2158 keV level in the decay of Cobalt 60 is Wolfson's[7] detection of a weak externally converted gamma ray of this energy. The 826 keV transition from this level to the 1332 keV level is indicated by Copper 60 decay[1], and so is a branching ratio of 6.5 for $I(826\,\gamma)/I(2158\,\gamma)$.

Nevertheless, uncertainty remains about the population of the nickel states by the beta decay of $Co^{60}$. Recently, Hansen and Spernol[8] have

1 Rauch, F., Patter, D. M. van, Hinrichsen, P. F.: Nucl. Phys. A **124**, 145 (1969).
2 Ballini, R., Blair, A. G., Cindre, N., Delauny, J., Fouan, J. P.: Nucl. Phys. A **111**, 147 (1968).
3 Auerbach, N.: Phys. Rev. **163**, 1203 (1967).
4 Cohen, S., Lawson, R. D., Macfarlane, M. H., Pandya, S. P., Soga, M.: Phys. Rev. **160**, 903 (1967).
5 Plastino, A., Arvieu, R., Moszkowski, S. A.: Phys. Rev. **145**, 837 (1966).
6 Lederer, C. M., Hollander, J. M., Perlman, I.: Table of isotopes. New York: Wiley 1967.
7 Wolfson, J. L.: Can. J. Phys. **33**, 886 (1955).
8 Hansen, H. H., Spernol, A.: Z. Physik **209**, 111 (1968).

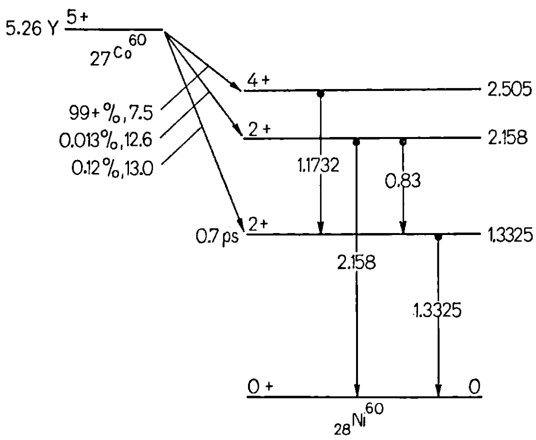


Fig. 1. The decay scheme of $Co^{60}$. All energies are in MeV

reported evidence for a third beta transition (670 keV) to an intermediate level. In addition, on the basis of a peak at 822 keV in their Ge(Li) gamma spectrum they propose that this level should be at 2155 keV (and not 2158). Raman [9], however, has cast doubt on this interpretation by intimating the 822 keV peak is an annihilation single-escape peak from the 1332 keV transition. The present experiment was designed to test this proposal.

## 2. Experiment and Results

The gamma spectra have been studied with a Nuclear Enterprises 40 cc trapezoidal Ge(Li) detector coupled to a 400 channel pulse height analyser. The detector had a nominal resolution of 3.5 keV (FWHM) for the 1332 keV line. The biassing was such that the spectra in the region 270–1400 keV were recorded in the analyser. Throughout the experiment the settings remained unchanged; and the energy calibration was made using the prominent $Ni^{60}$ lines and also the double escape peak at 310.5 keV. A separate energy measurement was made on the 822 keV $Ni^{60}$ peak, using the detector connected to a 1024 channel analyser.

The gamma spectra from $Co^{60}$ decay in the region 820 keV are shown in Fig. 2b. It is seen that a peak clearly exists at 822.1 keV. To ascertain whether the peak is the result of a single annihilation quantum escaping after pair production in the germanium crystal, isotopes of $Sc^{46}$, $Na^{22}$ and $Na^{24}$ were also studied. These elements have prominent gamma rays

9 Raman, S.: Z. Physik **228**, 387 (1969).

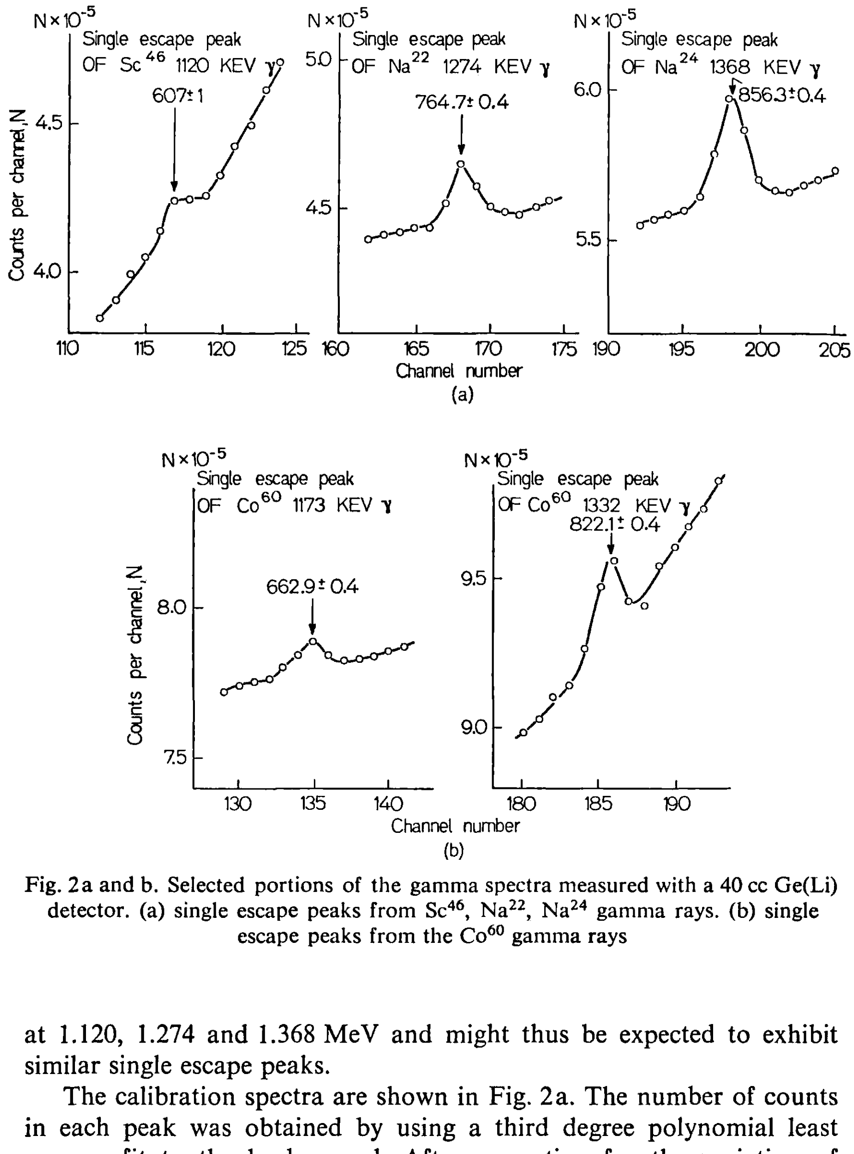


Fig. 2a and b. Selected portions of the gamma spectra measured with a 40 cc Ge(Li) detector. (a) single escape peaks from $Sc^{46}$, $Na^{22}$, $Na^{24}$ gamma rays. (b) single escape peaks from the $Co^{60}$ gamma rays

at 1.120, 1.274 and 1.368 MeV and might thus be expected to exhibit similar single escape peaks.

The calibration spectra are shown in Fig. 2a. The number of counts in each peak was obtained by using a third degree polynomial least squares fit to the background. After correction for the variation of efficiency with energy, the relative intensities of the single escape peaks were calculated. The line in Fig. 3 shows that the intensities are a smooth function of energy.

It may be seen that the $Co^{60}$ peak at 822 keV lies approximately on this line, and it is thus possible to conclude that the peak, suggested by

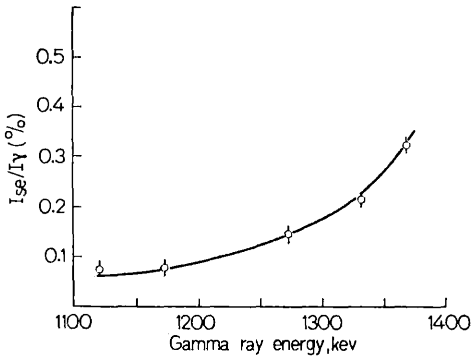


Fig. 3. Relative intensities of the single escape peaks shown as a function of the gamma ray energy

Hansen and Spernol to be a gamma transition, is a single escape peak of the 1332 keV transition. Further, from Fig. 3, it is possible to calculate an upper limit of 0.012% for the intensity of a possible gamma ray at this energy.

### 3. Conclusion

It is clear that our results discount the proposal by Hansen and Spernol[8] for a prominent level at 2155 keV. It may be noted that although these authors presented their $\beta$ spectrum, the fact that they omitted the Fermi-Kurie analysis makes it impossible to assess the significance of their statement that three straight lines resulted, indicating a third weak beta transition to the level in question of intensity $0.15 \pm 0.03$%.

Wolfson's value of $1.2 \times 10^{-3}$% for the intensity of the 2158 keV transition, and our measured limit on the intensity of the 826 keV line gives an upper value for the branching ratio of this level ($I(826\ \gamma)/I(2158\ \gamma)$) of 10. This is very different from the value 120 given by Hansen and Spernol[8] but is in agreement with the 6.5 of Rauch *et al.*[1].

The authors wish to thank Mr. and Mrs. R. N. Thomas, Mr. P. Pal and Professor H. O. W. Richardson for their help and interest; and to acknowledge the financial support from the Science Research Council. One of us (Z.A.) also wishes to thank the Government of the Union of Burma for the award of a scholarship.

Dr. P. Rice-Evans
Physics Department
Bedford College
Regents Park,
London N.W.1.
Great Britain

Zin Aung
Physics Department
Arts and Science University
Rangoon
Burma